NASA TECHNICAL MEMORANDUM

NASA TM X-2383

NASA TM X-2383

ATLAS-CENTAUR AC-18 PERFORMANCE EVALUATION FOR APPLICATIONS TECHNOLOGY SATELLITE ATS-5 MISSION

by Lewis Research Center Staff

Lewis Research Center
Cleveland, Ohio 44135

NATIONAL AERONAUTICS AND SPACE ADMINISTRATION • WASHINGTON, D. C. • NOVEMBER 1971

1. Report No.	2. Government Accession No.	3. Recipient's Catalog No.
NASA TM X-2383		

4. Title and Subtitle	5. Report Date
ATLAS-CENTAUR AC-18 PERFORMANCE EVALUATION FOR APPLICATIONS TECHNOLOGY SATELLITE ATS-5 MISSION	November 1971
	6. Performing Organization Code

7. Author(s)	8. Performing Organization Report No.
Lewis Research Center	E-6284
	10. Work Unit No.
	491-02

9. Performing Organization Name and Address	11. Contract or Grant No.
Lewis Research Center National Aeronautics and Space Administration Cleveland, Ohio 44135	
	13. Type of Report and Period Covered
	Technical Memorandum

12. Sponsoring Agency Name and Address	14. Sponsoring Agency Code
National Aeronautics and Space Administration Washington, D. C. 20546	

15. Supplementary Notes

16. Abstract

This report contains an evaluation of the performance of the Atlas-Centaur launch vehicle AC-18 in support of the Applications Technology Satellite 5 (ATS-5) mission. The Atlas-Centaur with the ATS-5 spacecraft was successfully launched from Eastern Test Range on August 12, 1969, and the ATS-5 was placed in the required highly elliptical transfer orbit with apogee near synchronous altitude. From this orbit the ATS-5, using its apogee motor, achieved the desired near-synchronous circular equatorial orbit. All launch vehicle systems performed satisfactorily. This concluded a planned series of five ATS launches. Atlas-Agena vehicles launched the first three ATS spacecraft and Atlas-Centaur vehicles launched the last two.

17. Key Words (Suggested by Author(s))	18. Distribution Statement
Atlas applications Centaur applications Launch vehicle Application Technology Satellite	Unclassified - unlimited

19. Security Classif. (of this report)	20. Security Classif. (of this page)	21. No. of Pages	22. Price*
Unclassified	Unclassified	145	$3.00

* For sale by the National Technical Information Service, Springfield, Virginia 22151

CONTENTS

ATLAS-CENTAUR AC-18 PERFORMANCE EVALUATION FOR APPLICATIONS TECHNOLOGY SATELLITE ATS-5 MISSION

Lewis Research Center

I. SUMMARY

by Roy K. Hackbarth

The Atlas-Centaur launch vehicle AC-18, with the Applications Technology Satellite 5 (ATS-5) spacecraft, was successfully launched from Eastern Test Range Complex 36A at 0601:04 eastern standard time on August 12, 1969. An indirect mode of ascent was used wherein the Atlas boost phase and a Centaur first powered phase placed the Centaur/ATS-5 in an elliptical parking orbit with a perigee altitude of 180.8 kilometers (97.6 n mi) and an apogee altitude of 5158.4 kilometers (2785.8 n mi). After a 25-minute coast in this orbit, a Centaur second powered phase placed the Centaur/ATS-5 in a highly elliptical transfer orbit with a perigee altitude of 2147.2 kilometers (1159.4 n mi) and an apogee altitude of 36 645.6 kilometers (19 787.2 n mi). The Centaur oriented to the attitude required by ATS-5 at the apogee of the transfer orbit and separated the ATS-5. The Centaur then performed a maneuver which increased the rate of separation and also placed Centaur in an orbit different from that of ATS-5.

The ATS-5 coasted for approximately $5\frac{1}{2}$ hours to the apogee of the transfer orbit. Its apogee motor was then fired and the ATS-5 achieved near-synchronous circular equatorial orbit. However, due to stability problems, the ATS-5 assumed an undesirable spin-stabilized mode and gravity gradient stabilization was not attempted.

The Atlas-Centaur performed satisfactorily and achieved all flight objectives. This report presents an evaluation of Atlas-Centaur performance in support of the ATS-5 mission, from lift-off through completion of the Centaur post-separation maneuver performed after spacecraft separation.

II. INTRODUCTION

by Roy K. Hackbarth

The primary purpose of the Applications Technology Satellite 5 (ATS-5) mission was to demonstrate precision spacecraft stabilization in synchronous orbit by use of gravity gradient techniques. The objectives of the Atlas-Centaur launch vehicle AC-18 were to inject the ATS-5 into the proper elliptical transfer orbit (apogee near synchronous altitude), to aline the ATS-5 to the required apogee motor firing vector, to initiate spacecraft separation, and to perform a post-separation maneuver to ensure adequate orbital separation from ATS-5.

This was the last in a planned series of five ATS missions. The launch vehicles for this series were the responsibility of the Lewis Research Center. Atlas-Agena vehicles launched the first three ATS spacecraft and Atlas-Centaur vehicles launched the last two. ATS-1 was successfully placed into orbit in December 1966. ATS-2, launched in April 1967, did not attain the proper orbit due to failure of the Agena engine to start for its second powered phase. ATS-3 was successfully placed into orbit in November 1967. ATS-4, launched in August 1968, did not attain the proper orbit due to failure of the Centaur main engine to restart for its second powered phase.

AC-18, launched on August 12, 1969, was the 12th operational Centaur and the sixth to employ the indirect (two Centaur powered phases) mode of ascent. This mode consists of an Atlas boost phase and Centaur first powered phase to achieve a parking orbit, a Centaur coast in this orbit, and a Centaur second powered phase to achieve final orbit.

The trajectory for the ATS-4 and ATS-5 missions required placing the spacecraft in a highly elliptical transfer orbit (apogee near synchronous altitude) from which the spacecraft would achieve circular synchronous orbit with firing of its fixed-impulse apogee motor. Initially the ATS-5 trajectory was planned to be like that of ATS-4. However, because the weight of ATS-5 was increased, a different (or optimized) trajectory was required to accomplish the ATS-5 mission within the performance capability of the launch vehicle. This optimization resulted in, as compared to ATS-4, a more elliptical parking orbit, a yaw maneuver during Centaur first powered phase, and a shorter coast time in parking orbit with injection of Centaur/ATS-5 into transfer orbit at the first equatorial crossing.

Changes to the initial ATS-5 configuration were required because of the changed trajectory and because of changes to preclude failure of the Centaur main engine to restart, as occurred on the ATS-4 mission. These changes included elimination of a second hy-

drogen peroxide bottle because of a shorter coast period (25 min versus 61 min), extensive modifications to the hydrogen peroxide boost pump feed system and aft bulkhead area to eliminate the possibility of hydrogen peroxide freezing in the boost pump feedlines, and provisions to separate the spacecraft if the Centaur main engines failed to restart or shut down prematurely.

This report presents an evaluation of the performance of the Atlas-Centaur launch vehicle systems in supporting ATS-5 mission objectives.

III. LAUNCH VEHICLE DESCRIPTION

by Eugene E. Coffey and Roy K. Hackbarth

The Atlas-Centaur is a two-stage launch vehicle consisting of an Atlas first stage and a Centaur second stage connected by an interstage adapter. Both stages are 3.05 meters (10 ft) in diameter, and the composite vehicle is 35.6 meters (117 ft) in length. The vehicle weight at lift-off is approximately 147 048 kilograms (324 185 lbm). The basic structure of the Atlas and the Centaur stages utilizes thin-wall, pressure-stabilized main propellant tank sections of monocoque construction. Figure III-1 shows the Atlas-Centaur lifting off with the ATS-5 spacecraft.

The first-stage SLV-3C Atlas (fig. III-2) is 21.03 meters (69 ft) long. It is powered by a propulsion system consisting of a booster engine having two thrust chambers and with a total sea-level thrust of 1494×10^3 newtons (336×10^3 lbf), a sustainer engine with a sea-level thrust of 258×10^3 newtons (58×10^3 lbf), and two vernier engines with sea-level thrust of 2980 newtons (670 lbf) each. All engines use liquid oxygen and RP-1 (kerosene) as propellants and are ignited prior to lift-off. The booster engine thrust chambers are gimbaled for pitch, yaw, and roll control during the booster engine phase of the flight. This phase is completed at booster engine cutoff, which occurs when the vehicle acceleration reaches about 5.7 g's. The booster engine section is jettisoned 3.1 seconds later.

The sustainer engine and the vernier engines continue to thrust for the Atlas sustainer phase of the flight. During this phase the sustainer engine is gimbaled for pitch and yaw control, while the vernier engines are gimbaled for roll control only. The sustainer and vernier engines provide thrust until propellant depletion. The Atlas is severed from the Centaur by the firing of a shaped charge system located on the forward end of the interstage adapter. The firing of a retrorocket system then separates the Atlas/interstage adapter from the Centaur.

The Centaur second stage (fig. III-3) is about 9.1 meters (30 ft) long. It is a high-performance stage with a design specific impulse of approximately 442 seconds. The Centaur is powered by two main engines which use liquid hydrogen and liquid oxygen as propellants; it generates a total thrust of approximately 133.45×10^3 newtons (30 000 lbf). These engines are gimbaled to provide pitch, yaw, and roll control during Centaur powered flight. Fourteen hydrogen peroxide engines, mounted on the aft periphery of the oxidizer tank, operate during nonpowered phases of flight to provide various thrust levels for attitude control, for propellant settling and retention, and for vehicle reorientation.

The cylindrical section of the Centaur hydrogen tank is insulated with four jettisonable fiber-glass panels whose primary function is to reduce liquid-hydrogen boiloff. A fiber-glass nose fairing is used to provide an aerodynamic shield for the spacecraft, for the Centaur guidance equipment, and for the Centaur electronic equipment during ascent. The insulation panels and the nose fairing are jettisoned during the Atlas sustainer phase. The Applications Technology Satellite 5 (ATS-5) spacecraft is shown in figure III-4.

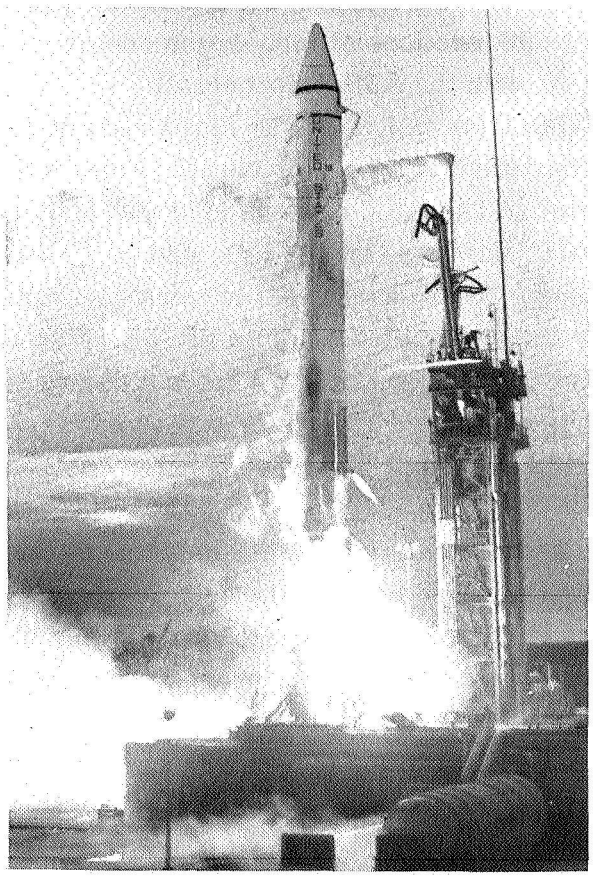

Figure III-1. - Atlas-Centaur lift off with ATS-5.

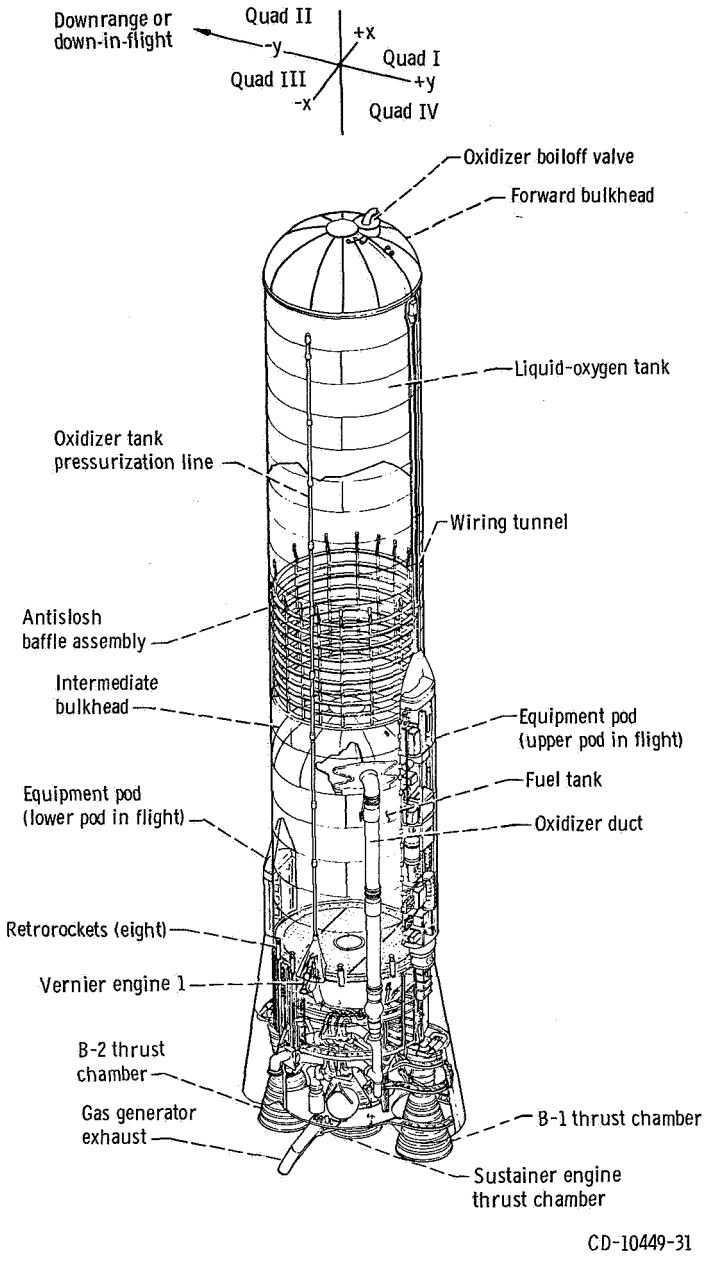

Figure III-2. - General arrangement of Atlas launch vehicle, AC-18.

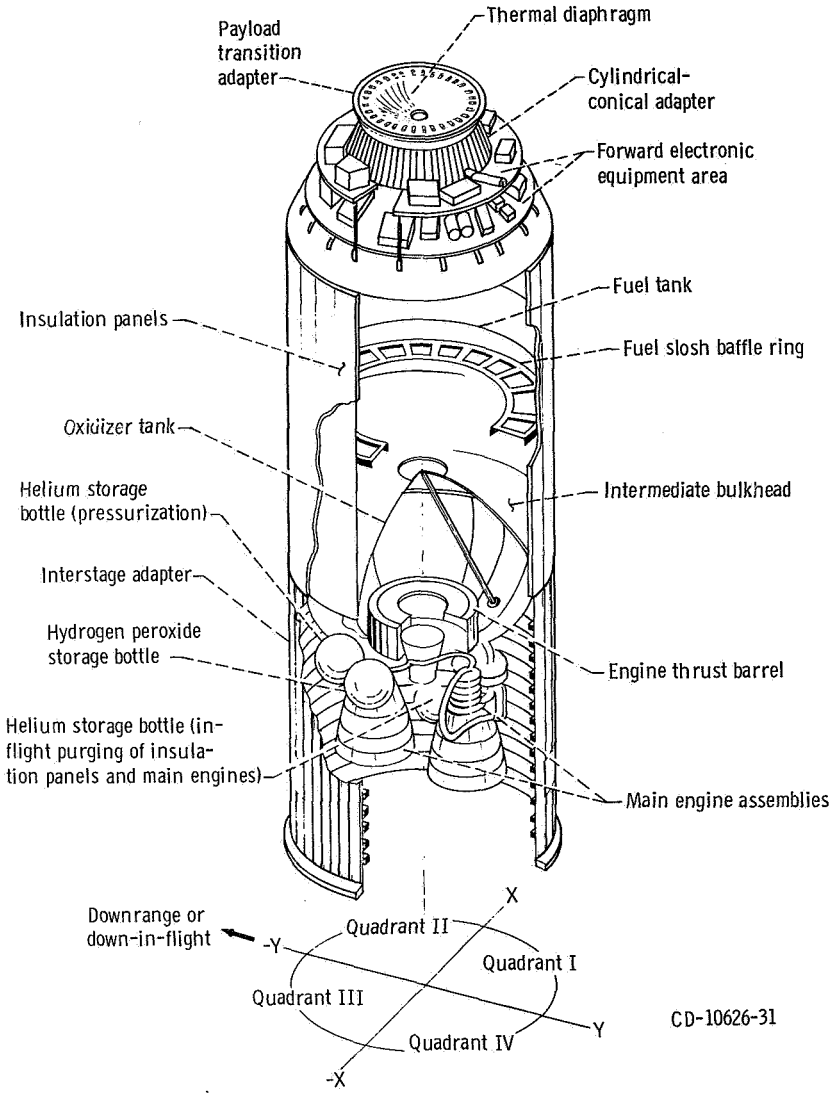

Figure III-3. - General arrangement of Centaur vehicle, AC-18.

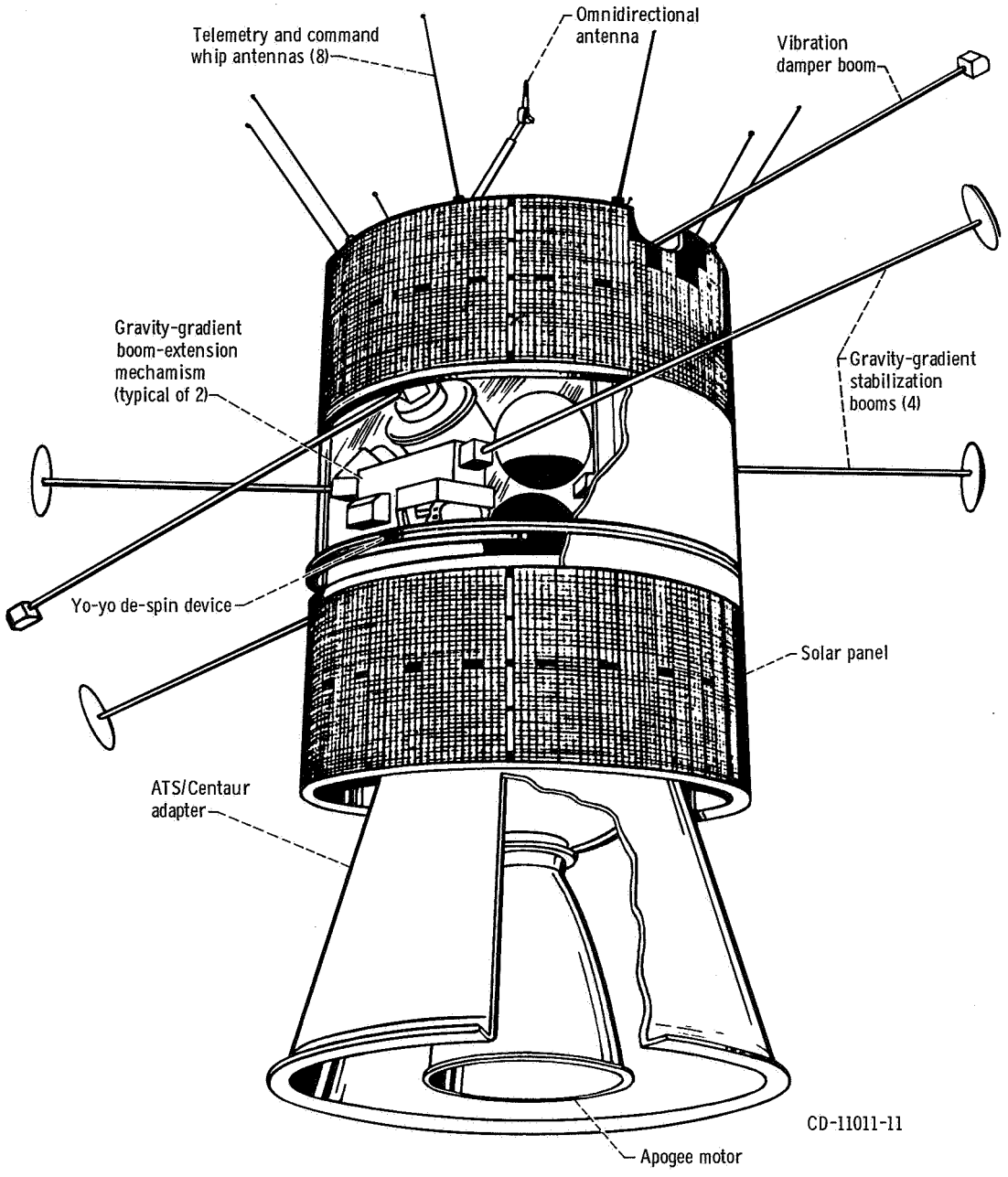

Figure III-4. - Configuration of Applications Technology Satellite, AST-5. (Spacecraft booms shown partially extended for illustrative purposes only; normal extension occurs after separation of adapter and apogee motor.)

IV. MISSION PERFORMANCE

by Roy K. Hackbarth

The Atlas-Centaur launch vehicle AC-18 with the Applications Technology Satellite 5 (ATS-5) was successfully launched from Eastern Test Range Complex 36A at 0601:04 hours e.s.t. on August 12, 1969. The ATS-5 was placed in the proper elliptical transfer orbit and all launch vehicle objectives were achieved. The ATS-5, through firing of its apogee motor, attained the desired nearly synchronous circular equatorial orbit. However, because of ATS-5 stability problems, gravity gradient stabilization was not attempted, and the ATS-5 remained on station in a spin-stabilized mode.

ATLAS FLIGHT PHASE

Ignition and thrust buildup of the Atlas engines were normal. The vehicle lifted off (T + 0 sec) with a combined vehicle weight of 147 048 kilograms (324 185 lbm) and a thrust-weight ratio of 1.2. Two seconds after lift-off, the Atlas began a programmed roll from the launch pad azimuth of 105° to the required flight azimuth of 97°. This flight azimuth was attained at T + 15 seconds and the vehicle then began a programmed pitchover maneuver which lasted through booster engine cutoff. For this period of flight, guidance was accomplished by pitch and yaw programs which had been selected and stored in the Centaur computer during launch countdown. The programs are selected on the basis of trajectory requirements and predicted structural loading determined from prelaunch upper-wind soundings.

Vehicle steady-state acceleration during the booster engine powered phase was according to the mission plan. The Centaur guidance system issued the booster engine cutoff signal when the vehicle acceleration reached 5.65 g's (specification is 5.70±0.113 g's). About 3 seconds later, at T + 154.9 seconds, the Atlas programmer issued the staging command to separate the booster engine section from the vehicle. Staging transients were small and were damped within 2 seconds.

Steering by the Centaur guidance system was initiated about 8 seconds after Atlas booster engine staging. At the start of guidance steering the vehicle was slightly off the steering vector by about 5° nose down. The guidance system corrected the attitude error and issued commands to continue pitchdown during the Atlas sustainer phase. The Centaur insulation panels were jettisoned at T + 196.5 seconds and the nose fairing was

jettisoned at T + 233.3 seconds. Vehicle angular rates resulting from the jettisoning of the insulation panels and nose fairing were small.

Sustainer and vernier engine system performance was satisfactory throughout the flight and cutoff occurred at T + 251.6 seconds from liquid-oxygen depletion, the planned mode. Vehicle acceleration just prior to sustainer engine cutoff was 1.86 g's. Coincident with sustainer engine cutoff, the guidance steering commands to the Atlas flight control system were disabled and the vehicle was in a free-flight mode. Also the Centaur main engines were driven towards center (null) to maintain clearance between the engines and the interstage adapter during Atlas/Centaur separation.

The Atlas/Centaur separation command was issued by the Atlas flight programmer at T + 253.6 seconds. A linear shaped charge cut the forward end of the interstage adapter, and eight retrorockets on the Atlas were fired to move the Atlas/interstage adapter away from the Centaur. The transients during separation were small and comparable to those experienced on similar flights. Proper clearances were maintained during separation.

CENTAUR FLIGHT PHASE

Centaur First Powered Phase

The main engine start sequence for the Centaur was initiated prior to sustainer engine cutoff with propellant boost pump start at T + 215.7 seconds. The required net positive suction pressure to prevent boost pump cavitation (during the near-zero-gravity period from sustainer engine cutoff to main engine start) was assured by increasing pressure in the propellant tanks. Eight seconds prior to main engine start, prestart valves were opened to permit liquid-hydrogen flow to chill the engine turbopumps. This chilldown ensures against cavitation of the main engine turbopumps. At T + 263.1 seconds the ignition command was issued. Rapid and uniform thrust buildup occurred and engine thrust increased to flight levels.

Inertial guidance steering for the Centaur stage was enabled 4 seconds after engine start command. At this time the Centaur attitude was about 2^{o} nose down and 16^{o} nose right relative to the guidance steering vector. These attitude differences were composed of small attitude errors induced during Atlas/Centaur staging, and a programmed yaw-left maneuver initiated at this time to reduce orbit inclination. These attitude differences were corrected in about 12 seconds. Vehicle performance throughout the first powered phase was normal.

Main engine shutdown was commanded by Centaur guidance at T + 639.0 seconds. Shutdown transients were similar to those experienced on past flights. The Centaur engine thrust duration was about 3.2 seconds shorter than predicted. On all other opera-

tional Centaur flights the thrust durations were longer than predicted. Starting with AC-18, the thrust and specific impulse values used in trajectory design were changed to more closely reflect actual performance on past flights. The new values reduced the differences between predicted and actual performance. However, additional flights will be required to determine the validity of the new values. The propellant utilization system performed satisfactorily and controlled the fuel and oxidizer flow rates to the engines.

Centaur Coast Phase

At main engine first cutoff, the Centaur/ATS-5 began a 25-minute orbital coast. The hydrogen peroxide thrusters provided attitude control throughout the coast period. During the first 15 minutes, the inertial guidance system provided attitude error information to the flight control system to aline the Centaur roll axis with the flightpath velocity vector. During the last 10 minutes, the inertial guidance system issued small incremental attitude changes to reorient the Centaur/ATS-5 to the desired attitude for Centaur second powered phase.

The coast phase control mode sequence started with firing of two of the four 222-newton (50-lbf) thrust engines at main engine cutoff. This thrust level provided a vehicle acceleration of 7×10^{-3} g's to suppress any disturbances of the liquids induced by main engine cutoff transients and to settle the residual propellants. After 76 seconds these two engines were commanded off and two of the 13.5-newton (3-lbf) thrust engines were commanded on. This provided a low-level acceleration to retain the propellants in a settled condition.

Forty seconds prior to main engine restart the thrust level was increased to 444 newtons (100 lbf) by again firing two of the 222-newton (50-lbf) thrust engines, and the two 13.5-newton (3-lbf) thrust engines were commanded off. The increased thrust level gave additional assurance of settled propellants for main engine second start. At the same time, the hydrogen tank pressure was increased by injecting helium gas into the ullage. Engine prestart valves were opened 17 seconds prior to engine start to allow liquid hydrogen to flow through and chill down the lines and engine components. Tank pressurization, thermal conditioning of the engines, and control of the propellants throughout the coast phase were satisfactory and supported restart of the main engines.

Centaur Second Powered Phase

The Centaur main engines restarted on command at T + 2143.1 seconds. At this same time, the 444-newton (100-lbf) thrust for propellant control was terminated, guid-

ance steering was inhibited, and the attitude control engines were enabled for a period of 20 seconds. (Attitude control and changes to timed events and guidance functions were incorporated on AC-18 to provide for spacecraft separation in the event the main engine failed to restart or premature engine shutdown occurred.) Four seconds after main engine restart, guidance steering was resumed to attain the velocity vector required for injection of Centaur/ATS-5 into the highly elliptical transfer orbit. At T + 2213.9 seconds the injection velocity vector was achieved and the guidance system issued the command for engine shutdown. The thrust duration was 70.8 seconds, 0.4 second shorter than predicted. All systems performed satisfactorily during the second powered phase. Orbital insertion occurred at an altitude of about 2658 kilometers (1435 n mi).

SPACECRAFT REORIENTATION AND SEPARATION

Coincident with main engine cutoff, the hydrogen vent valve was unlocked to permit reduction of tank pressure, and the oxidizer tank pressure was increased by injection of helium gas. This was done to prevent reversal of the bulkhead between the two tanks. Also two of the four 13.5-newton (3-lbf) thrust engines were commanded on to prevent venting of liquid hydrogen. At this same time the attitude control engines were commanded on and the guidance system generated steering vectors to reorient the Centaur and ATS-5 to the pointing vector required for later firing of the ATS-5 apogee motor. Ten seconds after main engine cutoff the hydrogen vent valve was locked and the two 13.5-newton (3-lbf) thrust engines were commanded off. Oxidizer tank pressurization was terminated 20 seconds later. Reorientation was essentially completed 90 seconds after main engine cutoff. The Centaur had turned through an angle of about 150°, resulting in a nose aft-down attitude.

After reorientation, ATS-5 separation was delayed about 45 seconds to attain minimum vehicle residual rates at separation. At T + 2349.0 seconds the Centaur issued the command for spacecraft separation. The spacecraft V-band explosive bolts were fired and separation springs separated the ATS-5 from Centaur. Residual angular rate of the Centaur just prior to separation was extremely small. The ATS-5 now trailed the Centaur in essentially the same orbit.

CENTAUR POST-SEPARATION MANEUVER

Six seconds after spacecraft separation the Centaur initiated a post-separation manmaneuver to increase its separation distance from ATS-5 and to alter the Centaur's orbit. A guidance pointing vector was issued at T + 2355.1 seconds and the Centaur pitched down toward the earth. The Centaur rotated through about 101° in the pitch plane, point-

ing about 50^{o} forward of the local vertical in the orbit plane. This direction would result in Centaur being in a higher energy orbit than ATS-5 after a Centaur thrust period.

At T + 2411.0 seconds, reorientation was completed and two 222-newton (50-lbf) thrust engines were commanded on for 8 seconds. These engines were then commanded off and two 13.5-newton (3-lbf) thrust engines were commanded on for a period of 100 seconds. At T + 2519.0 seconds the two engines were commanded off and the propellant discharge sequence was commanded. The Centaur main engines were gimbaled to aline the thrust vector with the guidance-generated steering vector. The engine prestart valves were opened and residual propellants were allowed to discharge through the engines. The thrust from the propellant discharge and the hydrogen peroxide engines provided the desired separation from ATS-5.

The post-separation maneuver was completed at T + 2769.0 seconds with closing of the engine prestart valves. At this same time, two of the 222-newton (50-lbf) thrust engines were commanded on to determine the amount of residual hydrogen peroxide. The engines fired for 49 seconds, indicating a residual of about 15.3 kilograms (33.3 lbm) of usable hydrogen peroxide. At T + 2819.1 seconds, all electrical power was removed from the Centaur system, except C-band and telemetry. The Centaur was then in a non-stabilized flight mode.

ATS-5 TRANSIT TO SYNCHRONOUS ORBIT

Immediately after separation from Centaur the ATS-5 was spun-up to about 95 rpm to provide spin stabilization until it reached its permanent earth station. During the $5\frac{1}{2}$-hour transit to synchronous altitude an excessive amount of control gas was required to control nutation. Consequently, the apogee motor was fired at the first apogee of the transfer orbit, rather than the second apogee as planned. The desired near-circular synchronous equatorial orbit was attained, thereby verifying that the Centaur provided proper orientation and satisfactory separation of ATS-5.

After apogee motor firing, nutation of the spin axis could not be adequately controlled and this caused ATS-5 to become spin stabilized about an undesired axis. During drift of ATS-5 to its permanent station, commands were issued in an attempt to correct the condition. The desired spin axis was reestablished; however, the direction of spin was reversed. De-spin of the spacecraft could not be accomplished from this reversed direction of spin. Consequently, extension of the booms, which were to provide gravity gradient stabilization, was not attempted.

V. TRAJECTORY AND PERFORMANCE

by John J. Nieberding

MISSION PLAN

The AC-18 mission plan required the Atlas-Centaur launch vehicle to inject the ATS-5 spacecraft in a highly elliptical transfer orbit (apogee near synchronous altitude) from which ATS-5 achieves near-synchronous circular orbit by firing its fixed-impulse apogee motor. The Atlas first places the Centaur/ATS-5 on a suborbital coast ellipse through two powered phases - a booster phase and a sustainer phase. After the Atlas' powered phases are complete, the Centaur/ATS-5 separates from Atlas and the Centaur first powered phase places the Centaur/ATS-5 into an elliptical parking orbit. This orbit has an apogee altitude of 5163 kilometers, a perigee altitude of 181 kilometers, and an orbital inclination of 26.76°. After injection into this parking orbit, the Centaur/ATS-5 coasts (for about 25 min) until it crosses the equator for the first time. At this time, the Centaur second powered phase accelerates the Centaur/ATS-5 from the parking orbit into a highly elliptical transfer orbit with an apogee altitude of about 37 000 kilometers and a perigee altitude of about 2100 kilometers and reduces the orbital inclination from 26.76° to 17.60°.

After Centaur main engine second cutoff, the Centaur executes a turning maneuver, mostly out of the orbital plane, of approximately 150°. This maneuver orients the spacecraft to the inertial attitude required at apogee of the transfer orbit. After this reorientation, the spacecraft separates from the Centaur. The Centaur then performs a post-separation maneuver by turning generally towards earth and then begins thrusting with the hydrogen peroxide engines and discharging residual propellants. This thrusting maneuver occurs with the Centaur's nose pointing about 50° forward of the local vertical in the direction of motion.

The spacecraft coasts in the transfer orbit for about 17 hours ($1\frac{1}{2}$ orbits) in a spin stabilization mode. This stabilization maintains the inertial attitude provided by the Centaur at spacecraft separation. A few minutes after reaching the second apogee of the transfer orbit, while crossing the equator, the spacecraft motor fires to accomplish the orbital plane change of 15.13° and to accelerate the spacecraft into the desired nearly circular final orbit. This orbit is inclined 2.47° to the equator. At spacecraft motor burnout, the spacecraft is at about 81° west longitude and 2° north latitude. From this position, it drifts at the rate of about 5° per day westward until it reaches the desired

longitude of 108° west, where it is commanded by ground control to assume a nearly stationary position. Figure V-1 illustrates the mission profile.

TRAJECTORY RESULTS

Lift-off Through Booster Phase of Atlas Flight

Actual wind conditions, as measured by a weather balloon sent aloft near the time of lift-off, are presented in figures V-2 and V-3. To minimize angle of attack, and hence aerodynamic structural loading, under these actual wind conditions throughout the booster phase of flight, pitch program PP31 and yaw program YP0 were selected.

Radar tracking and Centaur inertial guidance data indicated that the flightpath during the Atlas booster phase was very close to that predicted. The transonic region, the time span when the vehicle passes through Mach 1, occurred from about T + 60 to T + 65 seconds. During this period, the axial load factor (thrust acceleration in g's) was nearly constant (fig. V-4) because of high aerodynamic drag. Maximum dynamic pressure occurred at about T + 82.5 seconds. Atlas booster engine cutoff (BECO) occurred at T + 151.8 seconds, 1.1 seconds earlier than predicted, when the vehicle axial load factor reached 5.65. The axial load factor at BECO is designed to be 5.7±0.113. The altitude at BECO was about 2.9 kilometers (1.6 n mi) less than predicted, while the velocity was about 187 kilometers per hour (170 ft/sec) less than predicted. (See figs. V-5 to V-7.) These deviations were well within tolerances. Table V-I presents the predicted versus the actual sequence of events.

Atlas Sustainer Phase

An abrupt decrease in acceleration occurred at booster engine cutoff. This decrease is shown in figure V-4 and also in figure V-5, where a change in slope indicates a change in acceleration. A small increase in acceleration occurred at T + 154.9 seconds when the booster engine section, weighing 3351 kilograms (7389 lbm), was jettsoned. Atlas and Centaur weight summaries are presented in tables V-II and V-III. Following booster engine section jettison, the constantly decreasing vehicle propellant weight caused the axial acceleration to increase smoothly until sustainer and vernier engine cutoff occurred, at T + 251.6 seconds. However, small perturbations, resulting from jettisoning the 520-kilogram (1146-lbm) insulation panels at T + 196.5 seconds and the 970-kilogram (2138-lbm) nose fairing at T + 233.3 seconds, were noted during this period. Sustainer engine cutoff (SECO) occurred 2.9 seconds later than predicted. This

longer firing time is attributed to a greater quantity of propellant available for the sustainer phase because of the early BECO. At SECO the altitude was 3.3 kilometers (1.8 n mi) lower than expected, and the velocity was about 23 kilometers per hour (21 ft/sec) higher than expected, both well within tolerance.

Centaur Main Engine First Powered Phase and Coast Phase

Atlas/Centaur separation was timed to occur 1.9 seconds after SECO; Centaur main engine first start (MES-1) was timed for 11.5 seconds after SECO. Since SECO was late, these two events were also late. The increase in velocity and acceleration following Centaur main engine first start (at T + 263.1 sec) is shown in figures V-4 and V-5. Early in the Centaur first powered phase, a yaw maneuver to the left was performed to slightly reduce the parking orbit inclination. Main engine first cutoff occurred at T + 639.0 seconds.

During the latter portion of this powered phase, the actual acceleration was slightly higher than predicted (fig. V-4). As a result, the required cutoff energy and angular momentum were achieved with a Centaur thrust duration 3.2 seconds shorter than predicted.

AC-18 was the first Centaur flight whose predicted trajectory was biased to compensate for the Centaur low thrust and high specific impulse usually observed on Centaur flights. As a result, the Centaur's powered phase was not longer than predicted as had been the case on previous flights.

At Centaur main engine first cutoff, the 25-minute coast phase began with two 222-newton (50-lbf) thrust hydrogen peroxide engines programmed on for 76 seconds to settle the Centaur propellants. The actual and predicted parking orbit parameters which are compared in table V-IV, include the effect of the two 222-newton thrust engines. At T + 715 seconds the 222-newton (50-lbf) thrust engines were programmed off and two 13.3-newton (3-lbf) thrust hydrogen engines were programmed on for propellant retention. About 600 seconds prior to main engine second start the Centaur began to reorient to the attitude required for the second powered phase. At 41 seconds prior to main second start the 13.3-newton (3-lbf) thrust engines were programmed off and the 222-newton (50-lbf) thrust engines were programmed on to settle the propellants for Centaur main engine second start.

Centaur Main Engine Second Powered Phase

At T + 2143.1 seconds the Centaur engines restarted and thrusted for 70.8 seconds, 0.4 seconds less than predicted. At restart, the vehicle had just crossed the equator for

the first time. At second cutoff, the Centaur began to reorient, through an angle of about 150^{o}, to the attitude required for spacecraft separation. This attitude was then inertially maintained until spacecraft apogee motor firing. The spacecraft separated from Centaur at T + 2349.0 seconds. The transfer orbit of the spacecraft is described in table V-V.

Centaur Post-Separation Maneuver

At T + 2355.1 seconds the Centaur began its post-separation maneuver, whereby it turned (approximately 101^{o}) generally towards earth and then began thrusting with the hydrogen peroxide engines and the expulsion of residual propellants. This thrusting maneuver, which occurred with the Centaur's nose pointing about 50^{o} forward of the local vertical in the direction of motion, added energy to the orbit. This resulted in a higher apogee altitude than that of the spacecraft. The resulting Centaur orbit is described in table V-VI.

The mission plan was for the spacecraft to coast in the transfer orbit for $1\frac{1}{2}$ orbits (17 hr) and to fire its apogee motor near the second apogee of the transfer orbit. However, due to spacecraft stability problems, the apogee motor was fired at first apogee, after the spacecraft had traversed only one-half of the transfer orbit (about $5\frac{1}{2}$ hr). The resulting ATS-5 final orbit is described in table V-VII.

TABLE V-I. - FLIGHT EVENTS RECORD, AC-18

Event	Programmed time, sec	Predicted time, sec	Actual time, sec
Lift-off	T + 0.0	T + 0.0	T + 0.0
Booster engine cutoff	BECO	T + 152.9	T + 151.8
Booster jettison	BECO + 3.1	T + 156.0	T + 154.9
Insulation panel jettison	BECO + 45	T + 197.9	T + 196.5
Nose fairing jettison	BECO + 82	T + 234.9	T + 233.3
Sustainer engine cutoff; start Centaur programmer	SECO	T + 248.9	T + 251.6
Atlas/Centaur separation	SECO + 1.9	T + 250.8	T + 253.6
Centaur main engine first start	SECO + 11.5	T + 260.4	T + 263.1
Centaur main engine first cutoff; start propellant settling engines	MECO-1	T + 639.5	T + 639.0
Stop propellant settling engines; start propellant retention engines	MECO-1 + 76	T + 715.5	T + 715.0
Start reorientation for Centaur second start	MES-2 - 600	T + 1541.0	T + 1541.0
Stop propellant retention engines; start propellant settling engines	MES-2 - 40	T + 2101.0	T + 2102.1
Centaur main engine second start; stop propellant settling engines	MES-2	T + 2141.0	T + 2143.1
Centaur main engine second cutoff; start propellent settling engines; start alining Centaur roll axis to spacecraft separation vector	MECO-2	T + 2212.2	T + 2213.9
Stop propellant settling engines	MECO-2 + 10.0	T + 2222.2	T + 2223.9
Separate spacecraft	MECO-2 + 135.0	T + 2347.2	T + 2349.0
Start alining Centaur roll axis for post-separation maneuver	MECO-2 + 140.0	T + 2352.2	T + 2355.1
Start propellant settling engines	MECO-2 + 197.0	T + 2409.2	T + 2411.0
Stop propellant settling engines; start propellant retention engines	MECO-2 + 205.0	T + 2417.2	T + 2419.0
Stop propellant retention engines; start Centaur "blowdown"	MECO-2 + 305.0	T + 2517.2	T + 2519.0
Stop Centaur "blowdown"	MECO-2 + 555.0	T + 2767.2	T + 2769.0
Electrical system turn-off	MECO-2 + 605.0	T + 2817.2	T + 2819.1

TABLE V-II. - CENTAUR WEIGHTS SUMMARY, AC-18

Component	Weight	
	kg	lbm
Basic hardware:		
Body	525	1 158
Propulsion group	509	1 122
Guidance group	152	335
Fluid systems group	129	285
Electrical group	130	286
Separation group	35	78
Basic flight instrumentation	109	240
Mission peculiar equipment	122	269
Total	1 711	3 773
Jettisonable hardware:		
Nose fairing	970	2 138
Insulation panels	520	1 146
Ablated ice	23	50
Total	1 513	3 334
Centaur residuals at MECO-2:		
Liquid hydrogen	24	54
Liquid oxygen	143	315
Gaseous hydrogen	28	62
Gaseous oxygen	79	174
Hydrogen peroxide	24	53
Helium	2	5
Ice	5	12
Total	305	675
Centaur expendables:		
Main impulse hydrogen	2 258	4 977
Main impulse oxygen	11 204	24 701
Gas boiloff on ground, hydrogen	7	15
Gas boiloff on ground, oxygen	0	0
In-flight chill hydrogen	32	71
In-flight chill oxygen	46	102
Booster-phase vent hydrogen	24	53
Booster-phase vent oxygen	30	66
Sustainer-phase vent hydrogen	14	30
Sustainer-phase vent oxygen	27	60
Engine shutdown loss hydrogen:		
First shutdown loss	3	6
Second shutdown loss	3	6
Engine shutdown loss oxygen:		
First shutdown loss	6	13
Second shutdown loss	6	13
Parking-orbit vent hydrogen	2	5
Parking-orbit vent oxygen	0	0
Parking-orbit leakage hydrogen	1	1
Parking-orbit leakage oxygen	1	2
Hydrogen peroxide	83	183
Helium	2	5
Total	13 749	30 309
Total tanked weight	17 278	38 091
Minus ground boiloff	7	15
Total Centaur weight at lift-off	17 271	38 076

TABLE V-III. - ATLAS WEIGHT SUMMARY, AC-18

Component	Weight	
	kg	lbm
Booster jettison weight:		
Booster dry weight	2 863	6 312
Booster residuals	472	1 041
Unburned lubrication oil	16	36
Total	3 351	7 389
Sustainer jettison weight:		
Sustainer dry weight	2 720	5 996
Sustainer residuals (above and below pump inlets)	433	954
Interstage adapter	477	1 051
Unburned lubrication oil	8	17
Total	3 638	8 018
Flight expendables:		
Main impulse RP-1	37 738	83 199
Main impulse oxygen	83 878	184 919
Helium-panel purge	2	5
Oxygen vent loss	7	15
Lubrication oil	84	186
Oxygen boiloff - booster phase	134	296
Oxygen boiloff - sustainer phase	81	178
Total	121 924	268 798
Ground expendables:		
Fuel	239	526
Oxidizer	807	1 780
Lubrication oil	1	3
Exterior ice	24	54
Liquid nitrogen in helium shrouds	113	250
Preignition gaseous oxygen loss	204	450
Total	1 388	3 063
Total tanked weight	130 301	287 268
Minus ground expendables	1 388	3 063
Total Atlas weight at lift-off	128 913	284 205
Spacecraft weight	864	1 904
Total Atlas/Centaur/spacecraft lift-off weight	147 048	324 185

TABLE V-IV. - PARKING ORBIT PARAMETERS, AC-18

Parameter	Units	Predicted value[a]	Actual value[b]
Epoch	sec	T + 715.543	T + 720.9
Perigee altitude	km	180.6	180.8
	n mi	97.5	97.6
Apogee altitude	km	5163.0	5158.4
	n mi	2787.8	2785.3
Semimajor axis	km	9050.0	9047.8
	n mi	4886.6	4885.4
Eccentricity	----	0.275268	0.27508
Inclination	deg	26.760	26.785
Period	min	142.8	142.7
Energy, C_3	km^2/sec^2	-44.04	-44.07
	ft^2/sec^2	-4.740426×10^8	-4.743656×10^8

[a]Based on preflight trajectory from the AC-18 firing tables.
[b]Based on Centaur guidance telemetry.

TABLE V-V. - TRANSFER ORBIT PARAMETERS, AC-18

Parameter	Units	Predicted value	Actual value
Epoch	sec	T + 2347.2	T + 2349.0
Perigee altitude	km	2147.8	2147.2
	n mi	1159.7	1159.4
Apogee altitude	km	36 661.3	36 645.6
	n mi	19 795.5	19 787.2
Semimajor axis	km	25 782.8	25 774.6
	n mi	13 921.6	13 917.2
Eccentricity	----	0.66928	0.66924
Inclination	deg	17.604	17.600
Period	min	686.6	686.4
Energy, C_3	km^2/sec^2	-15.461	-15.473
	ft^2/sec^2	-1.664208×10^8	-1.665499×10^8

TABLE V-VI. - CENTAUR ORBITAL PARAMETERS AFTER POST-SEPARATION MANEUVER

Parameter	Units	Predicted value	Actual value[a]
Epoch	sec	T + 2817.2	T + 2852.0
Perigee altitude	km	2176	2187
	n mi	1175	1181
Apogee altitude	km	37 294	37 471
	n mi	20 137	20 233
Semimajor axis	km	26 113	26 208
	n mi	14 100	14 151
Eccentricity	----	0.67240	0.67316
Inclination	deg	17.60	17.59
Period	min	699.9	703.7
Energy, C_3	km^2/sec^2	-15.264	-15.209
	ft^2/sec^2	-1.64306390×10^8	-1.63712047×10^8

[a]Based on ETR tracking data.

TABLE V-VII. - SPACECRAFT FINAL ORBIT PARAMETERS, ATS-5[a]

Parameter	Units	Predicted value	Actual value
Epoch	sec	T + 63 555.0	T+25 140.0
Semimajor axis	km	42 561	42 627
	n mi	22 981	23 071
Eccentricity	----	0.009356	0.013150
Inclination	deg	2.467	2.617
Right ascension of ascending node	deg	(b)	276.1
Perigee altitude	km	35 786	35 784
	n mi	19 323	19 322
Apogee altitude	km	36 582	36 908
	n mi	19 753	19 929

[a]These parameters are presented for information only. They are not a measure of the launch vehicle accuracy since the spacecraft supplied significant velocity to itself during the transfer orbit and since the spacecraft apogee motor fired at first apogee instead of the second apogee as planned.

[b]Launch-time dependent, therefore, not predicted.

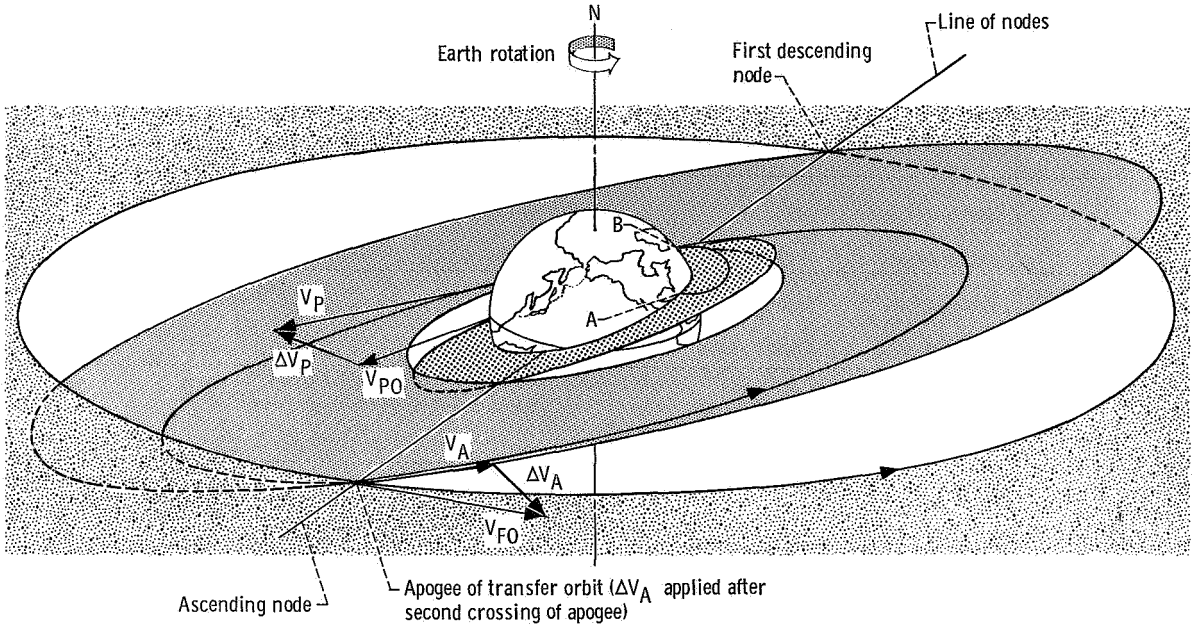

V_P transfer orbit perigee velocity
ΔV_P Centaur second-powered-phase velocity increment
V_{PO} velocity in parking orbit
V_A transfer orbit apogee velocity
ΔV_A apogee-motor-firing velocity increment
V_{FO} velocity in final orbit

Parking orbit plane
Transfer orbit plane
Stationary orbit plane

Figure V-1. - Planned flight profile, AC-18.

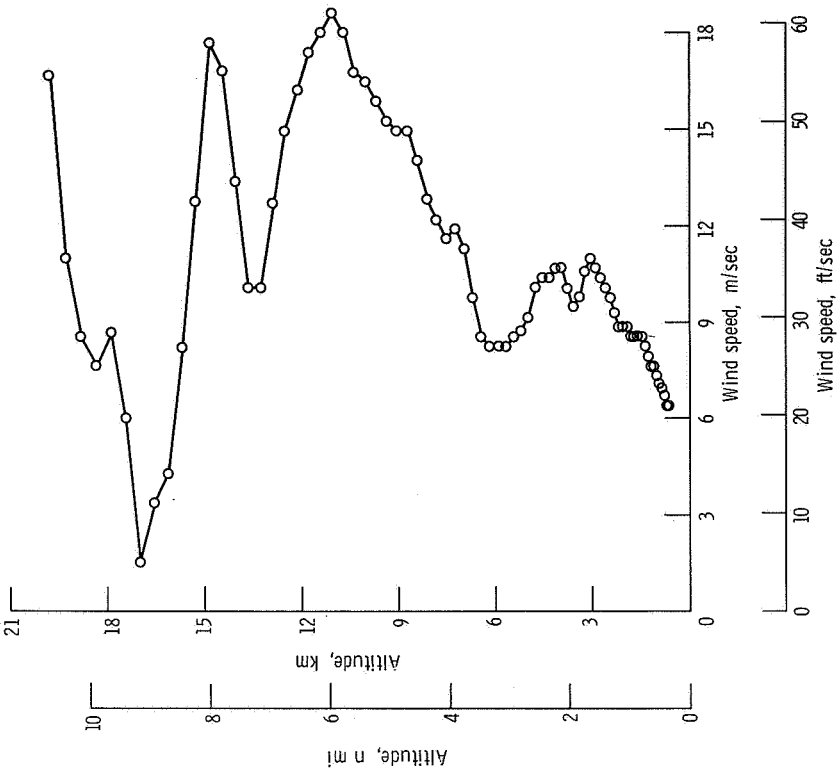

Figure V-3. - Altitude as function of wind speed, AC-18.

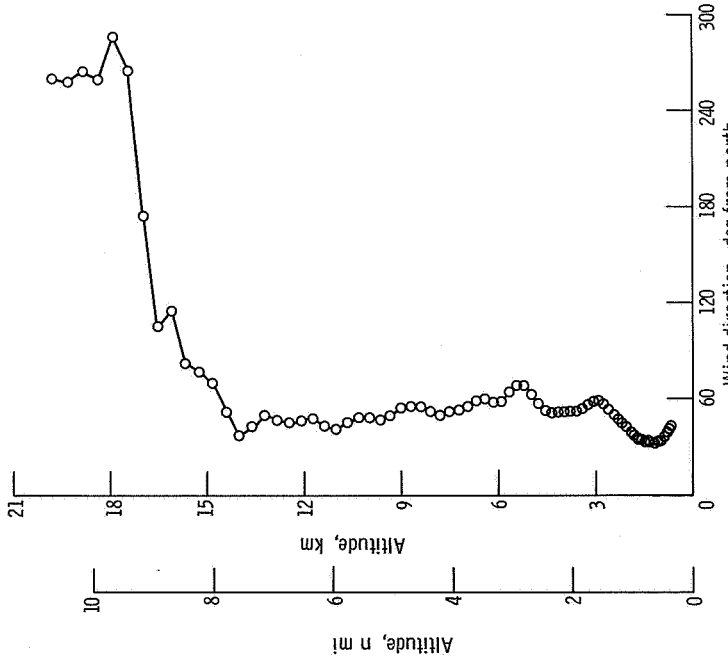

Figure V-2. - Altitude as function of wind direction, AC-18.

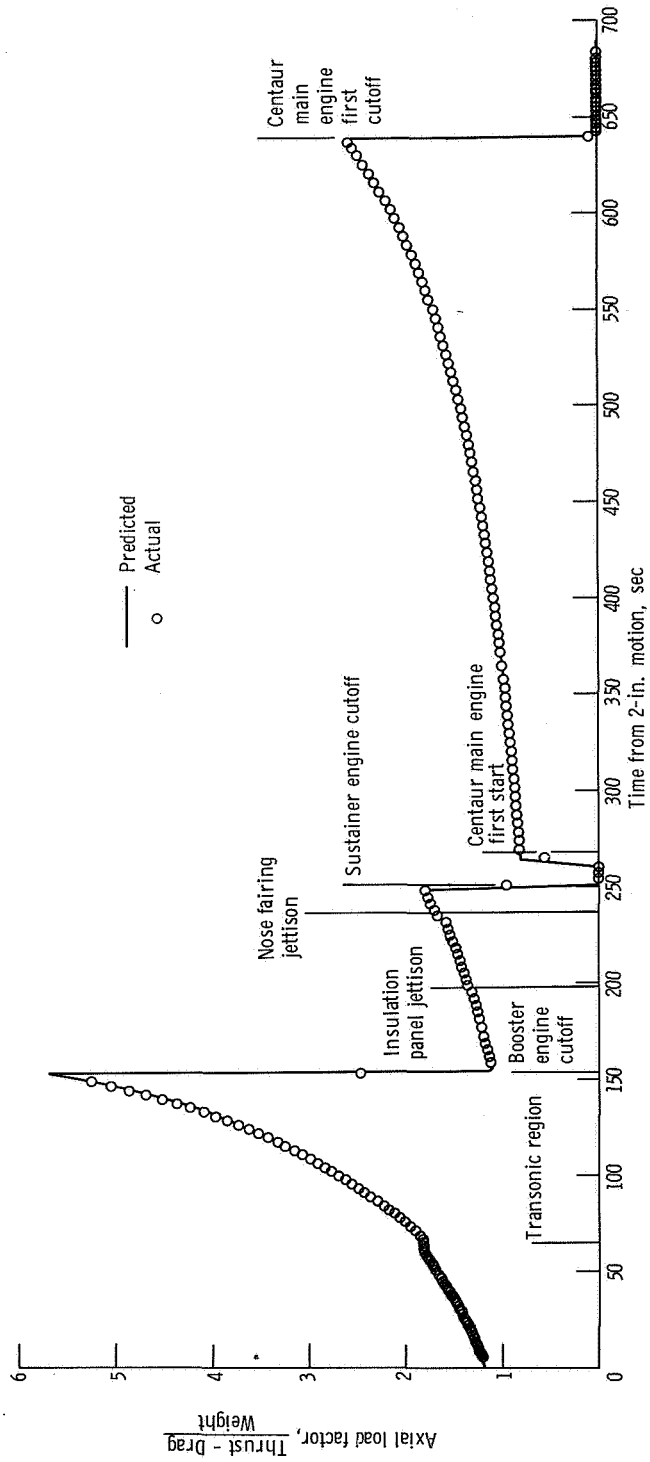

Figure V-4. - Axial load factor as function of time, AC-18.

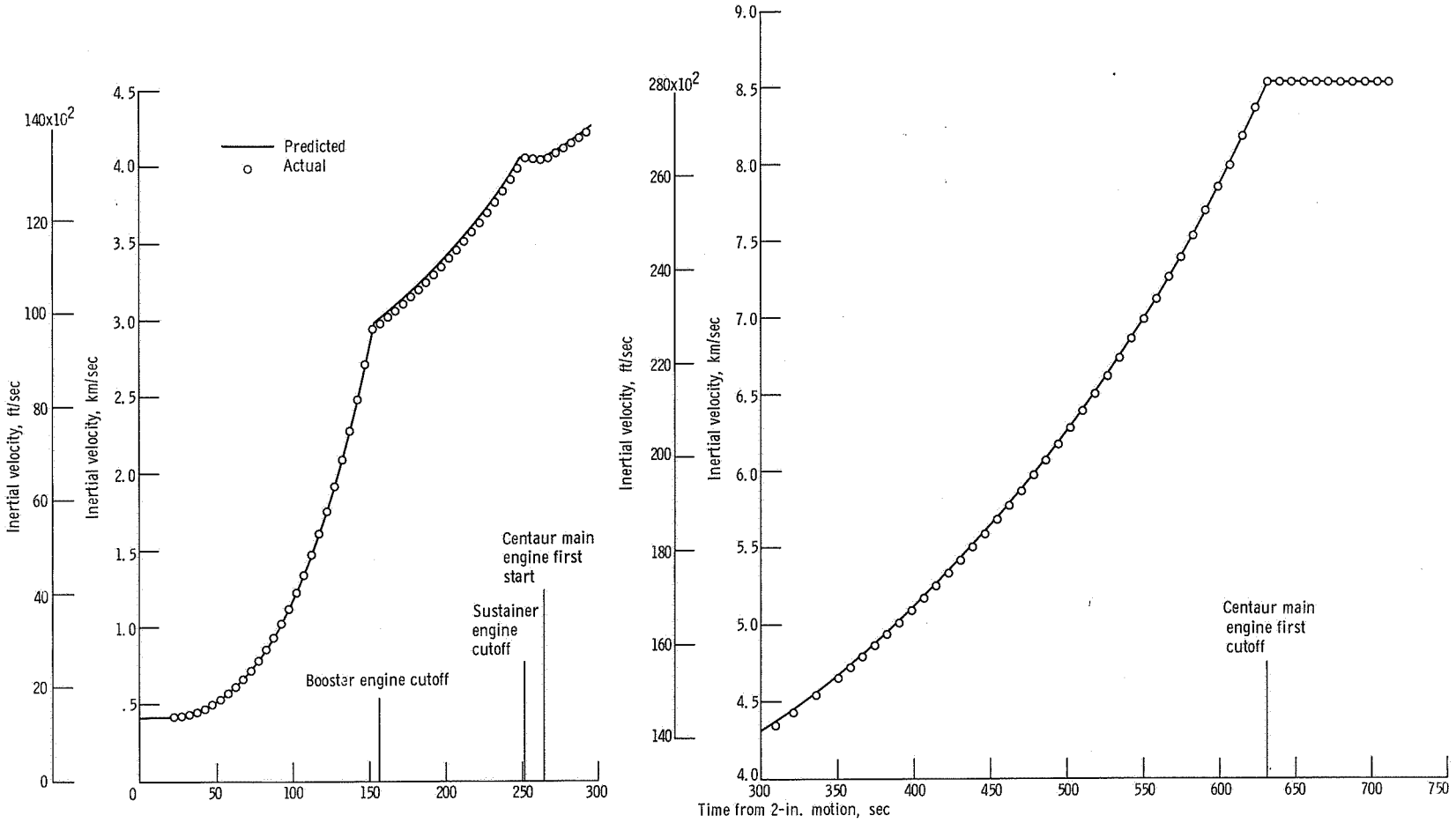

Figure V-5. - Inertial velocity as function of time, AC-18.

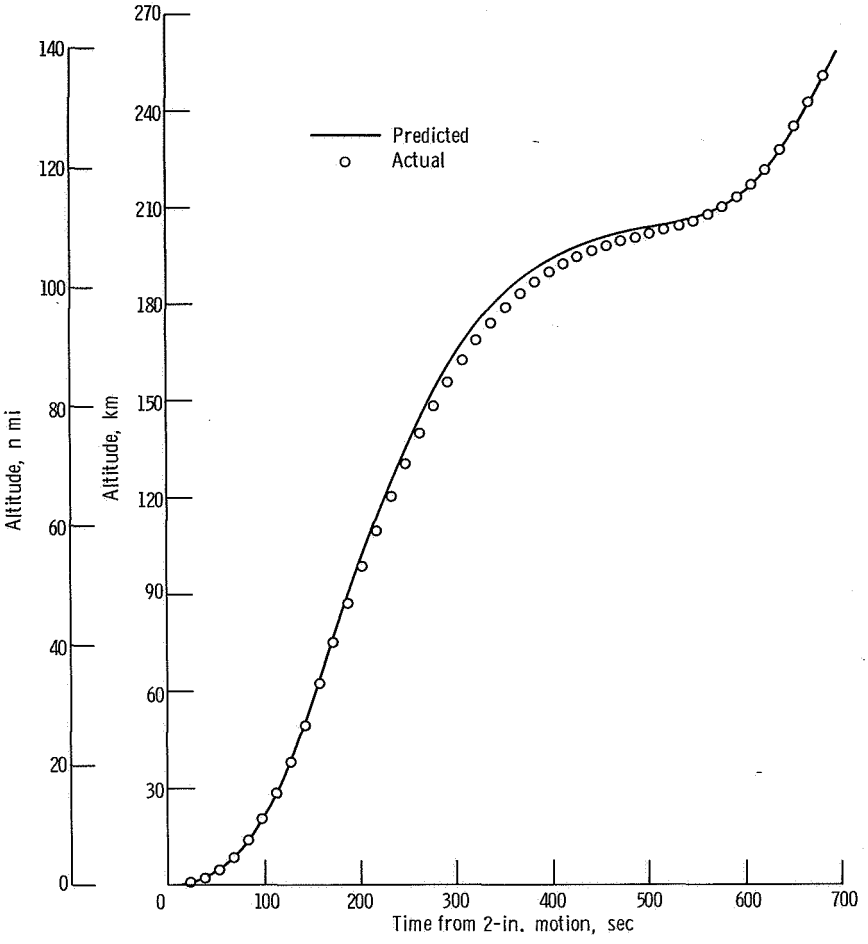

Figure V-6. - Altitude as function of time, AC-18.

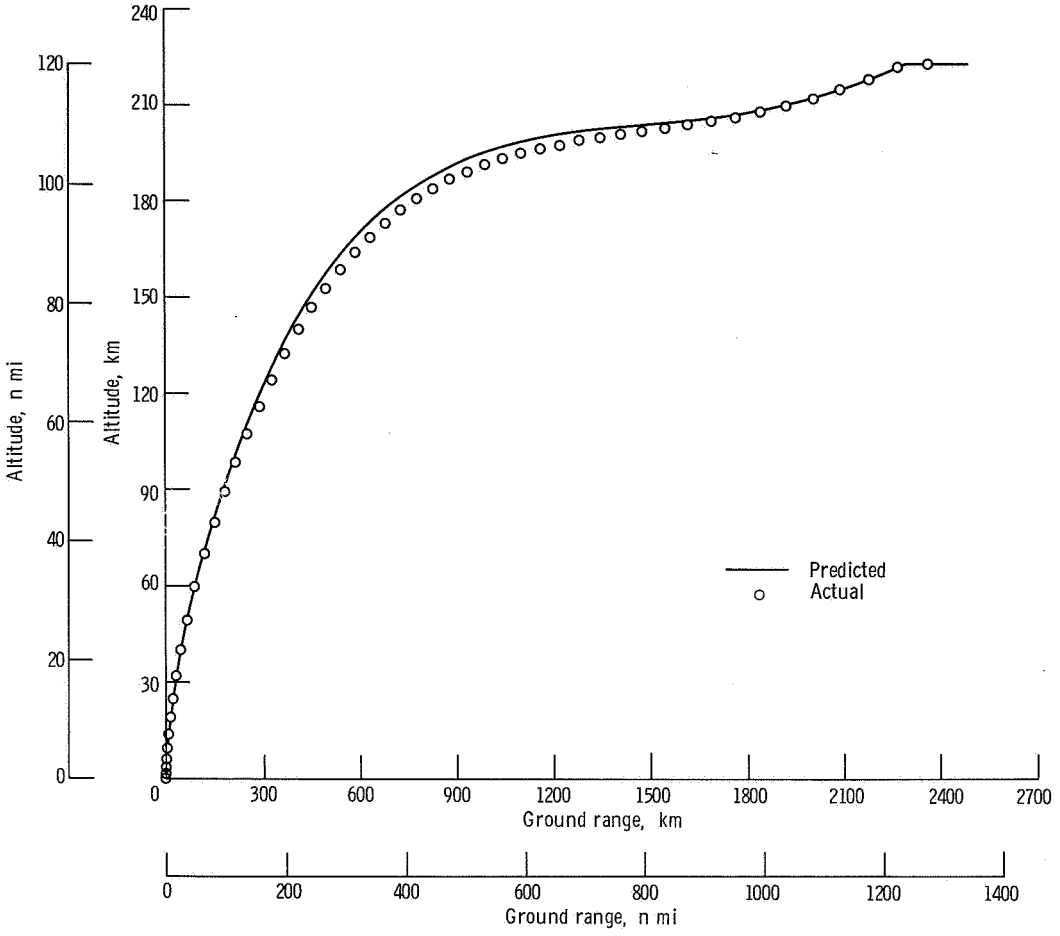

Figure V-7. - Altitude as function of ground range, AC-18.

VI. LAUNCH VEHICLE SYSTEM ANALYSIS

PROPULSION SYSTEMS

by Charles H. Kerrigan and Donald B. Zelten

Atlas Engines

System description. - The Atlas engine system (fig. VI-1) consists of a booster engine, a sustainer engine, two vernier engines, an engine start tank system, and an electrical control system. The engines use liquid oxygen and RP-1 (kerosene) for propellants. During engine start, electrically fired pyrotechnic igniters are used to ignite the gas generator propellants for driving the turbopumps; and hypergolic igniters are used to ignite the propellants in the thrust chambers of the booster, sustainer, and vernier engines. The pneumatic control of the engine system is discussed in a following section PNEUMATIC SYSTEMS.

The booster engine, rated at 1494×10^3 newtons (336×10^3 lbf) thrust at sea level, consists of two gimbaled thrust chambers, propellant valves, two oxidizer and two fuel turbopumps driven by one gas generator, a lubricating oil system, and a heat exchanger. The sustainer engine, rated at 258×10^3 newtons (58×10^3 lbf) thrust at sea level, consists of a thrust chamber, propellant valves, one oxidizer and one fuel turbopump driven by a gas generator, and a lubricating oil system. The entire sustainer engine system gimbals. Each vernier engine is rated at 2.98×10^3 newtons (670 lbf) thrust at sea level, and propellants are supplied from the sustainer turbopump. The vernier engines gimbal for roll control.

The engine-start-tank system consists of two spherical helium-pressurized propellant tanks for liquid oxygen and RP-1 (kerosene), each approximately 51 centimeters (20 in.) in diameter. This system supplies starting propellants (oxidizer and fuel) for the gas generators and the vernier engines, and fuel only for the booster and sustainer engines for a period of approximately 2 seconds; thereafter the turbopumps provide the propellants to sustain the engines.

System performance. - The performance of the Atlas propulsion system was satisfactory. During the engine start phase, valve opening times and starting sequence events were within tolerances. The flight performance of the engines was evaluated by comparing measured parameters with the expected values. These are tabulated in table VI-I. Booster engine cutoff occurred at T + 151.8 seconds when the axial acceleration reached

5.65 g's. Sustainer engine cutoff and vernier engine cutoff were due to liquid-oxygen depletion, the planned shutdown mode, and occurred at T + 251.6 seconds. Transients were normal during shutdown of all engines.

After booster engine cutoff, thrust chamber pressure data for both vernier engines showed gradual, and sometimes erratic, decreases from expected operating values. However, these low pressure indications were not substantiated by the number 1 vernier engine liquid-oxygen inlet pressure, which was satisfactory. Since the propellants for both vernier engines are supplied from the same source, the vernier engine operation is considered to be satisfactory. The erratic behavior of the chamber pressure data probably resulted from a buildup of carbon in the instrumentation sense port. This behavior has occurred on several previous flights.

Centaur Main Engines

System description. - The Centaur main engine system (see engine system schematic, fig. VI-2) consists of two engines identified as C-1 and C-2. Each engine is gimbal mounted and has its own oxidizer and fuel turbopump, thrust chamber, solenoid control valves, propellant valves, and spark igniter system. The engines are capable of making multiple starts after long coast periods in space. Propellants are liquid oxygen and liquid hydrogen. The rated thrust of each engine is 66 700 newtons (15 000 lbf) at an altitude of 61 000 meters (200 000 ft).

These engines operate by the "topping cycle" principle: pumped fuel, after circulating through the thrust chamber tubes, is expanded through a turbine which drives the propellant pumps. This routing of fuel through the thrust chamber tubes serves the dual purpose of cooling the thrust chamber walls and of adding energy to the fuel (hydrogen) prior to expansion through the turbine. After passing through the turbine, the fuel is injected into the combustion chamber. The pumped oxidizer is supplied directly to the combustion chamber after passing through the propellant utilization (mixture ratio control) valve.

Pneumatically operated valves start and stop propellant flow to the engines. Helium pressure to these valves is supplied through engine-mounted solenoid valves which are controlled by electrical signals from the vehicle control system. Ignition is accomplished by means of a spark igniter recessed in the propellant injector face. The thrust level is maintained by regulating the amount of fuel bypassed around the turbine as a function of combustion chamber pressure.

An additional pressure transducer was installed in the C-2 engine to investigate lower-than-expected thrust chamber pressure values noted during several previous Centaur flights. The range of this transducer was 252 to 286 newtons per square centimeter (365 to 415 psia); the regular transducer range is 0 to 345 newtons per square

centimeter (0 to 500 psia). Special instrumentation was also added to the C-2 engine thrust controller to determine skin temperature, body cavity pressure, and vibration levels. This instrumentation was to aid in determining if low thrust chamber pressure is related to operation of the thrust controller, as chamber pressure is the parameter most directly affected by the thrust controller.

System performance - main engine first powered phase. - The main engine prestart signal was issued as programmed, 8 seconds prior to the engine start signal. During this period the turbopumps were prechilled by allowing oxidizer and fuel to flow through the turbopumps and to discharge overboard. Turbopump surface temperature data indicated the prechill was satisfactory. Propellant pressures and temperatures at the pump inlets were satisfactory during the prestart period. Main engine first start was commanded at T + 263.1 seconds. The start transients were normal. Steady-state operating performance of the engine was satisfactory and was evaluated by comparing measured parameters with expected values. These data are tabulated in table VI-II. The signal for main engine cutoff was generated by the guidance system and occurred at T + 639 seconds. Engine shutdown sequences were normal.

System performance - main engine second powered phase. - The coast period between main engine powered phases was 25 minutes, as planned. Turbopump prechill duration for the main engine second start sequence was 17 seconds as planned. A satisfactory prechill was achieved, and main engine second start was commanded at T + 2143.1 seconds. Engine start transients, steady-state operation, and shutdown sequences were satisfactory. Main engine cutoff was commanded by the guidance system at T + 2213.9 seconds. Performance values are tabulated in table VI-II. The propellant blowdown to provide thrust for the post-separation maneuver started at T + 2519 seconds and ended upon command at T + 2769 seconds. This was performed by opening the pump inlet valves, which allowed propellants remaining in the tanks to discharge through the main engines.

Special instrumentation. - The special instrumentation installed to investigate low thrust chamber pressure (see system description for details) produced data that compared favorably with normal and expected engine operating values.

Centaur Boost Pumps

System description. - A boost pump is used in each propellant tank to supply propellants to the main engine turbopumps at the required inlet pressures. Each boost pump is a mixed-flow centrifugal type and is powered by a hot-gas-driven turbine. The hot gas consists of superheated steam and oxygen from the catalytic decomposition of 90-percent-concentration hydrogen peroxide. Constant power is maintained on each turbine by metering the hydrogen peroxide through fixed-area orifices upstream of the

catalyst bed. A speed control system is provided on each turbine.

The configuration of the boost pumps and turbine drives on AC-18 is similar to that of AC-17, the preceding two-Centaur-powered-phase vehicle, except that the turbine speed control system was disabled on AC-18 by disconnecting the electrical harness at the overspeed valve. In addition, the plastic seats in the overspeed valves were removed to preclude any possibility of the seats obstructing the flow of hydrogen peroxide through the valve. The complete boost pump and hydrogen peroxide supply systems are shown in figures VI-3 to VI-6.

System performance. - Performance of the boost pumps was satisfactory for both operating periods. Performance data at selected times during boost pump operation are presented in tables VI-III and VI-IV. The boost pumps were started 47.4 seconds prior to main engine first start and continued to operate until main engine first cutoff at T + 639 seconds. The boost pumps were restarted 28 seconds prior to main engine second start and continued to operate until main engine cutoff at T + 2213.9 seconds. The turbine inlet pressure delay times (time from boost pump start signal to time of first indication of turbine inlet pressure rise) were less than 1 second for each start. Expected and actual steady-state performance data are shown in table VI-V for both operating periods. Differences between the ground test data and the flight data were within the accuracy tolerances of the instrumentation and telemetry systems.

Hydrogen Peroxide Engine and Supply System

System description. - The hydrogen peroxide engine and supply system (figs. VI-6 and VI-7) consists of 14 thruster engines, a supply bottle, and interconnecting tubing to the engines and boost pump turbines. The engines are primarily used during the nonpowered portions of the flight. Four 222-newton (50-lbf) thrust engines and four 13-newton (3-lbf) thrust engines are used primarily for propellant settling and retention and for the post-separation maneuver. Two clusters of three engines each are used for attitude control. Each cluster consists of two 16-newton (3.5-lbf) thrust engines and one 27-newton (6-lbf) thrust engine. Modes of operation are given in table VI-XVI, GUIDANCE AND FLIGHT CONTROL SYSTEMS section. Propellant is supplied to the engines from a positive-expulsion, bladder-type storage tank pressurized with helium to an absolute pressure of about 210 N/cm^2 (305 psi) by the pneumatic system. The hydrogen peroxide is decomposed in engine catalyst beds, and the hot gases are expanded through nozzles to provide thrust. Hydrogen peroxide is also used to drive the boost pump turbines. The hydrogen peroxide supply lines are equipped with heaters to maintain line temperatures between 278 and 322 K (40° and 120° F).

Vehicle configuration changes, from the previous two-powered-phase vehicle

(AC-17), were made as a result of suspected cryogenic leakage during the AC-17 flight. The leakage was believed to have frozen the hydrogen peroxide in a line and thereby prevented flow to the boost pumps. The boost pump hydrogen peroxide feedlines were rerouted to avoid areas of potential cryogenic leakage. A helium purge was added to the boost pump hydrogen peroxide feedlines to purge the lines of residual peroxide when the pumps were not operating. Openings in the liquid-oxygen-tank radiation shield in the vicinity of the hydrogen peroxide bottle and feedlines were covered. Cryogenic leak deflector shields and collector rings were installed in potential leak areas (fig. VI-7). Extensive instrumentation was added to monitor temperatures throughout the system (fig. VI-8 and table VI-VI). In addition to these changes, a single-bottle, instead of dual-bottle, hydrogen peroxide system was used because the hydrogen peroxide requirements for AC-18 were not as great as those for AC-17.

System performance. - The hydrogen peroxide engine and supply system performed satisfactorily. System temperature data are tabulated for various time periods of the flight in table VI-VII. All the data appeared normal, except for measurement CP361T. Separate discussion on this measurement is provided at the end of this section.

A hydrogen peroxide engine firing was performed after the post-separation maneuver to determine the hydrogen peroxide residuals. These data are useful in estimating propellant consumption rates. The 222-newton (50-lbf) thrust engines were fired in the V-half-on mode. These engines fired for approximately 49 seconds before the peroxide supply was depleted. Preflight estimate of the firing time, which was based on the estimated consumption rates at nominal engine firing duty cycles, was 36 seconds. Review of the engine firing times during the flight did not indicate any abnormally low duty cycles. Therefore the reason for the excess peroxide residual at the end of the mission is not known.

Temperature measurement CP361T analysis. - Measurement CP361T was located on the hydrogen peroxide feedline near the overspeed valve on the hydrogen boost pump. A plot of this measurement, along with the corresponding measurement (CP352T) on the line to the oxygen boost pump, is shown in figures VI-9(a) and (b). Immediately after lift-off, both these temperatures decreased normally due to termination of the warm-gas conditioning supply to the Centaur thrust section. At boost pump first start the temperatures increased rapidly as the relatively warmer hydrogen peroxide from the supply bottle flowed through the lines. During boost pump operation, measurement CP352T leveled out near the temperature of the hydrogen peroxide in the supply bottle. Measurement CP361T was expected to follow a similar trend, but instead continued to rise throughout boost pump first operation. A possible explanation of this increase is that CP361T had a better "view" of the hot liquid-hydrogen boost pump turbine than CP352T had of the oxygen boost pump turbine. Therefore, the effects of radiation from the hot turbines would be more pronounced on CP361T. Another possible explanation is the turbine exhaust gases and/or a hot gas leak in the turbine contributed to the heating of the

line to the hydrogen boost pump. At main engine first cutoff, measurement CP352T showed a pronounced increase, which was expected. It was caused by the termination of flow of the relatively cool hydrogen peroxide and by radiative heating from the hot turbine. At this same time period, measurement CP361T began to decrease. The reason for this is not clear. If we assume that the increase in temperature during boost pump operation was caused by radiation from the hot turbine, then with the termination of the flow of the relatively cool peroxide at main engine cutoff, an immediate increase in temperature would be expected; and this did not occur. If we assume that the heating during boost pump operation was caused by turbine exhaust gas and/or hot gas leakage, the temperature drop at main engine cutoff would be expected but then the increase in temperature starting at T + 875 seconds cannot be explained. Therefore neither theory agrees completely with the data. There was a very slight change (drop) in the hydrogen boost pump turbine inlet pressure at approximately T + 865 seconds, indicating that all the residual hydrogen peroxide had been purged from the feedline at this time. This would correlate with the theory that the increase in temperature starting at T + 875 seconds was caused by radiation heating of a dry line. After T + 1100 seconds, measurement CP361T indicates a gradual cooling trend. This was not abnormal if we assume that the peroxide line was being heated by radiation from the hot turbine and the turbine temperature was decreasing during the coast period. However, starting at T + 1370 seconds, measurement CP361T shows a very rapid cooling trend. There is no known explanation for this rapid cooling.

The general trend of the temperature of the hydrogen peroxide feedline to the hydrogen boost pump (CP361T) during and after the boost pump second operation was similar to that seen during and after the first operation. Definite oscillations were seen in the hydrogen boost pump turbine inlet pressure from main engine second cutoff to T + 2440 seconds, indicating the effects of purging the residual peroxide in the line through the turbine gas generator. The time of these oscillations corresponds very closely to the time period when measurement CP361T shows a decreasing temperature. Due to some of the unexplained excursions of measurement CP361T, consideration was given to the possibility of the data being erroneous possibly as a result of the temperature patch coming loose.

TABLE VI-I. - ATLAS PROPULSION SYSTEM PERFORMANCE, AC-18

Performance parameter	Units	Expected operating range	Flight values at-		
			T + 10 sec	Booster engine cutoff	Sustainer and vernier engine cutoff[a]
Booster engine:					
Thrust chamber 1 (B-1):					
Pressure, absolute	N/cm^2	389 to 414	398	398	(b)
	psi	565 to 600	576	576	(b)
Turbopump speed	rpm	6 225 to 6 405	6 379	6 369	(b)
Thrust chamber 2 (B-2):					
Pressure, absolute	N/cm^2	389 to 414	392	398	(b)
	psi	565 to 600	569	576	(b)
Turbopump speed	rpm	6 165 to 6 345	6 338	6 338	(b)
Gas generator chamber pressure, absolute	N/cm^2	351 to 382	373	373	(b)
	psi	510 to 555	540	540	(b)
Sustainer engine:					
Thrust chamber pressure, absolute	N/cm^2	469 to 493	483	476	483
	psi	680 to 715	700	690	700
Gas generator discharge pressure, absolute	N/cm^2	427 to 469	427	427	427
	psi	620 to 680	620	620	620
Turbopump speed	rpm	10 025 to 10 445	10 029	10 029	10 029
Vernier engine thrust chamber absolute pressure:					
Engine 1	N/cm^2	166 to 179	174	174	[c]149
	psi	240 to 260	252	252	[c]216
Engine 2	N/cm^2	166 to 179	166	116	[c]152
	psi	240 to 260	240	240	[c]220

[a]Values listed are just prior to SECO/VECO to preclude the effects of propellant depletion.

[b]Not applicable.

[c]Data invalid. See section PROPULSION SYSTEMS, Atlas Engines for explanation.

TABLE VI-II. - CENTAUR MAIN ENGINE SYSTEM PERFORMANCE, AC-18

Performance parameter	Units	Expected operating range	Flight values at-							
			Main engine first start + 80 sec[a]		Main engine first cutoff		Main engine second start + 10 sec[a]		Main engine second cutoff	
			C-1	C-2	C-1	C-2	C-1	C-2	C-1	C-2
Fuel pump inlet pressure, absolute	N/cm^2	16.2 to 24.1	20.7	21.3	18.6	18.3	23	22.8	23	22.8
	psi	23.5 to 33.9	30	30.9	27	26.5	33.3	33.0	33.3	33.0
Fuel pump inlet temperature	K	20.3 to 21.9	21.5	21.5	20.9	20.9	21.5	21.5	22.0	22.0
	^oF	-424 to -420	-421	-421	-422	-422	-421	-421	-420	-420
Oxidizer pump inlet pressure, absolute	N/cm^2	31.8 to 47.3	43.5	44	43.5	44	45.6	45.5	43.1	43
	psi	46.2 to 68.7	63	63.6	63	63.7	66.1	66.0	62.5	62.4
Oxidizer pump inlet temperature	K	95.6 to 101.6	98.2	98.2	97.0	97.0	97.7	97.7	97.0	97.0
	^oF	-287 to -277	-283	-283	-285	-285	-284	-284	-285	-285
Oxidizer pump speed	rpm	11 865 to 12 507	12 030	12 390	11 980	12 470	12 110	12 380	12 110	12 300
Fuel venturi upstream pressure, absolute	N/cm^2	492 to 528	511	513	513	515	517	523	509	515
	psi	714 to 766	740	743	744	747	750	759	737	747
Fuel turbine inlet temperature	K	192 to 228	213	215	207	211	194	197	216	216
	^oF	-114 to -49	-76	-72	-86	-80	-110	-103	-70	-70
Oxidizer injector pressure, differential	N/cm^2	24.8 to 38.6	30	32.8	28.5	32.4	28.7	28.8	29.8	30.8
	psi	36 to 56	43.5	47.6	41.3	47	41.6	41.7	43.2	44.6
Thrust chamber pressure, absolute	N/cm^2	267 to 275	270	270	268	270	270	270	270	270
	psi	387 to 399	392	391	388	392	392	392	392	392
Thrust[b]	N	65 500 to 68 200	66 800	66 300	66 200	66 300	66 800	66 300	66 800	66 300
	lbf	14 700 to 15 300	15 025	14 900	14 890	14 910	15 025	14 910	15 025	14 910

[a]Times at which engine component temperatures have stabilized and the propellant utilization values are in the null position.
[b]Thrust values computed from thrust chamber pressure data.

TABLE VI-III. - BOOST PUMP PERFORMANCE DATA FOR CENTAUR FIRST FIRING, AC-18

Performance parameter	Units	Flight values at-				
		Boost pump first start	Start engine chilldown	Main engine first start	Main engine start + 10 sec	Main engine first cutoff
Oxidizer boost pump turbine speed	rpm	0	38 700	37 930	33 000	33 250
Oxidizer boost pump turbine inlet pressure, absolute	N/cm^2	0	61.6	62.0	62.0	64.5
	psi	0	89.5	90.1	90.1	93.8
Oxidizer boost pump turbine bearing temperature	K	286	292	294	295	371
	^oF	56	66	70	72	209
Fluid temperature at oxidizer boost pump inlet	K	98.0	98.2	98.1	98.0	96.8
	^oF	-282.9	-282.1	-282.3	-282.7	-285.4
Differential pressure (head-rise) across oxidizer boost pump	N/cm^2	0	57.0	55.6	21.6	23.7
	psi	↓	82.7	80.6	31.4	34.4
Fuel boost pump turbine speed	rpm	↓	52 650	43 750	41 100	42 000
Fuel boost pump turbine inlet pressure, absolute	N/cm^2	↓	64.3	64.6	64.6	65.2
	psi	↓	93.4	93.9	93.9	94.7
Fuel boost pump turbine bearing temperature	K	290	295	296	299	380
	^oF	62	71	74	79	225
Fluid temperature at fuel boost pump inlet	K	21.0	21.0	21.1	21.1	20.0
	^oF	-421.3	-421.3	-421.4	-421.4	-423.1
Differential pressure (head-rise across fuel boost pump	N/cm^2	0	15.5	14.1	7.7	7.9
	psi	0	22.5	20.5	11.1	11.5

TABLE VI-IV. - BOOST PUMP PERFORMANCE DATA FOR CENTAUR SECOND FIRING, AC-18

Performance parameter	Units	Flight values at-				
		Boost pump second start	Start engine chilldown	Main engine second start	Main engine start + 10 sec	Main engine second cutoff
Oxidizer boost pump turbine speed	rpm	0	34 900	40 400	35 000	35 000
Oxidizer boost pump turbine inlet pressure, absolute	N/cm^2	0	65.4	65.4	65.4	66.4
	psi	0	94.9	94.9	94.9	96.3
Oxidizer boost pump turbine bearing temperature	K	410	410	412	412	420
	^oF	278	278	282	282	297
Fluid temperature at oxidizer boost pump inlet	K					
	^oF	-284.6	-284.7	-284.6	-285.1	-290.1
Differential pressure (head-rise across oxidizer boost pump	N/cm^2	0	42.9	56.3	23.4	23.0
	psi		62.3	81.6	34.0	33.3
Fuel boost pump turbine speed	rpm		36 450	45 050	41 100	41 800
Fuel boost pump turbine inlet pressure, absolute	N/cm^2		64.6	65.6	64.0	64.0
	psi		93.9	95.1	92.8	92.8
Fuel boost pump turbine bearing temperature	K	418	418	418	420	427
	^oF	292	292	292	296	308
Fluid temperature at fuel boost pump inlet	K	21.0	21.0	21.2	21.0	21.5
	^oF	-421.2	-421.3	-420.8	-421.3	-420.5
Differential pressure (head-rise) across fuel boost pump	N/cm^2	0	10.3	14.1	6.8	7.9
	psi	0	14.9	20.4	9.9	11.4

TABLE VI-V. - COMPARISON OF EXPECTED AND ACTUAL FLIGHT STEADY-STATE BOOST PUMP DATA, AC-18

Performance parameter	Units	Expected[a]	Centaur engine first firing, actual	Centaur engine second firing, actual
Liquid-oxygen-boost-pump turbine inlet pressure, absolute	N/cm^2	67.2	64.6	65.4
	psi	97.5	93.8	94.9
Liquid-hydrogen-boost-pump turbine inlet pressure, absolute	N/cm^2	66.1	65.3	64.6
	psi	96.0	94.7	93.9
Liquid-oxygen-boost-pump turbine speed	rpm	34 080	33 250	35 000
Liquid-hydrogen-boost-pump turbine speed	rpm	39 800	41 800	41 600
Liquid-oxygen-boost-pump headrise	N/cm^2	19.9	21.6	22.9
	psi	28.8	31.4	33.3
Liquid-hydrogen-boost-pump headrise	N/cm^2	7.5	7.7	7.5
	psi	10.9	11.1	10.9

[a]Values obtained from prelaunch component acceptance test.

TABLE VI-VI. - HYDROGEN PEROXIDE SYSTEM INSTRUMENTATION, AC-18

Measurement	Location (see fig. VI-8)
CP14T	P1 cluster fuel supply
CP40T	P2 cluster fuel supply
CP93T	Hydrogen peroxide bottle
CP344T	Liquid-oxygen-boost-pump hydrogen peroxide supply line
CP345T	Liquid-hydrogen-boost-pump hydrogen peroxide supply line
CP346T	Line between bottle and boost-pump feed valve
CP348T	Line between hydrogen-boost-pump catalyst bed and overspeed valve
CP349T	Line between oxygen-boost-pump catalyst bed and overspeed valve
CP350T	Aft radiation shield near bottle
CP352T	Oxygen-boost-pump supply line near overspeed valve
CP353T	Boost-pump feed valve body
CP354T	Oxygen-boost-pump line near tripod
CP355T	Hydrogen-boost-pump line near tripod
CP356T	Hydrogen-boost-pump line near propellant utilization package
CP357T	Hydrogen-boost-pump line reducer union
CP358T	Hydrogen-boost-pump line in quadrant 1
CP359T	Bottle outlet tee
CP360T	Helium purge line near feed valve
CP361T	Hydrogen-boost-pump line near overspeed valve
CP362T	Boost-pump supply line tee
CP692T	S3 engine chamber surface
CP730T	V1/S1 engine supply line
CP731T	V2/S2 engine supply line
CP738T	Supply line reducer union in quadrant 4

TABLE VI-VII. - HYDROGEN PEROXIDE SYSTEM TEMPERATURE DATA, AC-18

Measurement (see table VI-VI for location)	Lift-off, T + 0 sec		T + 100 sec		Boost pump start, T + 215.7 sec		T + 300 sec		Main engine first cutoff, T + 639 sec		T + 1100 sec		T + 1700 sec		Boost pump start, T + 2116 sec		Main engine start, T + 2143.1 sec		Main engine second cutoff, T + 2213.9 sec		T + 2400 sec		T + 2840 sec	
	K	°F	K	°F	K	°F	K	°F	K	°F	K	°F	K	°F	K	°F	K	°F	K	°F	K	°F	K	°F
CP355T	288	59	285	54	289	60	300	81	301	83	308	95	308	95	312	102	304	88	304	88	304	87	319	114
CP356T	289	61	287	57	291	64	304	88	302	85	304	88	304	88	305	89	301	82	302	84	305	89	309	96
CP357T	289	61	286	56	286	56	301	83	302	84	295	71	297	76	300	81	302	85	304	87	300	80	316	109
CP358T	298	77	289	60	292	66	305	90	302	84	301	82	303	86	302	84	300	81	300	80	302	84	307	94
CP359T	294	69	295	71	295	71	304	87	300	81	301	82	300	80	300	80	300	80	300	80	300	81	299	78
CP360T	286	56	284	51	286	56	286	55	283	50	305	90	310	98	307	94	307	94	306	91	303	86	305	90
CP361T	287	58	276	38	276	38	322	120	356	181	395	251	326	127	339	150	327	130	353	176	342	157	375	215
CP362T	286	56	285	54	285	54	303	86	305	89	301	82	300	81	302	85	305	90	305	90	305	89	304	88
CP692T	280	45	282	48	280	45	275	36	280	45	339	151	339	151	330	134	330	134	346	163	363	194	353	176
CP730T	303	86	299	79	302	84	302	84	299	78	303	86	304	88	303	86	302	85	302	85	306	91	304	88
CP731T	304	87	294	70	296	73	296	74	297	76	303	86	304	88	303	86	302	85	304	88	309	96	301	83
CP738T	301	83	299	79	299	79	299	78	294	70	303	86	302	84	299	79	299	79	298	77	301	83	301	83
CP14T	302	85	299	79	299	78	299	78	293	68	302	85	302	84	302	84	302	84	302	84	304	87	305	89
CP40T	296	74	292	66	292	67	292	66	289	60	302	85	304	87	302	85	301	83	301	83	306	92	302	84
CP93T	301	83	301	83	301	83	301	83	301	83	301	83	302	84	302	84	302	84	303	86	304	87	304	87
CP344T	295	71	289	61	295	72	304	88	303	86	309	97	306	92	306	91	301	83	302	84	308	95	295	71
CP345T	294	69	276	37	279	43	279	87	302	85	301	83	306	92	305	89	301	83	301	83	305	90	316	110
CP346T	296	73	296	73	294	70	304	88	305	90	297	76	295	71	293	68	304	88	304	88	300	81	294	70
CP348T	287	57	277	39	279	42	300	80	302	84	316	109	334	142	354	178	317	111	310	99	314	106	324	124
CP349T	289	61	277	39	282	48	301	82	305	89	311	100	321	118	331	136	312	103	307	93	301	82	321	118
CP350T	266	19	245	-19	250	-9	250	-9	239	-30	231	-44	238	-31	236	-35	235	-37	233	-40	232	-42	227	-50
CP352T	294	70	275	36	285	53	309	96	311	101	312	102	318	113	320	116	303	86	305	90	318	113	307	94
CP353T	288	59	287	57	287	57	294	70	300	80	299	79	303	86	304	87	304	88	305	90	305	90	304	87
CP354T	295	72	286	56	294	69	304	87	305	90	308	95	307	93	312	102	304	87	305	90	304	88	306	92

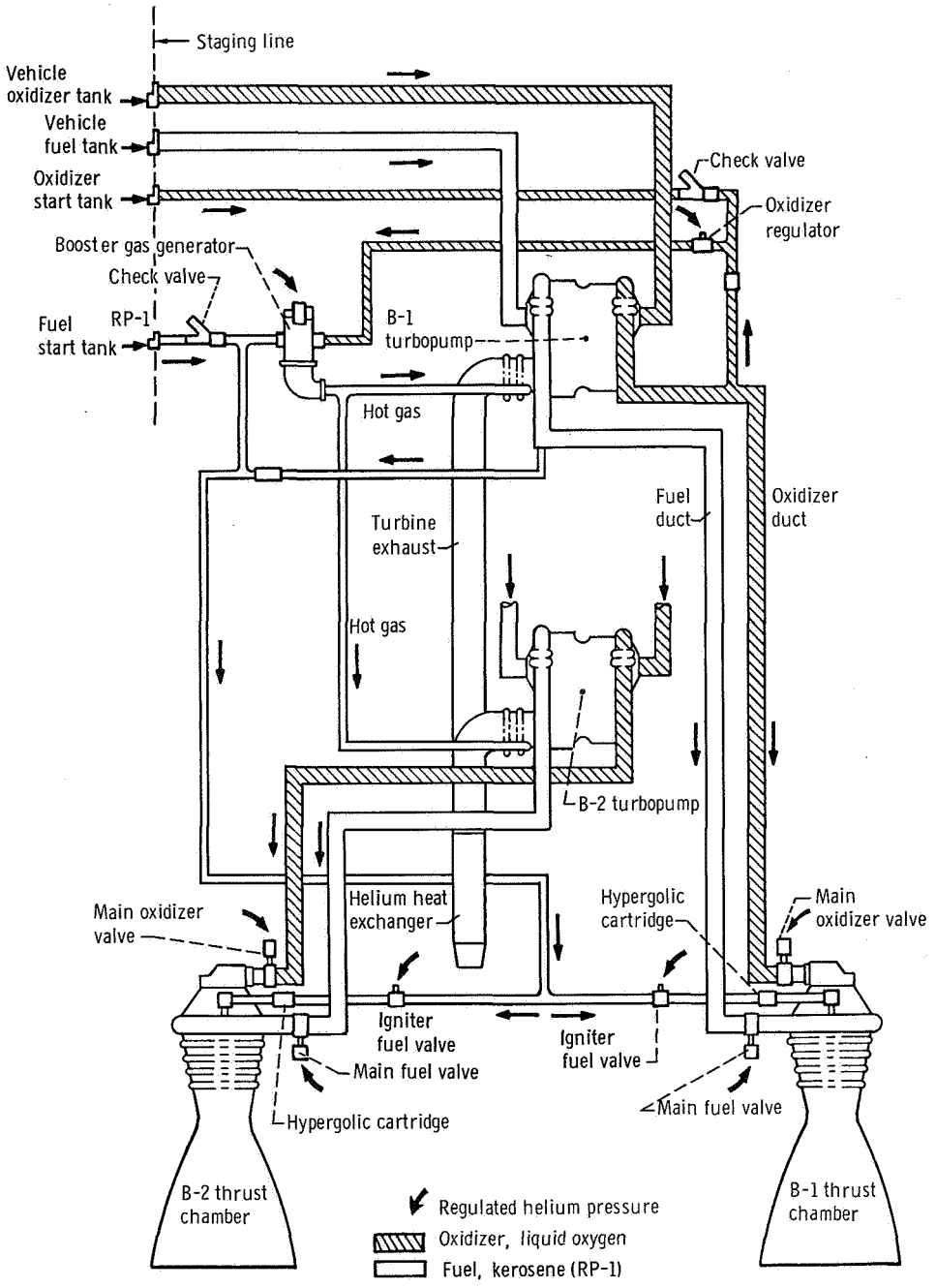

(a) Atlas vehicle booster engine.

Figure VI-1. - Atlas propulsion system, AC-18.

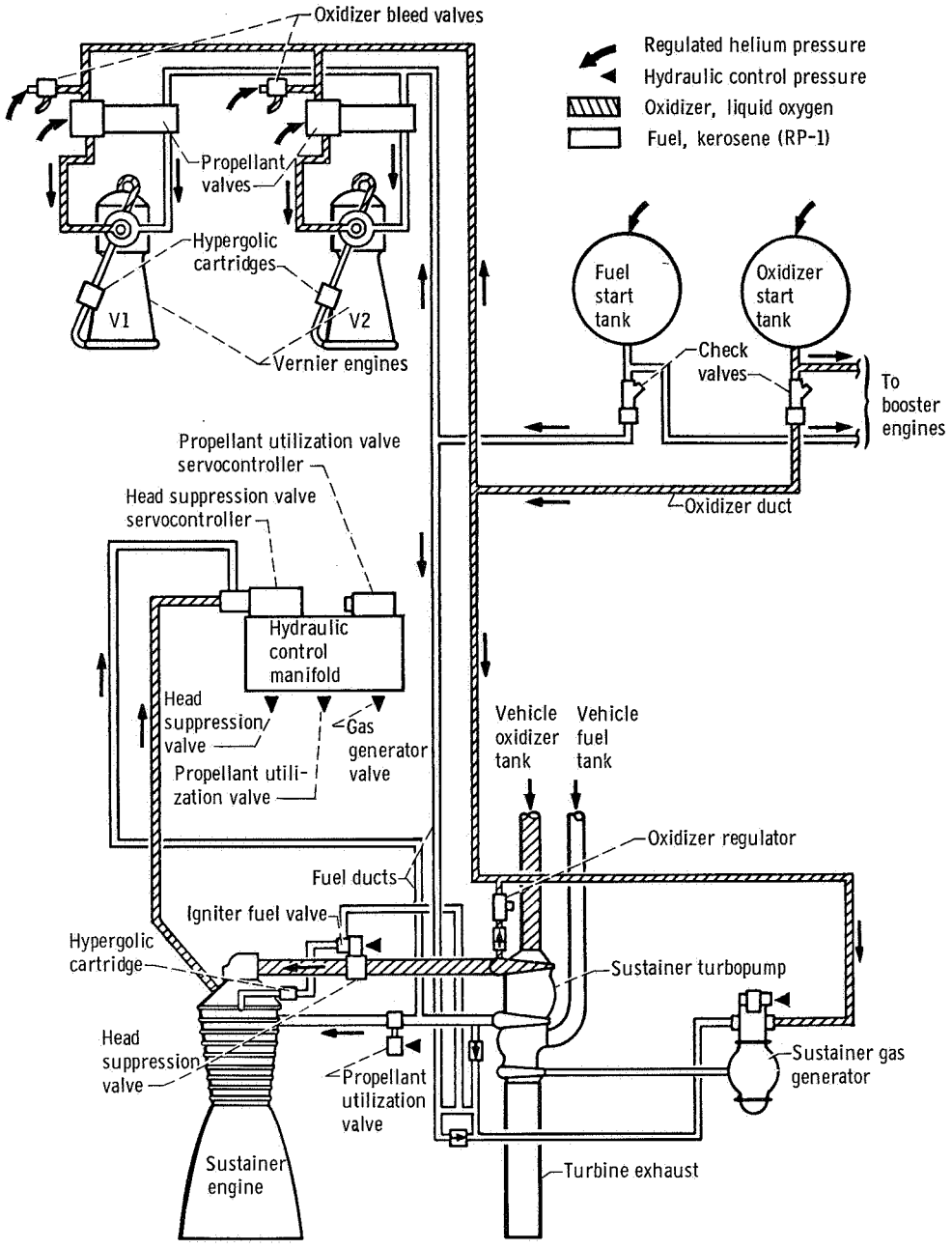

(b) Atlas vehicle sustainer and vernier engines.

Figure VI-1. - Concluded.

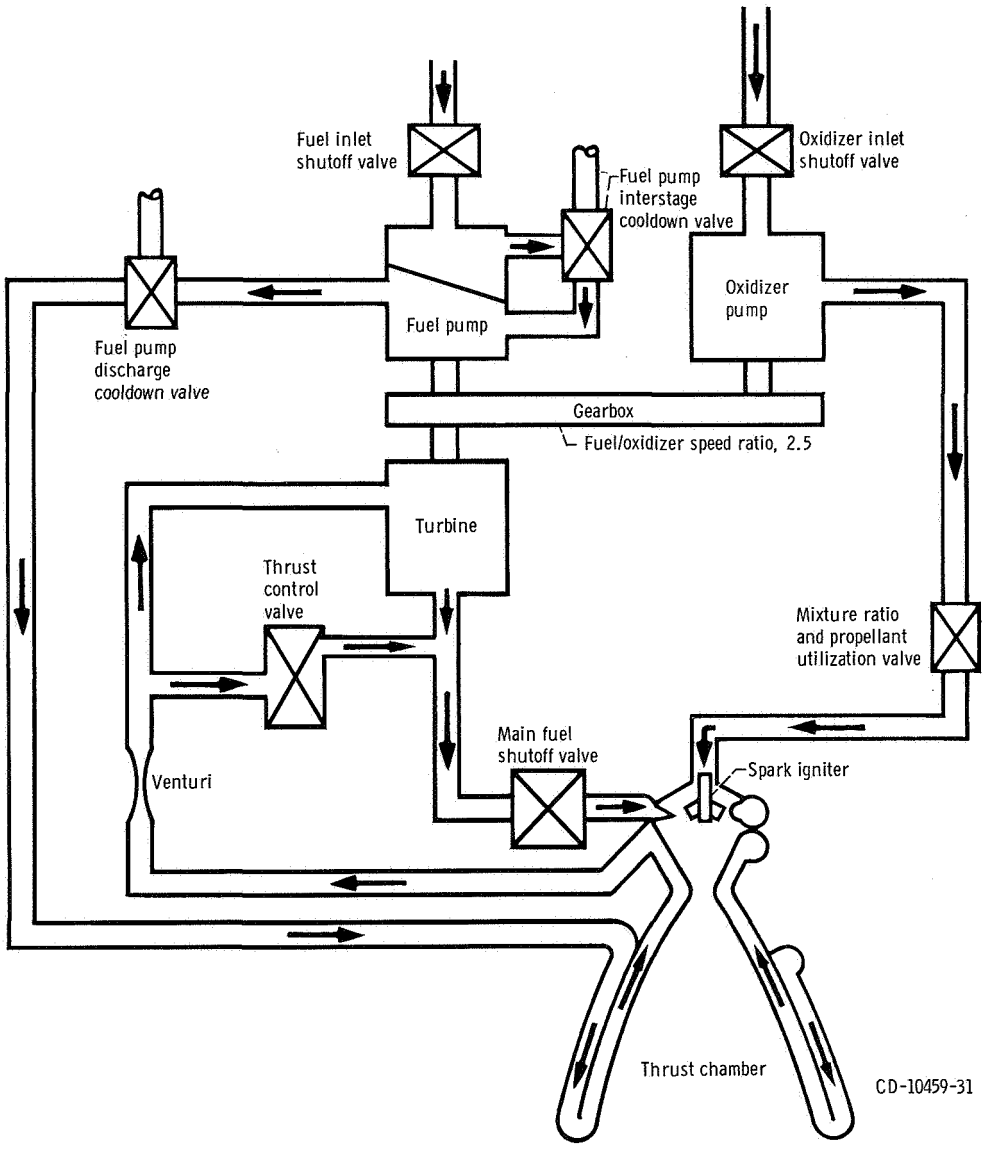

Figure VI-2. - Centaur propulsion system, AC-18.

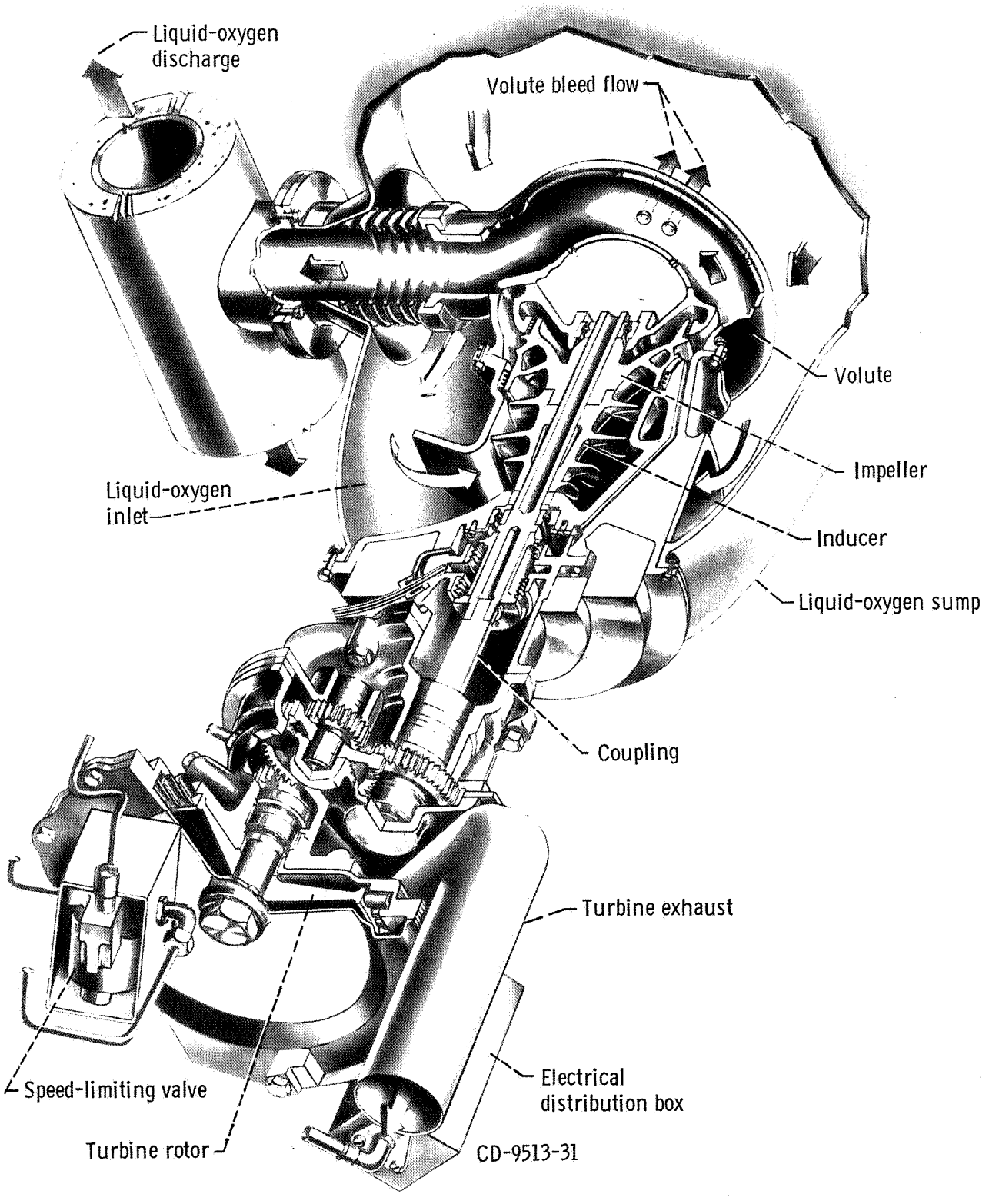

Figure VI-4. - Centaur liquid-oxygen boost pump and turbine cutaway, AC-18.

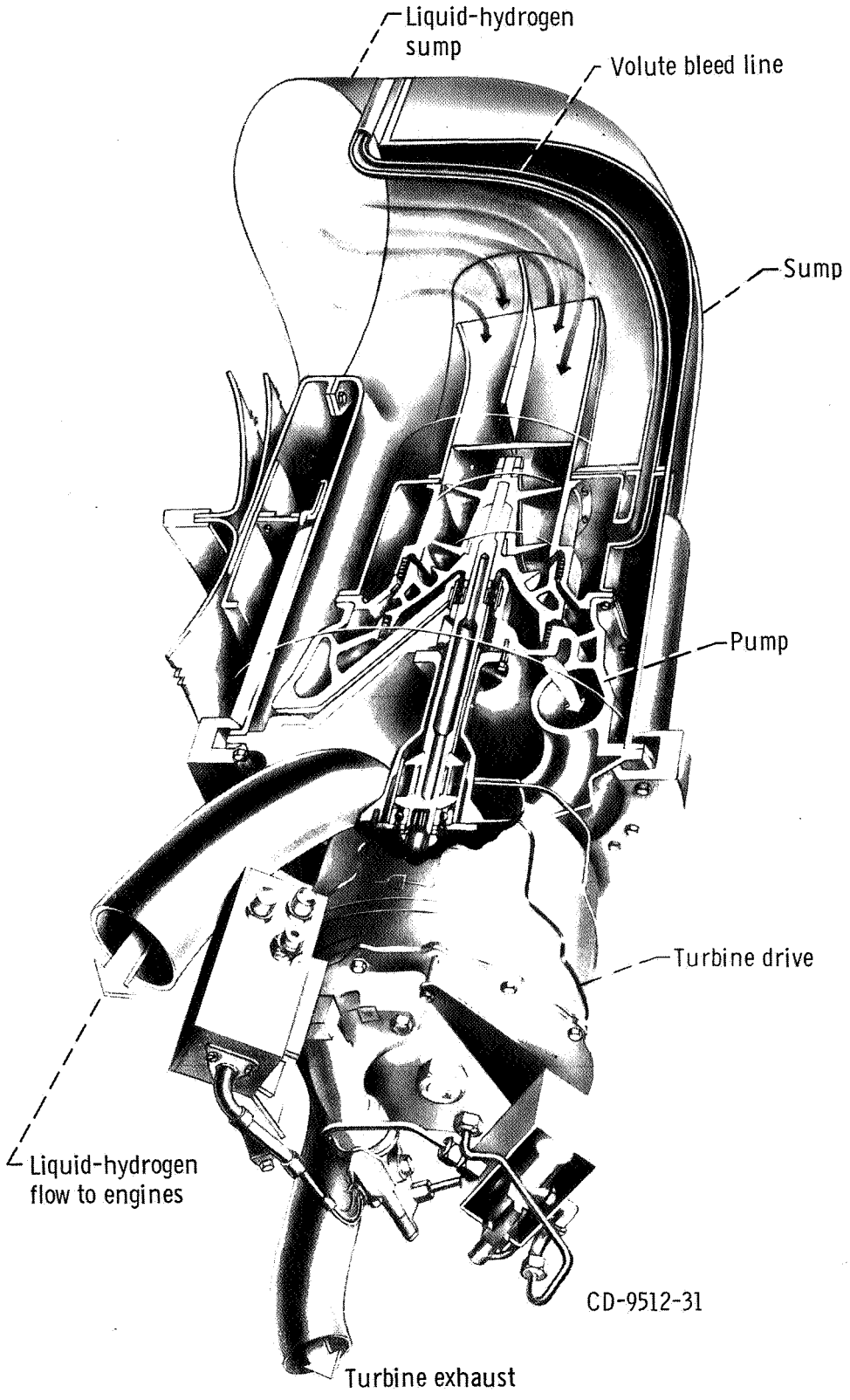

Figure VI-5. - Centaur liquid-hydrogen boost pump and turbine cutaway, AC-18.

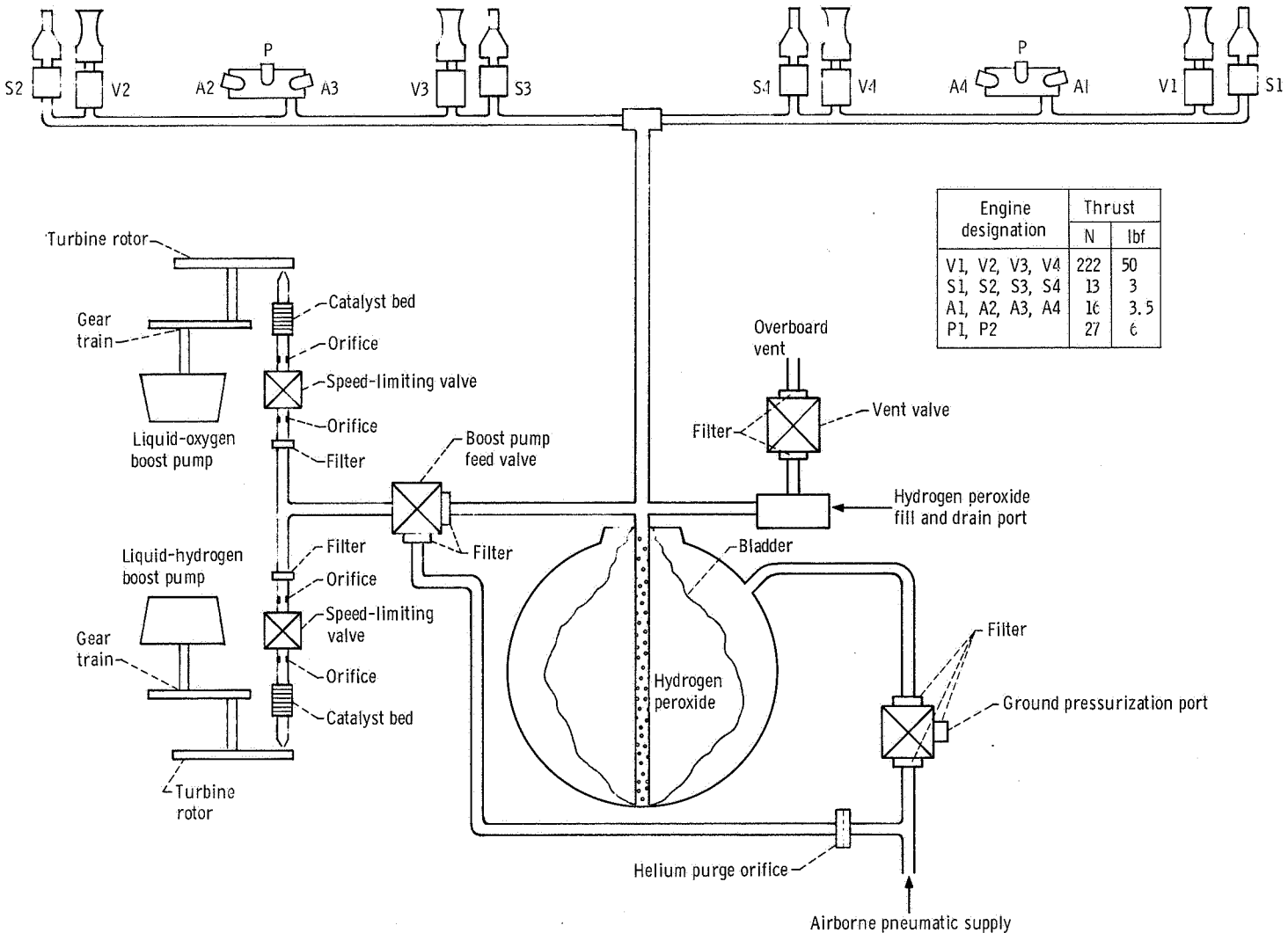

Figure VI-6. - Hydrogen peroxide engine and boost pump systems, AC-18.

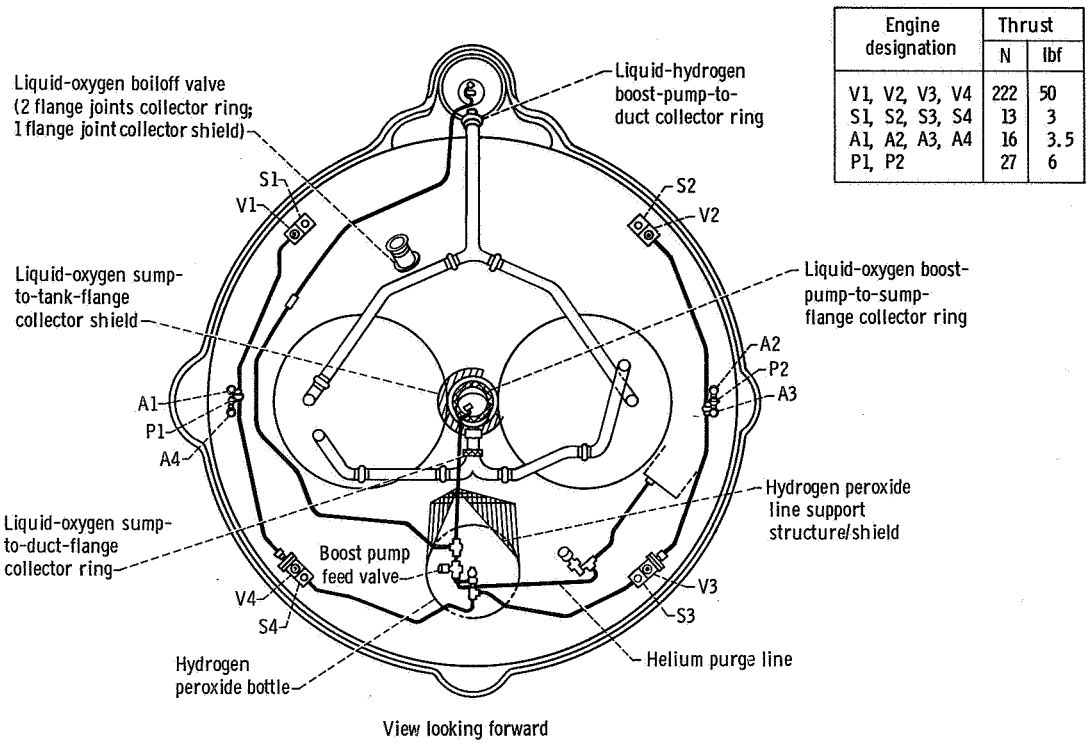

Figure VI-7. - Hydrogen peroxide system - cryogenic leak protection, AC-18.

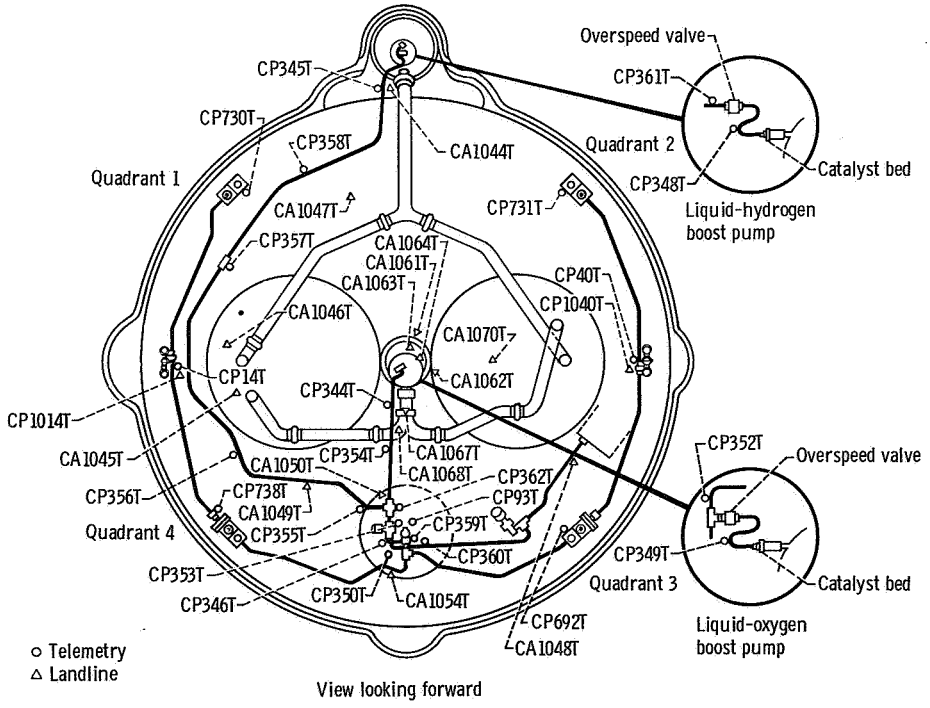

Figure VI-8. - Hydrogen peroxide system instrumentation, AC-18.

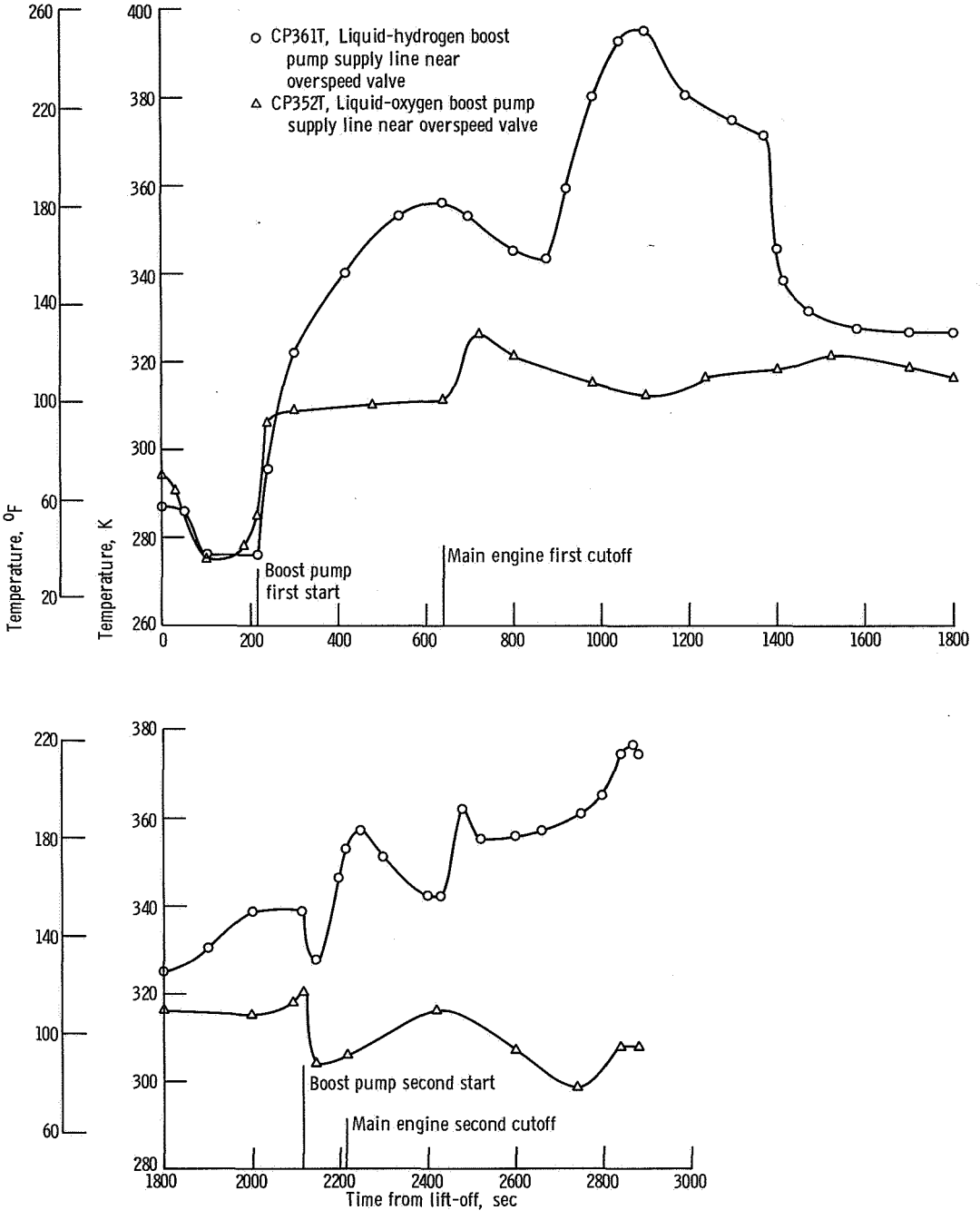

Figure VI-9. - Hydrogen peroxide feedline temperatures, AC-18.

PROPELLANT LOADING AND PROPELLANT UTILIZATION SYSTEMS

by Clifford H. Arth

Level Indicating Systems

System description. - The Atlas propellant level indicating system (fig. VI-10) consists of a portable sight gage assembly for RP-1 fuel (kerosene) loading and platinum hot-wire-type sensors for oxidizer (liquid oxygen) loading.

The fuel (RP-1) loading levels are determined by visual observation of the sight gage assembly, which is connected to the fuel probe by two sense lines. After tanking, the fuel sight gage assembly and sense lines are removed and the connection points on the vehicle are secured for flight.

The liquid-oxygen loading levels are determined from sensors located at discrete points in the oxidizer (liquid oxygen) tank. The sensing elements are a platinum hot-wire type (0.0025 cm (0.001 in.) diam) which have a linear resistive temperature coefficient. The sensors are supplied with a near-constant current of approximately 200 milliamperes and the voltage drop across a sensor reflects the resistance value of the sensor. When immersed in a cryogenic fluid (covered), the sensor has a low resistance and a low voltage drop. When uncovered, the sensor has a high resistance and therefore a high voltage drop.

The control unit with electronic trigger circuits and control relays supplies a signal to the propellant loading operator. These control relays are activated or de-activated by the voltage level of each sensor (i.e., covered or uncovered).

The Centaur propellant level indicating system (fig. VI-11) utilizes platinum hot-wire level sensors in both the liquid-oxygen and liquid-hydrogen tanks. This sensor system operates identically to those used in the Atlas liquid-oxygen tank.

System performance. - Atlas and Centaur propellant loading was satisfactorily accomplished. Atlas propellant weights were calculated using a density of 800 kilograms per cubic meter (49 lbm/ft^3) for the fuel, and a density of 1100 kilograms per cubic meter (69.29 lbm/ft^3) for the liquid oxygen. Centaur propellant weights were calculated using a density of 67.04 kilograms per cubic meter (4.19 lbm/ft^3) for the liquid hydrogen and a density of 1098 kilograms per cubic meter (68.6 lbm/ft^3) for the liquid oxygen. These calculated values are

Atlas propellant weight tanked, kg (lbm):	
Fuel (RP-1)	38 399 (84 656)
Oxidizer (liquid oxygen)	85 594 (188 702)
Centaur propellant weight at lift-off, kg (lbm):	
Fuel (liquid hydrogen)	2388 (5265)
Oxidizer (liquid oxygen)	11 542 (25 446)

Atlas Propellant Utilization System

System description. - The Atlas propellant utilization (PU) system (fig. VI-12) consists of two mercury manometer assemblies, a computer-comparator, a hydraulically actuated propellant utilization fuel valve, sense lines, and associated electrical harnessing. The system is used to ensure near-simultaneous depletion of the propellants and minimum propellant residuals at sustainer engine cutoff. This is accomplished by controlling the propellant mixture ratio (oxidizer flow rate/fuel flow rate) to the sustainer engine. During flight, the manometers sense propellant head pressures which are indicative of propellant mass. The mass ratio is then compared to a reference ratio (at lift-off the ratio is 2.27) in the computer-comparator. If needed, a correction signal is sent to the propellant utilization valve controlling the main fuel flow to the sustainer engine. The oxidizer flow is regulated by the head suppression valve. This valve senses propellant utilization valve movement and moves in the direction opposite to that of the propellant utilization valve. This opposite movement thus alters propellant mixture ratio to maintain constant propellant mass flow to the engine. The PU valve operates at the null position for the first 13 seconds (lockout) of flight to prevent oscillations of the valve during lift-off.

System performance. - The Atlas propellant utilization system operated satisfactorily. The propellant utilization system valve angles are shown in figure VI-13. The valve was in the fuel-rich position until just before booster engine cutoff, then oscillated between fuel rich and oxidizer rich until just before sustainer engine cutoff, when the valve was commanded to the oxidizer-rich position to ensure oxidizer depletion. The predicted and actual weights of residual propellant above the pump inlets at the sustainer engine cutoff are shown in the following table. These residuals include the trapped propellants and were calculated using the time the head sensing port uncovers as a reference. Propellants consumed from the time the port uncovers to sustainer engine cutoff include the effect of flow rate decay for a liquid-oxygen depletion.

Propellant	Units	Atlas propellant residuals	
		Predicted	Actual
Fuel (RP-1)	kg	131	120
	lbm	287	263
Oxidizer (liquid oxygen	kg	143	172
	lbm	315	378

Centaur Propellant Utilization System

System description. - The Centaur propellant utilization (PU) system (fig. VI-14) is used during flight to control the ratio of propellants consumed by the main engines and to assure minimum residuals. The probes (sensors) of the PU system are also used during tanking to indicate propellant levels within the range of these probes. In flight, the mass of propellant in each tank is sensed by a capacitance probe and compared in a bridge balancing circuit. If the mass ratio of propellants in the tanks varies from the predetermined value (5:1, oxidizer to fuel), an error signal is sent to the proportional servopositioners which control the liquid-oxygen flow control valves (one on each engine). When the mass ratio in the tanks is greater than 5:1, the liquid-oxygen flow is increased to return the ratio to 5:1. When the ratio is less than 5:1, the liquid-oxygen flow is decreased. The sensing probes do not extend to the top of the tanks, and therefore are not used for control until after the probes are uncovered at approximately 90 seconds after Centaur main engine first start. For this 90 seconds, the liquid-oxygen flow control valves are maintained at approximately 5:1 propellant mixture ratio. The valves are also commanded to the null position at approximately a 5:1 propellant mixture ratio 15 seconds before Centaur main engine second cutoff. This is done because the probes do not extend to the bottom of the tanks, and system control is lost when the liquid level depletes below the bottom of the probes.

System performance. - The Centaur propellant utilization system operated satisfactorily. The liquid-oxygen valve angles during flight are shown in figure VI-15. System control was enabled by the vehicle programmer at main engine first start plus 90.0 seconds. The valves at this time moved to the liquid-oxygen-rich stop, reaching the stop by main engine start plus 93.5 seconds, and remained there for approximately 35 seconds. The liquid-oxygen probe was uncovered at main engine start plus 95 seconds. The liquid-hydrogen probe uncovered 7.0 seconds later. During the 35 seconds the system corrected for 116.0 kilograms (255 lbm) of excess liquid oxygen. This correction consisted of

(1) Engine propellant consumption rate error accumulated during the first 90 seconds of engine firing
(2) Propellant loading error
(3) System bias to ensure liquid-oxygen depletion first
(4) System bias to compensate for propellant boiloff which occurs during the 25-minute Centaur coast

The valves oscillated about "null" throughout the period of the engine first firing. At main engine first cutoff, about 1945 kilograms (4280 lbm) of liquid oxygen and 409 kilograms (900 lbm) of liquid hydrogen remained in the propellant tanks.

During the main engine second firing the PU valves responded normally to changes

in the propellant quantities in the tanks. About 15 seconds prior to main engine second cutoff, the PU valves were commanded to null by the guidance system.

The following table shows the expected and actual weights of propellant residuals at main engine second cutoff:

Propellant	Units	Centaur propellant residuals	
		Expected	Actual
Liquid oxygen	kg	115	143
	lbm	254	315
Liquid hydrogen	kg	32.2	24.5
	lbm	70.8	54

The residuals remaining at main engine second cutoff would have provided for an additional 4.7 seconds of engine firing.

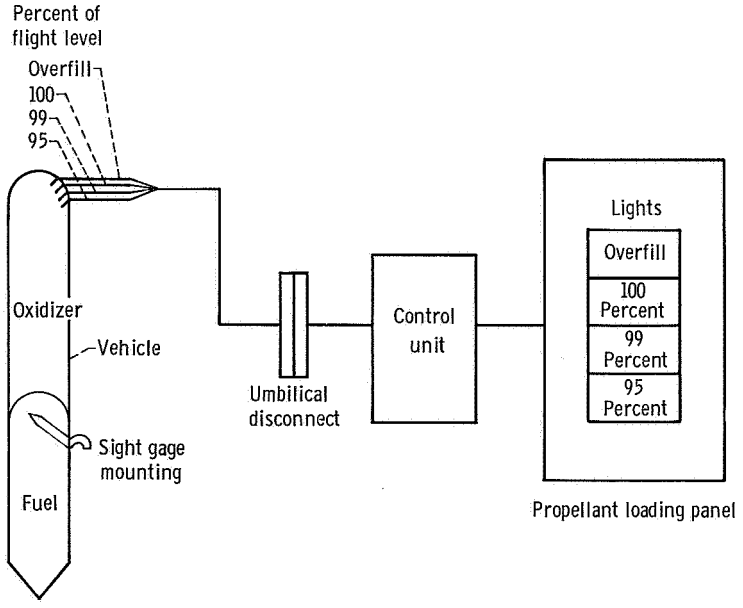

Figure VI-10. - Propellant level indicating system for Atlas propellant loading, AC-18.

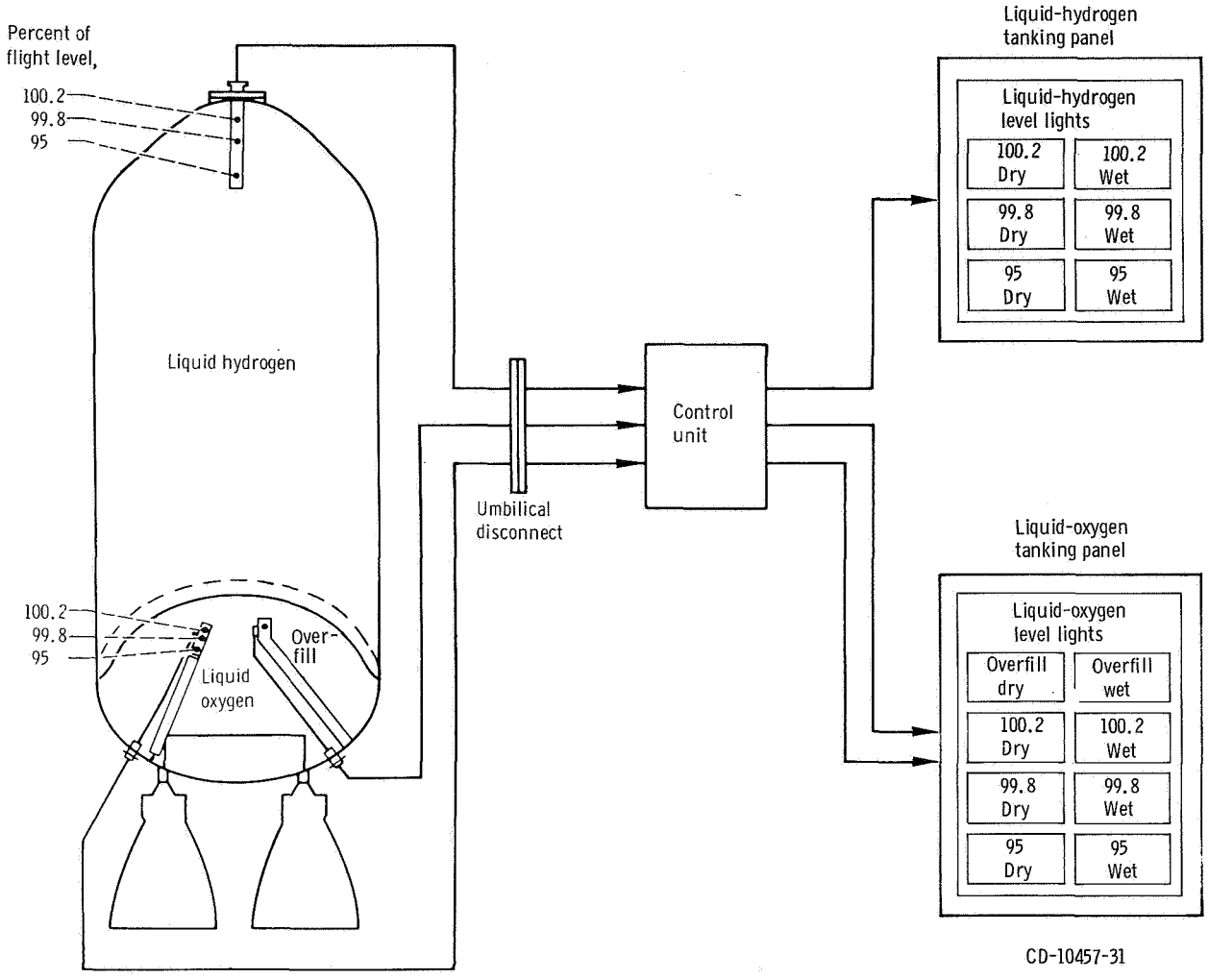

Figure VI-11. - Propellant level indicating system for Centaur propellant loading, AC-18.

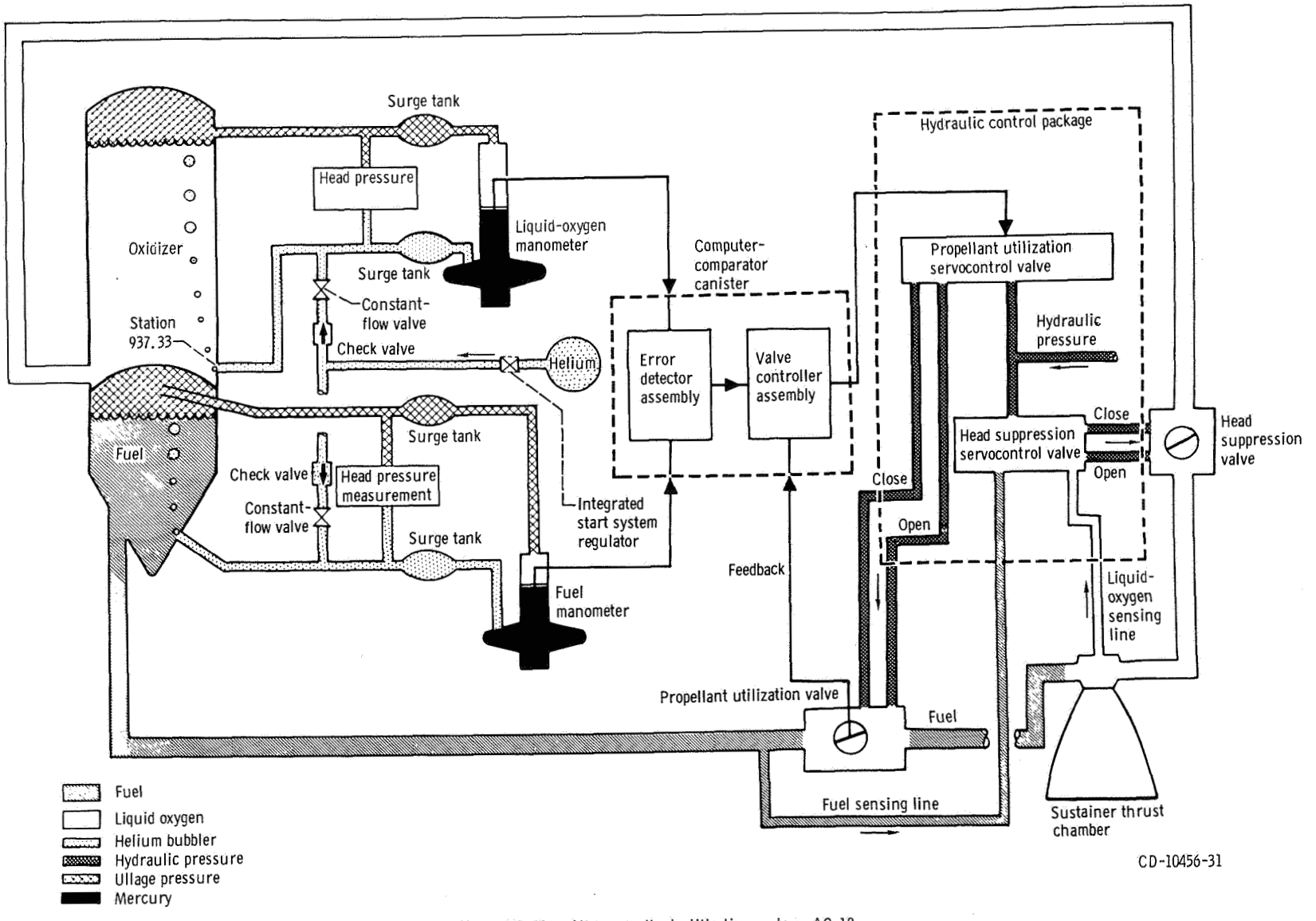

Figure VI-12. - Atlas propellant utilization system, AC-18.

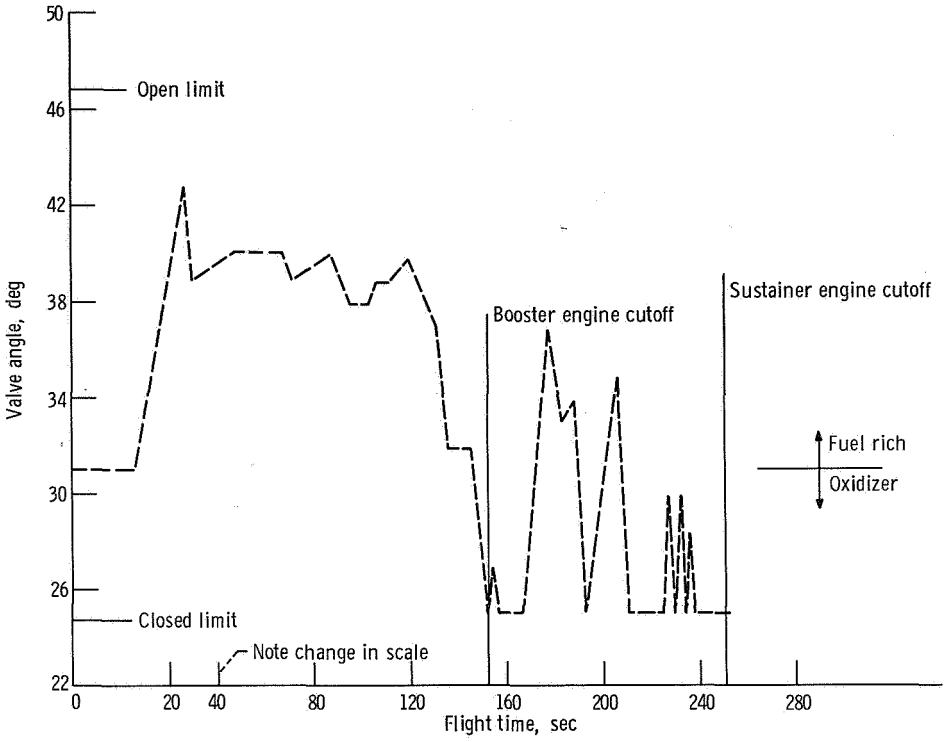

Figure VI-13. - Atlas propellant utilization valve angles, AC-18.

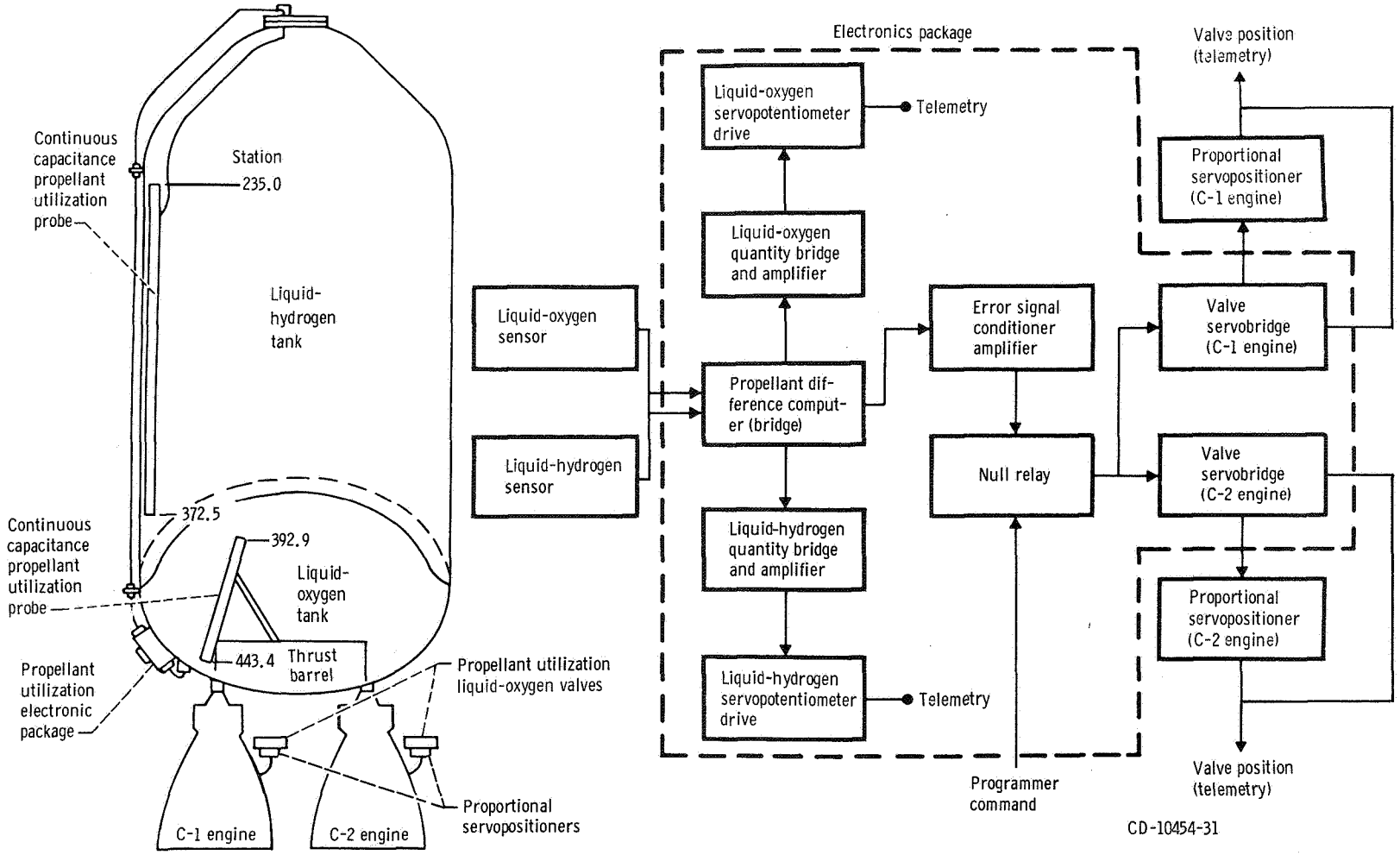

Figure VI-14. - Centaur propellant utilization system, AC-18.

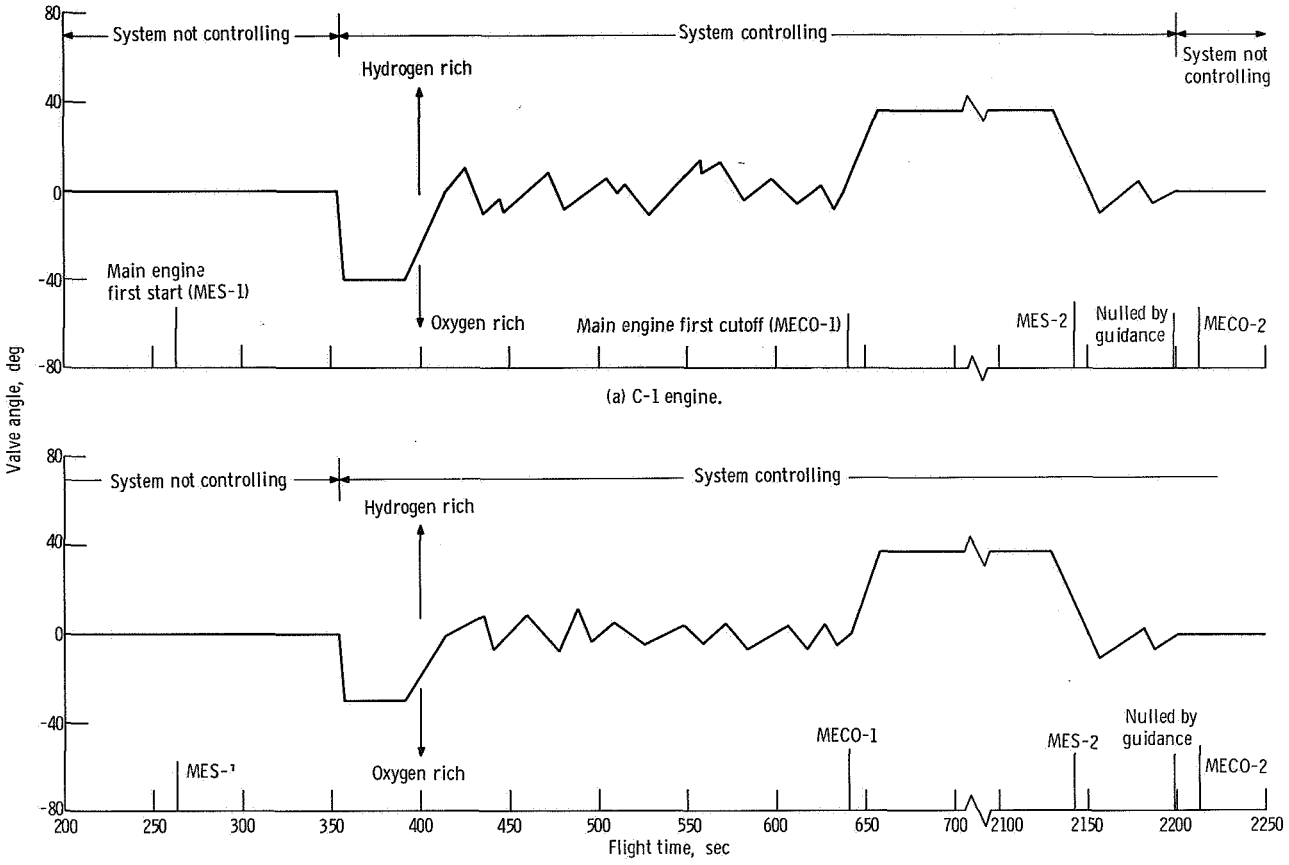

Figure VI-15. - Centaur propellant utilization valve angles, AC-18.

PNEUMATIC SYSTEMS

by Eugene J. Fourney and Richard W. Heath

Atlas

System description. - The Atlas pneumatic system supplies helium gas for pressurization of the propellant tanks and for various vehicle control functions. The system is comprised of three independent subsystems: propellant tank pressurization, engine control, and booster section jettison. The system schematic is shown in figure VI-16.

Propellant tank pressurization subsystem: This subsystem uses helium gas to maintain propellant tank pressures at required levels to support the pressure-stabilized tank structure and to satisfy the inlet pressure requirements of the engine turbopumps. In addition, helium is supplied from the fuel tank pressurization line to pressurize the hydraulic reservoirs and turbopump lubricant storage tanks. The subsystem consists of eight shrouded helium storage bottles, a heat exchanger, and fuel and oxidizer tank pressure regulators and relief valves.

The eight shrouded helium storage bottles with a total capacity of 967 000 cubic centimeters (59 000 cu in.) are mounted in the jettisonable booster engine section. The bottle shrouds are filled with liquid nitrogen during prelaunch operations to chill the helium in order to provide a maximum storage capacity at a pressure of 2342.3 N/cm^2 (3400 psia). The liquid nitrogen drains from the shrouds at lift-off. During flight the cold helium passes through a heat exchanger located in the booster engine turbine exhaust duct and is heated before being supplied to the tank pressure regulators. Pressurization control of the propellant tank pressurization subsystem is switched from the ground to the airborne system at about T - 60 seconds. Airborne regulators are set to control fuel tank gage pressure between 44.1 and 46.6 N/cm^2 (64 and 67 psi) and oxidizer tank pressure between 19.77 and 24.12 N/cm^2 (28.7 and 35.0 psi). From approximately T - 60 seconds to T + 20 seconds the liquid-oxygen regulator sense line is biased by a helium "bleed" flow into the liquid-oxygen-tank regulator sensing line which senses ullage pressure. The bias causes the regulator to control tank pressure at a lower level than the normal regulator setting. Depressing the liquid-oxygen-tank pressure increases the differential pressure across the bulkhead between the propellant tanks. The increased differential pressure counteracts the launch transient loads that act in a direction to cause bulkhead reversal. At T + 20 seconds the bias is removed by closing explosively actuated valves, and the ullage pressure in the liquid-oxygen tank increases to the normal regulator control range. The increased pressure then provides sufficient vehicle structural stiffness to withstand bending loads during the remainder of the ascent.

Pneumatic regulation of tank pressure is terminated at booster engine section jetti-

son. Thereafter the fuel tank pressure decays slowly. The oxidizer tank pressure is augmented by liquid-oxygen boiloff.

Engine control subsystem: This subsystem supplies helium pressure for actuation of engine control valves, for pressurization of the engine start tanks, for purging booster engine turbopump seals, and for the reference pressure to the regulators which control oxidizer flow to the gas generator. Control pressure in the system is maintained through Atlas/Centaur separation. These pneumatic requirements are supplied from a 76 000-cubic-centimeter (4650-cu-in.) helium storage bottle pressurized to a gage pressure of about 2342.6 N/cm^2 (3400 psi) at lift-off.

Booster engine jettison subsystem: This subsystem supplies pressure for release of the pneumatic staging latches to separate the booster engine section. A command from the Atlas flight control system opens two explosively actuated valves to supply helium pressure to 10 piston-operated staging latches. Helium for the system is supplied by a single 14 260-cubic-centimeter (870-cu-in.) bottle charged to a gage pressure of 2342.6 N/cm^2 (3400 psi).

System performance. - The Atlas pneumatic system performance was satisfactory during flight. Performance data are shown in table VI-VIII.

Propellant tank pressurization subsystem: Control of the propellant tank pressures was switched from the ground pressurization control unit (PCU) to the airborne regulators at approximately T - 60 seconds. Ullage pressures were properly controlled throughout the flight.

The fuel tank pressure regulator controlled at a gage pressure of about 44.65 N/cm^2 (64.8 psi) until termination of pneumatic control at booster engine section jettison. During the sustainer phase, the fuel tank ullage pressure decreased normally and was 38.58 N/cm^2 (56.0 psi) at sustainer and vernier engine cutoff.

The oxidizer tank ullage gage pressure was steady at 21.01 N/cm^2 (30.5 psi) after switching from the PCU to the airborne regulator. This pressure decreased to 19.77 N/cm^2 (28.7 psi) at engine start and then increased slightly to 20.12 N/cm^2 (29.2 psi) by T + 20 seconds. At this time the regulator sense line bias was terminated and the liquid-oxygen-tank ullage pressure increased to 23.29 N/cm^2 (33.8 psi). Four seconds was required for the ullage pressure to stabilize. The liquid-oxygen-tank pressure remained within the required limits until termination of pneumatic regulation at booster engine section jettison. After jettison the ullage pressure decreased from 23.56 N/cm^2 (34.2 psi) to 22.05 N/cm^2 (32.0 psi) at sustainer and vernier engine cutoff.

Engine control subsystem: The booster and sustainer engine control regulators provided the required helium pressure for engine control throughout the flight.

Booster section jettison subsystem: Subsystem performance was satisfactory. The explosive actuated valve was opened on command, allowing high-pressure helium to actuate the 10 booster staging latches.

Centaur

System description. - The Centaur pneumatic system (figs. VI-17(a) and (b)) consists of five subsystems: propellant tank venting, propellant tank pressurization, propulsion pneumatics, helium purge pneumatics, and nose fairing pneumatics.

Propellant tank venting subsystem: The structural stability of the propellant tanks is maintained throughout the flight by the propellant boiloff gas pressures. These pressures are controlled by a vent system on each propellant tank. The hydrogen tank vent system is comprised of two pilot-controlled, pressure-actuated vent valves and ducting. The hydrogen primary vent valve is fitted with a solenoid valve which locks the vent valve, preventing its opening. The hydrogen secondary vent valve does not have the control solenoid. The relief range of the secondary valve is 17.1 to 18.5 N/cm^2 (24.8 to 26.8 psia) and is above that of the primary valve, which is 13.1 to 14.8 N/cm^2 (19 to 21.5 psia). This prevents overpressurization of the hydrogen tank when the primary vent valve is locked. The vented hydrogen gas is ducted overboard through a single vent in the nose fairing. After fairing jettison the gas is vented overboard through two opposed nozzles so as to produce no thrust. The oxygen tank vent system uses a single vent valve which is fitted with the control solenoid valve. Its operating range is 20 to 22 N/cm^2 (29 to 32 psia). The vented oxygen gas is ducted overboard through the interstage adapter. The duct, which remains with the Centaur after separation from the interstage adapter, is oriented to aline the venting thrust vector with the vehicle center of gravity.

The vent valves are commanded to the locked mode at specific times (1) to permit the hydrogen tank pressure to increase during the atmospheric ascent to satisfy the structural requirements of the pressure-stabilized tank, (2) to permit controlled pressure increases in the tanks to satisfy the boost pump pressure requirements, (3) to restrict oxygen venting during nonpowered flight to avoid vehicle disturbing torques, and (4) to restrict hydrogen venting to nonhazardous times. (A fire could conceivably occur during the early part of the atmospheric ascent if a plume of vented hydrogen washes back over the vehicle and is exposed to an ignition source. A similar hazard could occur at Atlas booster engine staging when residual oxygen envelops a large portion of the vehicle.)

Propellant tank pressurization subsystem: The propellant tank pressurization subsystem supplies helium gas in controlled quantities for in-flight pressurization in addition to that provided by the propellant boiloff gases. It consists of a normally closed solenoid valve and orifice for each propellant tank, and a pressure switch assembly which senses oxygen tank pressure. The solenoid valves and orifices provide a metered flow of helium to both propellant tanks for step pressurization during the main engine start sequence, and to the oxygen tank at main engine cutoff. The pressure sensing switch controls the pressurization of the oxygen tank during the main engine start sequence.

Propulsion pneumatic system: The propulsion pneumatic subsystem supplies helium gas at regulated pressures for actuation of main engine control valves and pressurization of the hydrogen peroxide storage bottle. It consists of two pressure regulators, which are referenced to ambient pressure, and two relief valves. Pneumatic pressure supplied through the engine controls regulator is used for actuation of the engine inlet valves, the engine chilldown valves, and the main fuel shutoff valve. The peroxide pressure regulator, located downstream of the engine controls regulator, further reduces the pressure to provide expulsion pressurization for the hydrogen peroxide storage bottle and the boost pump feedline purge. The boost pump feedline purge was used for the first time on this flight. A relief valve is located downstream of each regulator to prevent overpressurization.

Helium purge subsystem: A ground/airborne helium purge subsystem was used to prevent cryopumping and icing under the insulation panels and in propulsion system components. A common airborne distribution system is used for prelaunch purging from a ground helium source and in-flight purging from an airborne helium storage bottle. This subsystem distributes helium gas for purging the cavity between the hydrogen tank and the insulation panels, the seal between the cylindrical section of the nose fairing and the forward bulkhead, the propellant feedlines, the boost pumps, the ducts for the engine chilldown vents, the engine thrust chambers, and the hydraulic power packages. The umbilical connection for charging the airborne bottle could also be used to supply the purge from the ground source should an abort occur after disconnection of the ground purge supply line.

Nose fairing pneumatic subsystem: The nose fairing pneumatic subsystem provides the thrust required to jettison the nose fairing. It consists of a nitrogen storage bottle and an explosive actuated valve with an integral thruster nozzle in each fairing half. Release of the gas through the nozzles provides the necessary thrust to propel the fairing halves away from each other and from the vehicle.

System performance. - The performance of the Centaur pneumatic system was satisfactory.

Propellant tank pressurization and venting subsystems: The ullage pressures in the hydrogen and oxygen tanks are shown in figure VI-18. At T - 8 seconds the hydrogen primary vent valve was locked, which subsequently resulted in an increase in the tank pressure. The pressure increased to the relief setting of the hydrogen secondary vent valve, which then began to regulate the tank pressure. The secondary valve relief absolute pressure was 18.1 N/cm^2 (26.3 psi). The tank pressure rise rate until the valve relieved was 3.10 N/cm^2/minute (4.45 psi/min). At T + 90 seconds the hydrogen primary tank vent valve was enabled and then regulated the tank pressure. The hydrogen primary vent valve was again locked at the beginning of Atlas booster engine jettison and remained locked for 7 seconds. At Atlas sustainer engine cutoff the primary hydrogen

vent valve was locked again, and the tank was pressurized with helium for 1 second as a part of the Centaur main engine start sequence. The pressure increased approximately 0.9 N/cm^2 (1.3 psi) during this 1-second period, and then decreased as the warm helium in the tank was cooled by the hydrogen gas.

The ullage pressure in the oxygen tank remained relatively constant due to steady-state venting for the first 30 seconds of flight until the increasing vehicle acceleration began to suppress the propellant boiling enough to allow the pressure to decrease. The pressure decreased and then varied between 20.4 N/cm^2 (29.6 psi) and 22.3 N/cm^2 (32.4 psi) until Atlas booster engine cutoff. At that time the sudden reduction in the acceleration caused an increase in the liquid-oxygen boiloff and a resulting pressure rise in the tank. As thermal equilibrium was reestablished in the tank, the pressure decreased to its original level.

Sixty-two seconds after Atlas booster engine cutoff the oxygen tank vent valve was locked and the helium pressurization of the oxygen tank was initiated. The tank pressure increased to the upper limit of the pressurization switch, which terminated the pressurization. As the helium gas was cooled in the tank, the pressure decreased until the heat input, principally from the boost pump recirculation flow, increased the boiloff and caused the pressure to increase again until Centaur main engine first prestart. The pressure then decreased gradually until Centaur main engine first start, at T + 263 seconds, when it decreased abruptly to the saturation pressure of the ullage gas.

The ullage pressures in both propellant tanks decreased normally during the main engine operation. After main engine cutoff at T + 639 seconds, the hydrogen primary vent valve was enabled while the oxygen vent valve remained locked.

During the coast period following the engine cutoff, the hydrogen tank pressure increased to the regulating range of the primary vent valve and was regulated by that valve until the beginning of the second prestart sequence. The oxygen tank ullage pressure rapidly rose to 20.3 N/cm^2 (29.4 psia) within 30 seconds after main engine cutoff and remained at that level for approximately 600 seconds. At that time, it began to rise gradually until the tank was pressurized in preparation for the main engine second start.

At T + 2103 seconds the hydrogen primary vent valve was locked and helium was injected into both propellant tanks. The pressurization of the oxygen tank was timed to last 18 seconds. The pressure sensing switch, which was used during the main engine first start sequence, was bypassed. During this 18-second period the oxygen tank ullage pressure rose from 21.3 N/cm^2 (30.9 psia) to 22.9 N/cm^2 (33.3 psia) and remained at that level until the engines were started. The pressurization of the hydrogen tank was also a timed function, lasting 40 seconds. The pressure in the tank increased from 14.3 N/cm^2 (20.7 psia) to the relief setting of the secondary vent valve. The pressure was regulated by that valve until the engine start. During the engine operation the oxygen tank ullage pressure decreased to 19.6 N/cm^2 (28.4 psia) at main engine cutoff, while the hydrogen tank ullage pressure decreased to 14.7 N/cm^2 (21.3 psia).

At engine cutoff the oxygen tank was pressurized with helium for 30 seconds in order to preclude the possibility of the hydrogen tank pressure exceeding the oxygen tank pressure and reversing the intermediate bulkhead. During this period the tank pressure increased to 21.4 N/cm^2 (31.1 psia). The hydrogen tank pressure began to increase after engine cutoff, reaching 16.8 N/cm^2 (24.4 psia) by T + 2420 seconds. The pressure remained at this level until the post-separation maneuver was initiated and the propellant flow relieved the tank pressure (last part of fig. VI-18).

Propulsion pneumatic subsystem: The engine controls regulator and the hydrogen peroxide bottle pressure regulator maintained proper system pressure levels throughout the flight. The engine controls regulator output pressure was 321 N/cm^2 (466 psia) at T - 0, while that of the hydrogen peroxide bottle pressure regulator was 220 N/cm^2 (319 psia). The engine controls regulator output increased to a maximum of approximately 324 N/cm^2 (472 psia) after about 43 minutes of flight. This level is within the specified range, whose upper limit is 327 N/cm^2 (475 psia).

Helium purge gas subsystem: The total helium purge flow rate to the vehicle just prior to launch was 86 kilograms per hour (190 lbm/hr) which is within specifications. The differential pressure across the insulation panels after hydrogen tanking was 0.09 N/cm^2 (0.13 psi). The minimum allowable differential pressure required to prevent cryopumping and icing is 0.02 N/cm^2 (0.03 psi). At approximately T - 12 seconds the airborne purge system was activated, and at T - 4 seconds the ground purge was terminated.

Nose fairing pneumatic subsystem: There was no airborne instrumentation for this system. However, the nose fairing was properly jettisoned, which indicated the system functioned properly.

TABLE VI-VIII. - ATLAS PNEUMATIC SYSTEM PERFORMANCE, AC-18

Performance parameter	Measurement	Units	Design range	Flight values at-						Remarks
				T - 10 sec	T - 0 sec	T + 20 sec	T + 24 sec	Booster engine cutoff	SECO/VECO[a]	
Oxidizer tank ullage pressure, gage	AF1P	N/cm^2 psi	(b) (c)	21.01 30.5	19.77 28.7	20.12 29.2 (d)	23.29 33.8 (e)	23.56 34.2	22.05 32.0 (f)	Normal
Fuel tank ullage pressure, gage	AF3P	N/cm^2 psi	44.1 to 46.16 64.0 to 67.0	46.16 67.0	44.30 64.3	44.65 64.8	44.65 64.8	46.09 66.9	38.58 56.0 (f)	Normal
Intermediate bulkhead differential pressure	AF116P	N/cm^2 psi	0.345 (min.) 0.5 (min.)	13.99 20.3	15.57 22.6	12.47 18.1	9.30 13.5	17.23 25.0 (g)	15.85 23.0	Lowest value was 8.61 N/cm^2 (12.5 psi) at T + 1 second
Engine controls helium bottle pressure, absolute	AF291P	N/cm^2 psi	2342.60 (max.) 3400 (max.)	2342.6 3400	2342.3 3400	2270.3 3295	2246.1 3260	2001.5 2905	1956.8 2840	Normal
Booster helium bottle pressure, absolute	AF246P	N/cm^2 psi	2342.60 (max.) 3400 (max.)	2342.6 3400	2294.4 3330	1801.7 2615	1691.5 2455	606.3 880	----- ----- (f)	Normal
Booster helium bottle temperature	AF247T	K ^oF	85.9 to 77.6 -305 to -320 (prior to T - 0)	79.15 -317	79.15 -317	72.72 -329	70.94 -332	48.17 -373	----- ----- (f)	Normal

[a]Sustainer engine cutoff/vernier engine cutoff.

[b]19.77 to 22.25 N/cm^2 (28.7 to 32.2 psi) prior to lift-off.

[c]22.05 to 24.12 N/cm^2 (32.0 to 35.0 psi) after T + 24 sec.

[d]Signal from programmer to fire programmed pressure conax valves.

[e]Liquid-oxygen-tank ullage pressure at termination of programmed pressure.

[f]Helium supply bottles (booster) jettisoned with booster engine package at 3 sec after booster engine cutoff.

[g]Off scale.

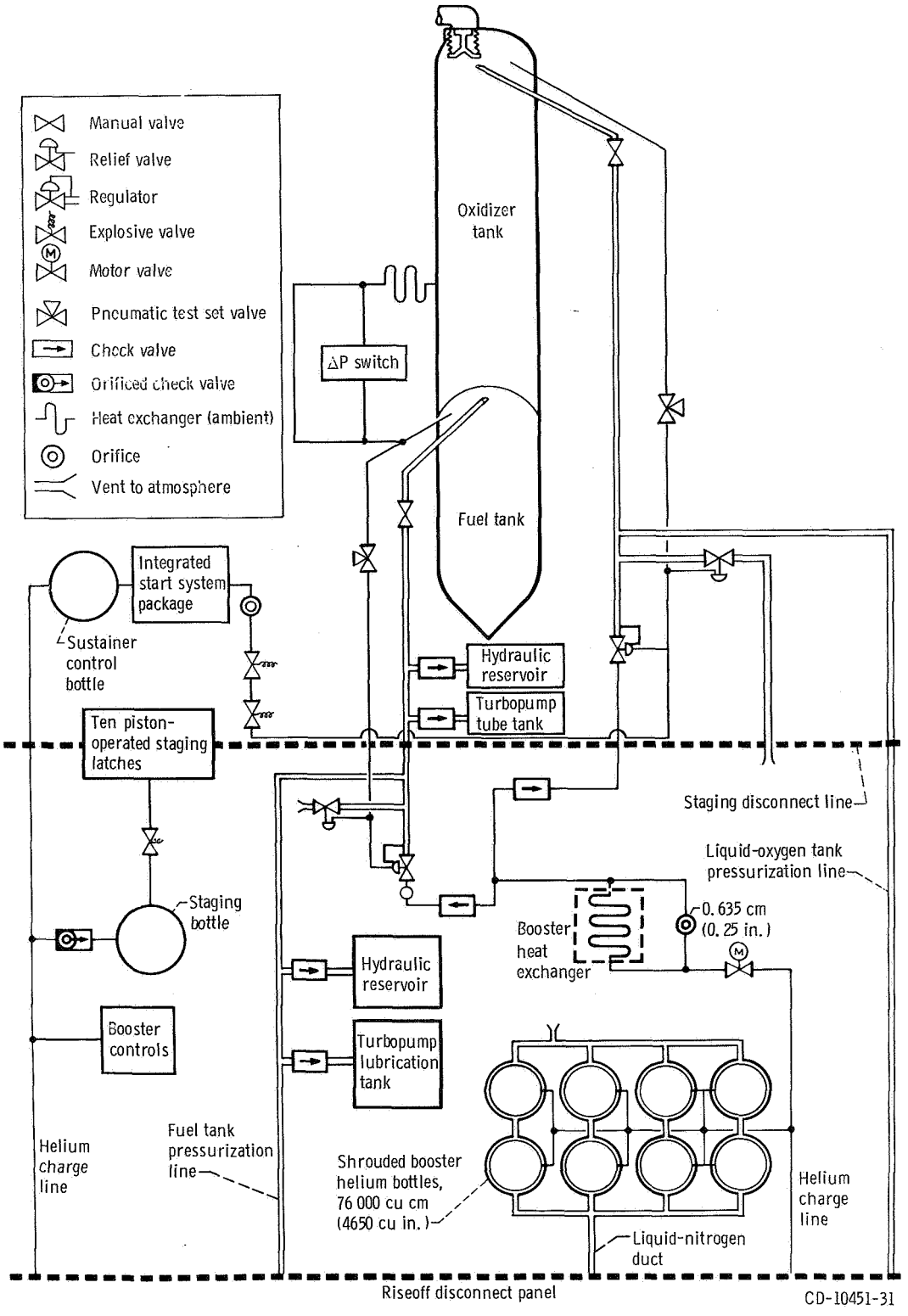

Figure VI-16. - Atlas vehicle pneumatic system, AC-18.

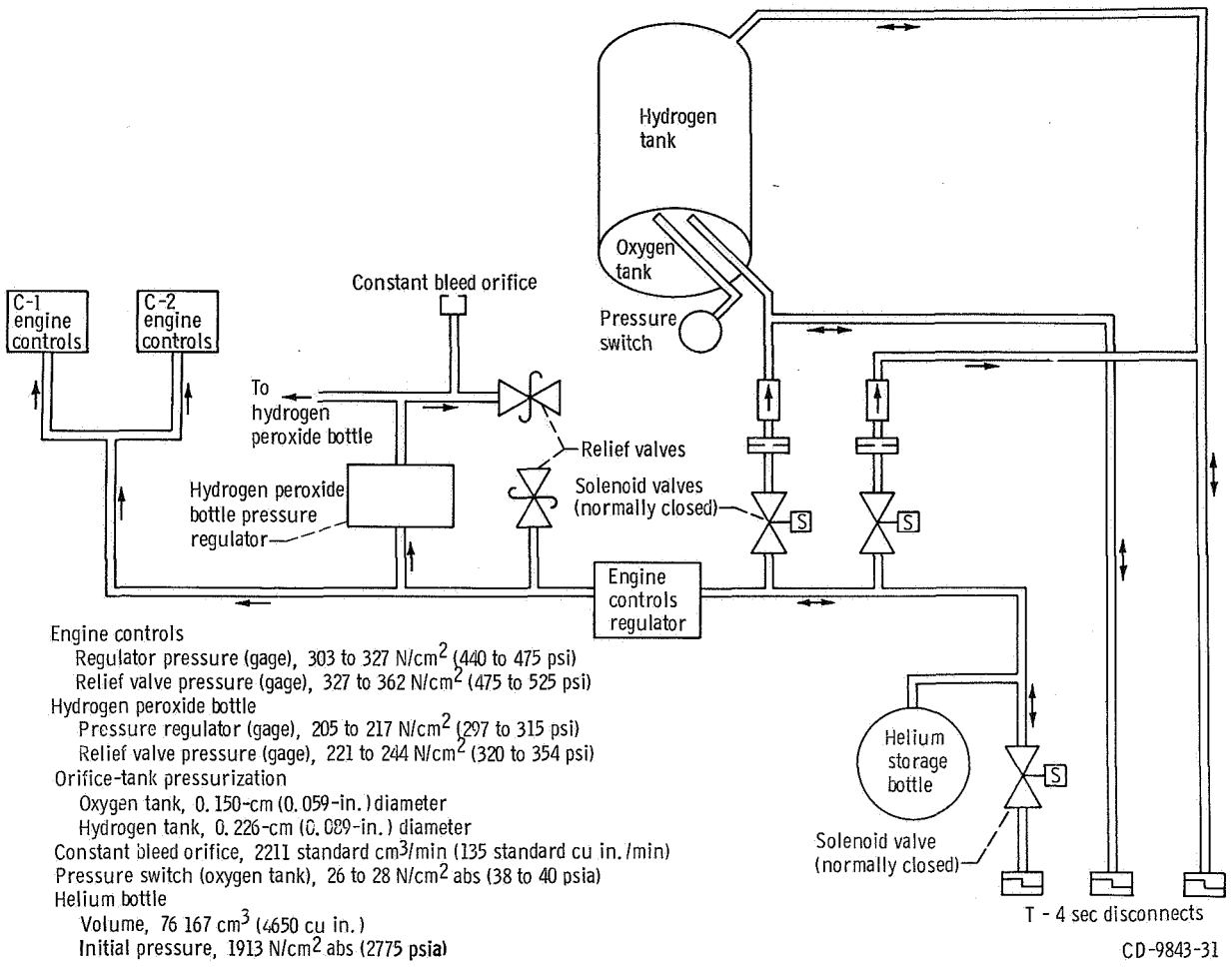

(a) Tank pressurization and propulsion pneumatics subsystems.

Figure VI-17. - Centaur pneumatics system, AC-18.

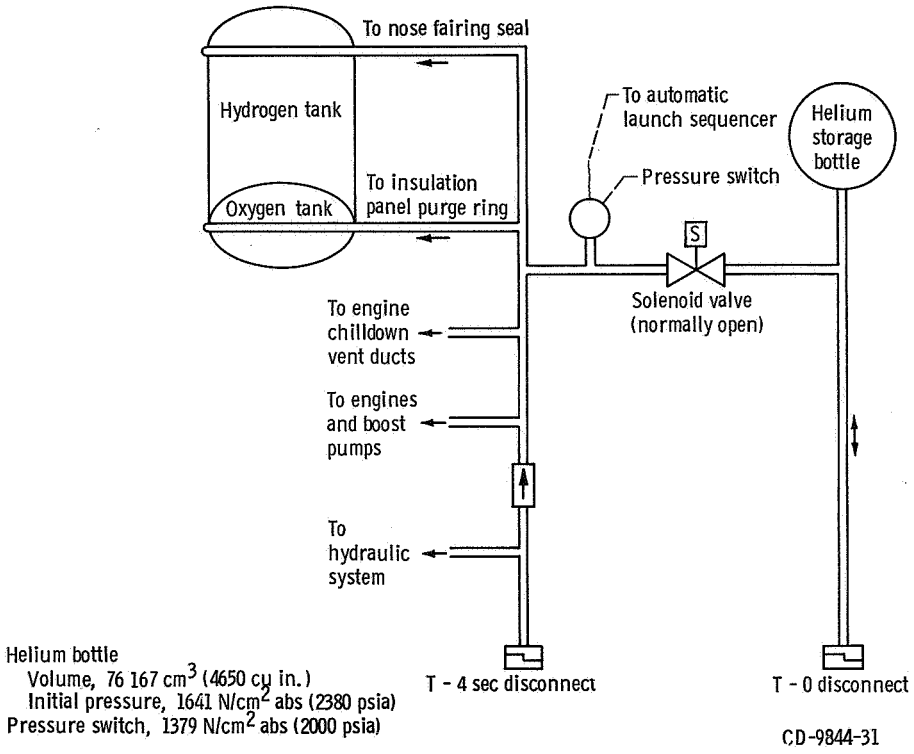

(b) Helium purge subsystem.

Figure VI-17. - Concluded.

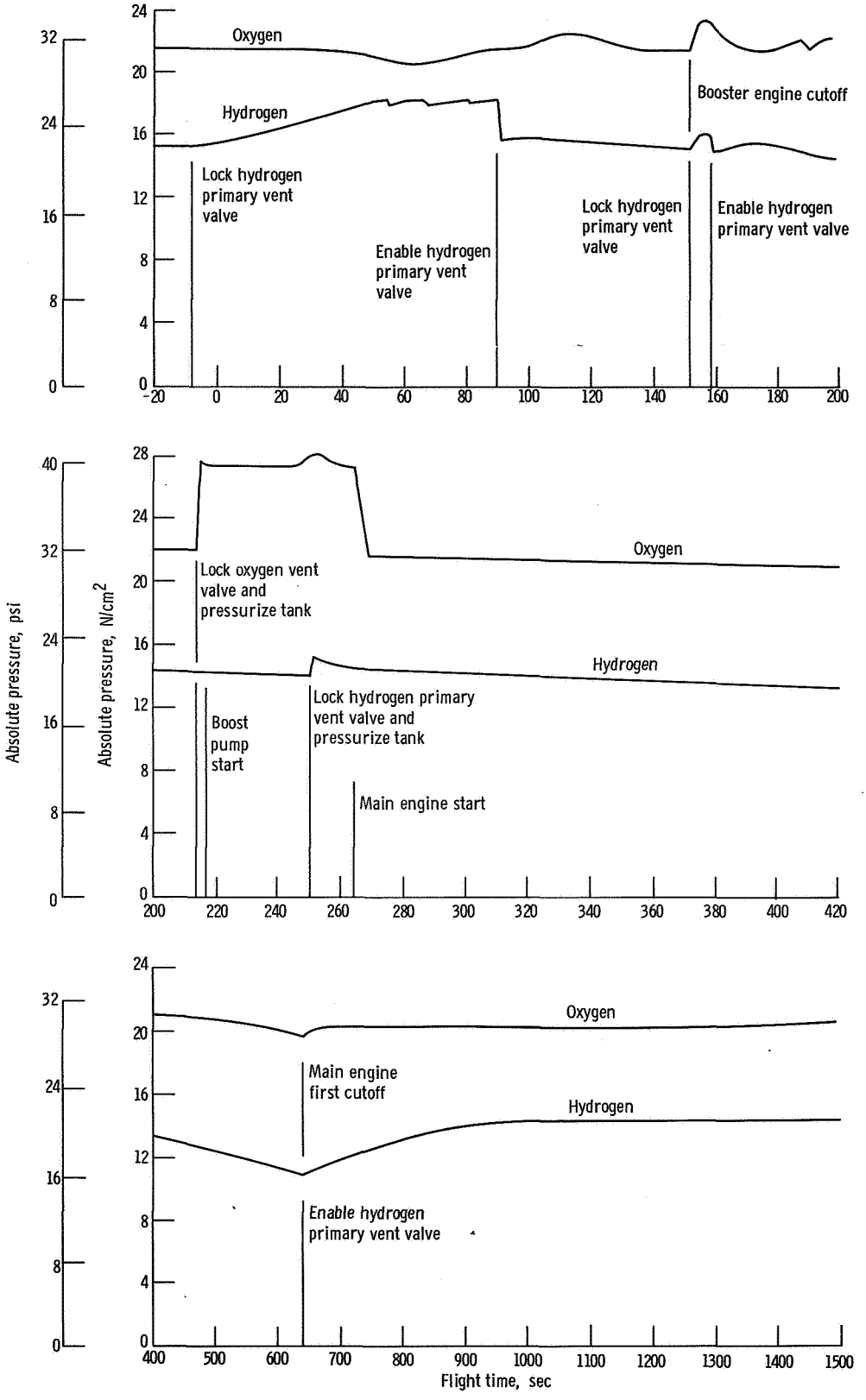

Figure VI-18. - Centaur tank pressure history, AC-18.

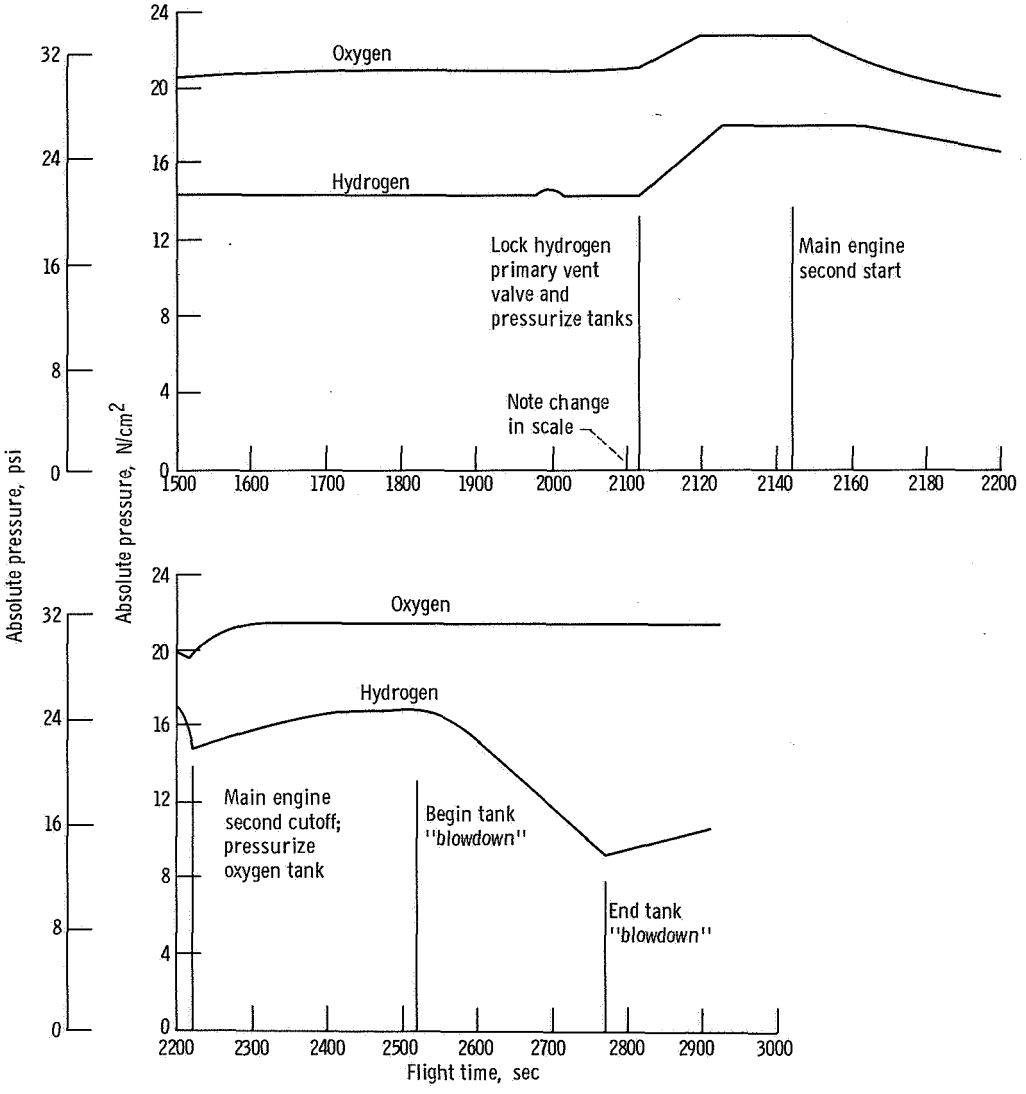

Figure VI-18. - Concluded.

HYDRAULIC SYSTEMS

by Eugene J. Fourney

Atlas

System description. - Two hydraulic systems (figs. VI-19 and VI-20) are used on the Atlas vehicle to supply fluid power for operation of sustainer engine control valves and for thrust vector control of all engines. One system is used for the booster engine thrust chambers and the other for the sustainer and vernier engines.

The booster hydraulic system provides power solely for gimbaling the two booster thrust chambers. System pressure is supplied by a single, pressure-compensated, variable-displacement pump driven by the engine turbopump accessory drive. Additional components of the system include four servocyclinders, a high-pressure relief valve, an accumulator, and a reservoir. Engine gimbaling in response to flight control commands is accomplished by the servocylinders, which provide separate pitch, yaw, and roll control during the booster engine phase of flight.

The sustainer and vernier hydraulic system is similar in components and function to the booster hydraulic system. In addition, the sustainer and vernier hydraulic system provides hydraulic power for sustainer engine control valves and for gimbaling of the two vernier engines. Vehicle roll control is accomplished during the sustainer phase by differential gimbaling of the vernier engines.

System performance. - Atlas hydraulic system performance was normal throughout the flight. Pressures were stable. The transfer of fluid power from ground to airborne hydraulic systems was normal. Pump discharge absolute pressures increased from 1240 N/cm^2 (1800 psi) at T - 2 seconds to flight levels of 2172 N/cm^2 (3150 psi) in less than 2 seconds. Starting transients produced a normal overshoot of about 10 percent in the pump discharge pressures. Flight data for the AC-18 Atlas hydraulic system are presented in table VI-IX.

Centaur

System description. - Two separate but identical hydraulic systems shown in figure VI-21, are used on the Centaur stage. Each system gimbals one main engine for pitch, yaw, and roll control. Each system consists of two servocylinders and an engine-coupled power package which contains a high- and a low-pressure pump, a reservoir, an accumulator, a pressure-intensifying bootstrap piston, and relief valves for pressure regulation. High pressure and flow are provided by a constant-displacement vane-type pump driven by the liquid-oxygen-turbopump accessory drive shaft. An electrically

powered recirculation pump is used to provide low pressure and flow for engine gimbaling requirements during prelaunch checkout, to aline the main engines prior to main engine start, and for limited thrust vector control during the Centaur post-separation maneuver.

System performance. - The hydraulic system performed properly throughout the flight. System pressures and temperatures were normal. System performance data are presented in table VI-X. The C-1 and C-2 hydraulic recirculation pumps were commanded on for 15 seconds by a Centaur timer discrete 11 seconds prior to main engine first start to null the C-1 and C-2 engines. The C-1 and C-2 main hydraulic pumps increased system pressure to normal flight levels after engine start. At main engine first cutoff the hydraulic pumps stopped and the system pressures decreased normally to zero.

After a 25-minute coast period the main engines were restarted for the second powered phase. Twenty-eight seconds prior to main engine second start the C-1 and C-2 hydraulic recirculation pumps were commanded on for 48 seconds by a Centaur timer discrete in order to null the C-1 and C-2 engines. After main engine start the C-1 and C-2 main hydraulic pumps increased system pressure to normal flight levels. At second main engine cutoff the hydraulic pumps stopped and the system pressures decreased normally to zero.

At the start of the post-separation maneuver the C-1 and C-2 recirculation pumps were commanded on for 250 seconds to provide limited thrust vector control during this maneuver.

TABLE VI-IX. - ATLAS HYDRAULIC SYSTEM PERFORMANCE, AC-18

Performance parameter	Measurement	Units[a]	T - 20 sec	Peak pressure prior to lift-off	Lift-off	Booster engine cutoff	SECO/VECO[b]	Remarks
Booster hydraulic pump discharge pressure	AH3P	N/cm^2 psi	10.14 14.7	2316.7 3360	2171.9 3150	2123.6 3080	------ ------	Normal
Booster hydraulic accumulator pressure	AH33P	N/cm^2 psi	1241.1 1800	2440.8 3540	2102.9 3050	2061.6 2990	------ ------	Normal
Booster hydraulic system return pressure	AH224P	N/cm^2 psi	49.6 72	57.9 84	57.9 84	57.9 84	------ ------	Normal
Sustainer/vernier hydraulic pump discharge pressure	AH130P	N/cm^2 psi	0 0	2206.4 3200	2109.8 3060	2109.8 3060	2109.8 3060	Normal
Sustainer/vernier accumulator pressure	AH140P	N/cm^2 psi	1275 1850	2220.2 3220	2116.8 3070	2116.8 3070	2116.8 3070	Normal
Sustainer/vernier system return pressure	AH601P	N/cm^2 psi	53.8 78	53.8 78	53.8 78	49.6 72	49.6 72	Normal transients at engine start and shutdown; smooth rest of the flight

[a]All pressures are absolute.

[b]Sustainer engine cutoff/vernier engine cutoff.

TABLE VI-X. - CENTAUR HYDRAULIC SYSTEM PERFORMANCE, AC-18

Performance parameter	Measurement	Units	Flight values at-					
			Main engine first start (MES-1)	MES-1 + 10 sec	Main engine first cutoff (MECO-1)	Main engine second start (MES-2)	MES-2 + 10 sec	MECO-2
C-1 power package pressure, absolute	CH1P	N/cm^2 psi	84.0 122	795 1155	780 1135	84.0 122	795 1155	784 1140
C-1 manifold temperature	CH5T	K ^oF	295 70	299 78	351 172	326 128	335 143	346 164
C-2 power package pressure, absolute	CH3P	N/cm^2 psi	84.5 123	792 1152	781 1137	84.5 123	792 1152	781 1137
C-2 manifold temperature	CH6T	K ^oF	295 70	299 78	346 164	322 121	335 143	346 164

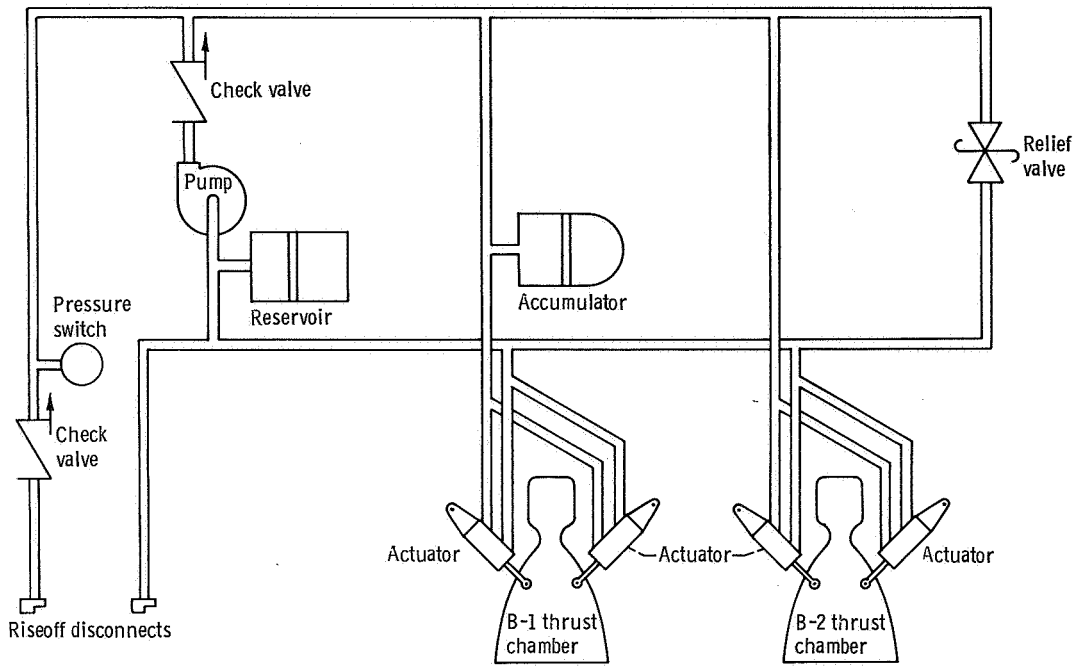

Figure VI-19. - Atlas booster hydraulic system, AC-18.

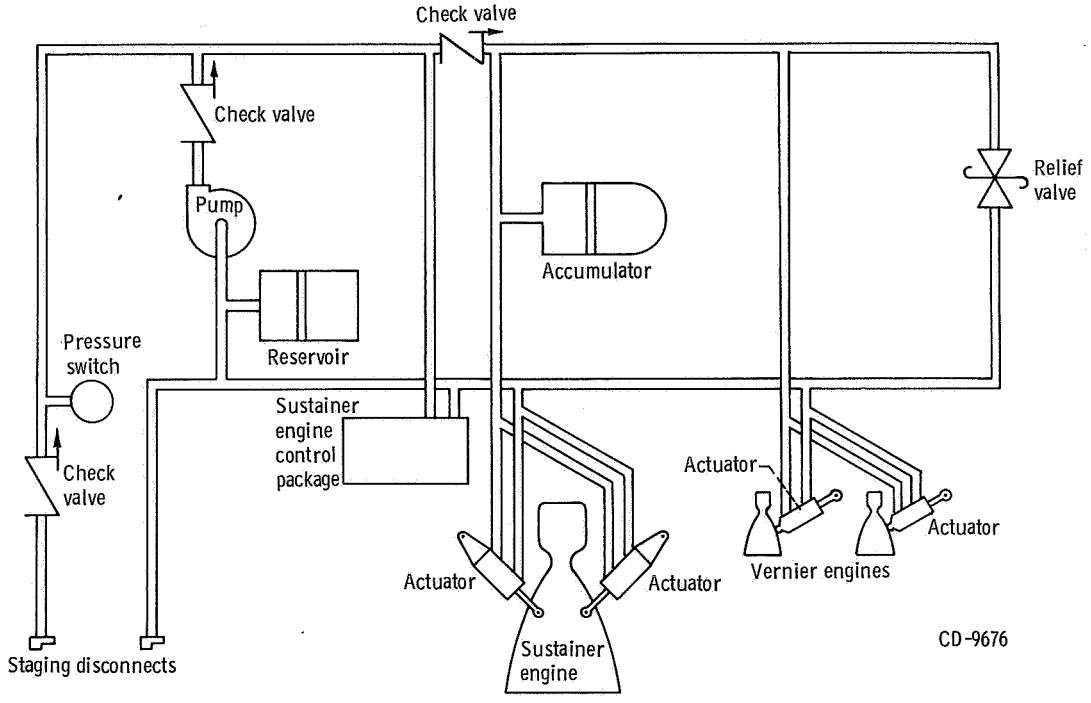

Figure VI-20. - Atlas sustainer hydraulic system, AC-18.

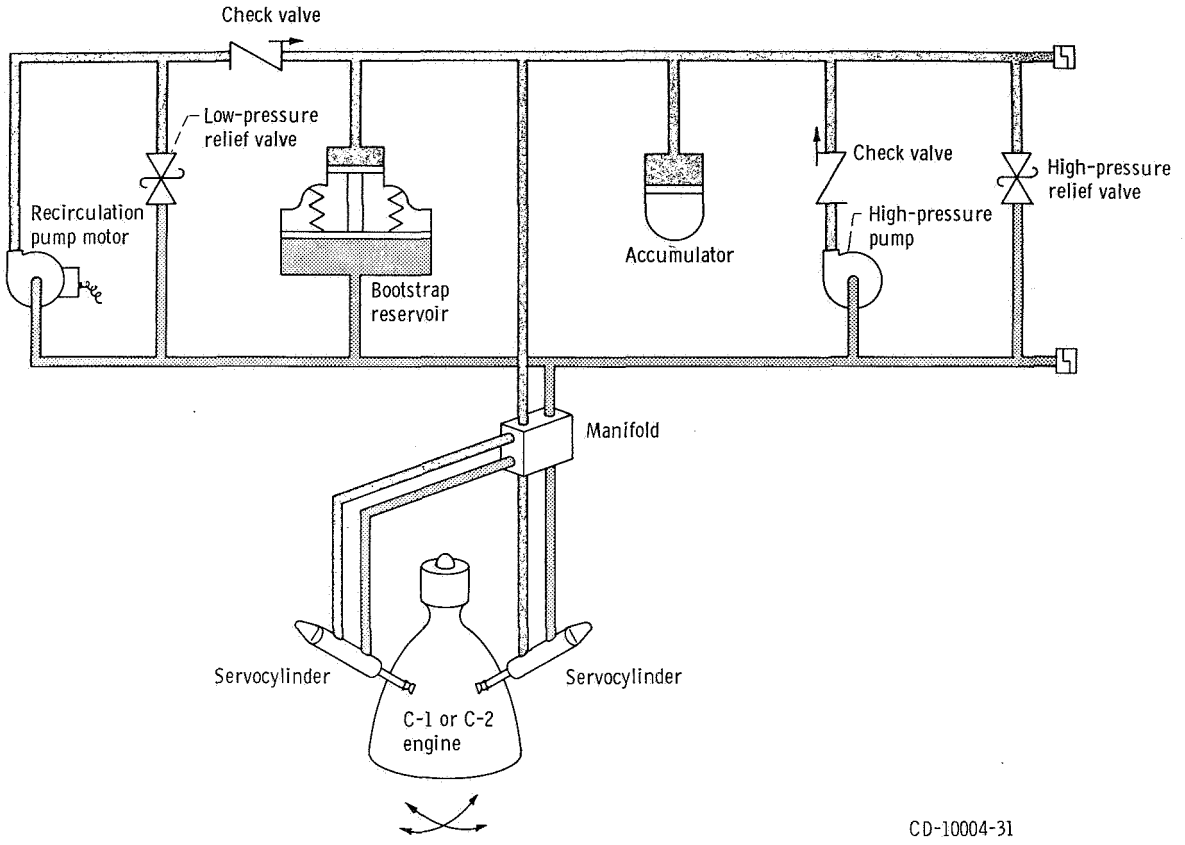

Figure VI-21. - Centaur hydraulic system, AC-18.

STRUCTURES

by James F. Harrington, Joseph E. Olszko, Richard T. Barrett,
Dana H. Benjamin, Thomas L. Seeholzer,
and Robert C. Edwards

Atlas and Interstage Adapter

System description - Atlas. - The Atlas structure consists primarily of a tank section and a jettisonable booster engine section. The forward end of the tank section mates with the interstage adapter and supports the Centaur and payload. The aft end mates with the booster engine section and supports the thrust loads of the booster and sustainer engines. The tank section is divided into a fuel tank and an oxidizer tank by an intermediate bulkhead. An ellipsoidal bulkhead encloses the forward end of the tank section and a thrust cone encloses the aft end. The sustainer engine is mounted on the thrust cone. Fairings on the tank section protect electronic equipment.

The primary structure is the propellant tanks. These tanks are thin-walled, pressure-stabilized, monocoque sections of welded stainless-steel construction (fig. VI-22). They require internal pressure in order to maintain structural stability. The tensile strength of the tank material determines the maximum allowable pressure in the propellant tanks.

The maximum allowable and minimum required tank pressures are presented in figure VI-23. They are computed using maximum design loads (as opposed to actual flight loads) with appropriate factors of safety. These tank pressure limits are not constant because aerodynamic loads, inertia loads, and ambient pressure vary during flight.

The Atlas vehicle is subjected to its highest bending load between T + 40 and T + 110 seconds. The bending, inertia, and aerodynamic drag create compressive loads in the fuel and oxidizer tank skin. These loads are resisted by internal pressure to prevent buckling of the skin.

The maximum allowable differential pressure between the oxidizer and fuel tanks is limited by the strength of the Atlas intermediate bulkhead. The fuel tank pressure must always be greater than the oxidizer tank pressure to stabilize the intermediate bulkhead (prevent bulkhead reversal).

This flight utilized an Atlas which was structurally damaged in the tank section during preparation for a previous mission. The six forward cylindrical skins were replaced.

The booster engine section structure consists of a thrust cylinder, nacelles, and fairings which house the booster engines and associated equipment.

This section is attached to the tank section by 10 helium-gas-operated latch mechanisms. These latches, as shown in figures VI-24(a) and (b), are located circumferen-

tially around the Atlas aft bulkhead thrust ring at station 1133. An explosive actuated valve supplies helium at a gage pressure of 2068 N/cm^2 (3000 psi) to the distribution manifold. The actuation of the latch mechanism results in the disengagement of the booster engine from the Atlas vehicle. Two jettison tracks (fig. VI-25) attached to the thrust ring are used to guide the booster engine section as it separates from the Atlas.

System description - interstage adapter. - The interstage adapter structure is a cylinder of aluminum skin and stringer construction that provides the structural tie between the Atlas and Centaur stages.

The Atlas/Centaur staging system, shown in figure VI-26, consists of a flexible linear shaped charge mounted circumferentially which severs the forward end of the interstage adapter at Centaur station 413; Atlas deceleration is provided by eight retrorockets mounted near the aft end of the Atlas.

System performance. - The Atlas ullage and bulkhead differential pressure profiles are compared with the design limits in figure VI-23. The Atlas oxidizer and fuel tank ullage pressures did not approach the maximum allowable pressure during flight. The oxidizer and fuel tank ullage pressures were greater than the minimum required to resist the combined bending and axial design loads between T + 40 seconds and T + 110 seconds. The bulkhead differential pressure was also within the maximum allowable and minimum required pressure limits for all periods of flight.

The increase of longitudinal inertia force was as expected. A maximum value of 5.65 g's was reached at booster engine cutoff. This value was less than the 5.813 g's maximum allowable.

Booster engine cutoff (BECO) occurred at T + 151.8 seconds and booster engine section staging occurred at T + 154.9 seconds. Staging was verified by data from the B-1 booster thrust chamber pitch actuator position instrumentation and from the vehicle axial (fine) accelerometer.

Atlas/Centaur staging was successful. Vehicle staging was commanded at T + 253.5 seconds and the flexible linear shaped charge severed the interstage adapter at station 413. The eight retrorockets, mounted around the aft end of the Atlas, fired 0.1 second later to decelerate the Atlas and provide separation from the Centaur. Accelerometer and other data indicated that all eight retrorockets functioned as expected for the flight. Figure VI-27 shows the separation distance between the Atlas and Centaur vehicles for the flight versus time. This figure also indicates clearance losses due to pitch and yaw motions of Atlas during separation.

The shaped-charge firing time, retrorocket firing time, and the results of the pitch and yaw motions as the Atlas cleared the aft end of the Centaur engines:

Shaped-charge firing time, sec	T + 253.51
Retrorocket firing time, sec	T + 253.61
Pitch clearance, nominal, cm (in.)	27.9 (11)
Pitch clearance loss, cm (in.)	4.60 (1.8)
Pitch clearance, actual, cm (in.)	23.3 (9.2)
Yaw clearance, nominal, cm (in.)	78.7 (31)
Yaw clearance loss, cm (in.)	10.7 (4.2)
Yaw clearance, actual, cm (in.)	68 (26.8)

Centaur

System description. - The Centaur structures consist of propellant tanks with an intermediate bulkhead, main engine thrust barrel, electronic equipment mounting structure, and adapters to attach the payload.

The Centaur primary vehicle structure is provided by the propellant tanks. These tanks are thin-walled, pressure-stabilized, monocoque sections of welded stainless-steel construction (fig. VI-28). They require internal pressure in order to maintain structural stability. The tensile stregnth of the tank material determines the maximum allowable pressure in the propellant tanks.

The tank locations and criteria which determine the maximum allowable and minimum required tank pressures during different phases of flight are described in figure VI-29. The maximum allowable and minimum required tank pressures presented in figure VI-30 are computed using maximum design loads (as opposed to actual flight loads) with appropriate factors of safety. These tank pressure limits are not constant because of varying loads and varying ambient pressure during flight.

The margin between oxidizer tank pressure and the maximum allowable pressure is least at booster engine cutoff (T + 151.8 sec), when the high inertia load causes maximum tension stresses on the aft bulkhead (fig. VI-30). The minimum required oxidizer tank pressure for intermediate bulkhead stability is always greater than the minimum pressure required for aft bulkhead stability.

The strength of the fuel tank is governed by the capability of the conical section of the forward bulkhead to resist hoop stress. Thus, the differential pressure across the forward bulkhead determines the maximum allowable fuel tank pressure.

The margin between fuel tank ullage pressure and the minimum required pressure is least during the following times:

(1) Prior to launch, when the payload and nose fairing impose compression loads on the cylindrical skin at station 409.6 because of gravity and ground winds

(2) From T + 0 to T + 10 seconds, when the payload and nose fairing impose compression loads on the cylindrical skin at station 409.6 from the longitudinal and lateral inertial loads and from the vibration loads

(3) From T + 40 to T + 110 seconds, when the Centaur is subjected to maximum bending moments (The combined loads from inertia, aerodynamic drag, and bending impose compression on the cylindrical skin at station 409.6.)

(4) At nose fairing jettison, when the nose fairing exerts inboard radial loads at station 218.9

The maximum differential pressure between the oxidizer and fuel tanks is limited by the strength of the Centaur intermediate bulkhead. This maximum allowable differential pressure is 15.9 N/cm^2 (23.0 psi). The oxidizer tank pressure must always be greater than the combined fuel tank pressure and hydrostatic pressure of the liquid hydrogen to stabilize the intermediate bulkhead (prevent bulkhead reversal).

There are three adapters that provide the structural tie between the Centaur and the separable payload (figs. III-3 and III-4). The aft adapter mounts on the Centaur forward bulkhead, the transition adapter mounts on the aft adapter, and the spacecraft adapter mounts on the transition adapter. The aft adapter is a truncated cone of aluminum sheet and stringer construction. The transition adapter is an inverted truncated cone of aluminum sheet and stringer construction with a fiber-glass thermal diaphragm containing air-conditioning ducts and nozzles. It is a new design similar to the adapter used on Surveyor missions. The spacecraft adapter is provided by the spacecraft agency. The spacecraft is attached to the spacecraft adapter by a V-band clamp. Two explosive bolts, located 180° apart in the clamp, are fired by the Centaur. Each explosive bolt contains one squib with dual bridgewires. When the bolts are severed, the V-band clamp is released and 10 springs between the spacecraft and the adapter provide the separation force. Eight lanyards and tension springs, attached from the periphery of the V-band to the spacecraft adapter, limit band excursion.

System performance. - The Centaur fuel and oxidizer tank ullage pressure profiles are compared with the design limits in figure VI-30.

The oxidizer tank pressure was less than the maximum allowable at booster engine cutoff and all other periods of flight. The oxidizer tank pressure was maintained above the minimum required for aft bulkhead stability during all periods of flight. The fuel tank ullage pressure was above the minimum required pressure and was below the maximum allowable pressure during all periods of flight.

The differential pressure across the Centaur intermediate bulkhead was less than the maximum allowable for all periods of flight. The oxidizer tank ullage pressure was always greater than the combined fuel tank ullage pressure and liquid-hydrogen hydrostatic pressure.

The spacecraft was successfully separated from the Centaur vehicle at T + 2349 seconds.

Jettisonable Structures

System description. - The Atlas-Centaur vehicle jettisonable structures are the hydrogen tank insulation panels and a nose fairing. The hydrogen tank insulation consists of four polyurethane-foam-filled fiber-glass honeycomb panels bolted together along the longitudinal axis to form a cylindrical cover around the Centaur tank. The panels are bolted at their aft end to a support on the Centaur vehicle (fig. VI-31). At the forward end, a circumferential Tedlar and fiber-glass laminated cloth forms a seal between the panels and the base of the nose fairing at station 219 (fig. VI-32). Separation of the four insulation panels is accomplished by firing of flexible linear shaped charges located at the forward, aft, and longitudinal seams. The shaped charge at the panel forward seam simultaneously severs the aft attachment of the nose fairing preparatory to fairing jettison at a later time in flight. Immediately following shaped-charge firing, the panels rotate about hinge points at their aft end (fig. VI-33) from the preload hoop tension, the center-of-gravity offset, and the in-flight residual purge pressure. The panels jettison free of the Centaur vehicle after approximately 45^{o} of panel rotation on the hinge pins.

The nose fairing is a fiber-glass skin and honeycomb structure of the type used on Surveyor missions. It consists of a cylindrical section approximately 1.83 meters (6 ft) long bolted to a conical section approximately 4.87 meters (16 ft) long. It is assembled in two jettisonable halves with the split line along the X-X axis as shown in figure VI-34. A subliming agent is applied to the fairing to limit temperature to maintain structural integrity.

In addition to the flexible linear shaped charge which severs the aft attachment, the nose fairing separation system consists of latches and thrusters. Eight pyrotechnically operated pin-puller latches release the fairing halves along the split line, as shown in figure VI-34. Separation force is provided by two nitrogen gas thrusters located at the forward end of the nose cone, one in each fairing half. Each fairing half is hinged at a single point on the Centaur hydrogen tank at station 219 on the Y-Y axis (fig. VI-34).

The following modifications were made to the Surveyor-type nose fairing for the ATS mission:

(1) Two 22.8-centimeter (9-in.) access doors, two electrical disconnects and harness assemblies, and four antenna ramps were added.

(2) Removable metal air-conditioning ducts replaced fiber-glass ducts bonded to the fairing.

(3) Split lines of the thermal bulkhead were modified to clear the transition adapter at nose fairing jettison.

(4) One split-line nose fairing longeron was notched to clear a spacecraft antenna.

System performance. - Flight data indicated that the insulation panels were jettisoned satisfactorily. The insulation panel jettison sequence was inititated by a command

signal issued from the Atlas programmer at T + 196.54 seconds. Following issuance of the command, the linear shaped charge fired to sever the panel attachments. Shaped-charge firing times were determined from accelerometers mounted on the payload aft adapter.

At 35° of panel rotation, breakwire transducers provided event time data. These transducers were attached to one hinge arm of each panel, as shown in figure VI-35. Since the breakwire data were monitored on commutated channels, the panel 35° position event times in the following table are mean times:

Insulation panel location, quadrant	Instrumented hinge arm location, quadrant	Insulation panel 35° rotation position event time, sec
I - II	1	T + 196.98
II - III	3	T + 196.99
III - IV	3	T + 196.97
IV - I	1	T + 196.98

The rotational velocity of each panel, assuming first motion at shaped-charge firing, was determined from the mean time of the 35° position. Panel velocities are presented in the following table:

Insulation panel location, quadrant	Insulation panel average rotational velocities from shaped-charge firing to mean time of 35° position, sec
I - II	80.2
II - III	78.4
III - IV	83.4
IV - I	80.1

The vehicle rates and dynamics response data indicated a completely satisfactory insulation panel jettison sequence.

The nose fairing was successfully jettisoned. The nose fairing jettison system was initiated by a command from the Atlas programmer at T + 233.3 seconds. The eight pyrotechnically operated pin pullers then unlatched the nose fairing split line. Approximately 0.5 second later the two nitrogen thrusters operated, causing the fairing halves to begin rotation about their hinge points. Nose fairing latch actuation and initiation of

the thruster operation were determined from accelerometer data. Rotation of each fairing half was sensed by disconnect pins in the electrical connectors, which separated after approximately 3^{o} of fairing rotation. The following table summarizes significant nose fairing separation event times:

Event	Nose fairing jettison time, sec
Split-line latch actuation	T + 232.791
Nitrogen thruster actuation	T + 233.301
3^{o} rotation position	[a]T + 234.433
(each fairing half)	[a]T + 234.433

[a]Commutated data.

During fairing jettison the payload compartment pressure remained at zero with no pressure surge occurring at thruster bottle discharge.

Vehicle Dynamic Loads

The Atlas-Centaur launch vehicle experiences dynamic loads from three major sources: (1) aerodynamics and acoustics; (2) transients from engines starting and stopping and from the separation systems; and (3) dynamic coupling between major systems.

The instruments used on AC-18 to determine dynamic loads and the parameters measured are

Instruments	Corresponding parameters
Low-frequency accelerometer	Vehicle longitudinal acceleration and vibration
Low-frequency accelerometers (6)	Spacecraft transition adapter longitudinal and tangential acceleration
Centaur pitch-rate gyro	Vehicle pitch-plane angular rate
Centaur yaw-rate gyro	Vehicle yaw-plane angular rate
Angle-of-attack sensor	Vehicle aerodynamic loads
High-frequency accelerometers (2)	Local spacecraft vibration

Launch vehicle longitudinal vibrations measured on this flight are compared with those of four other flights in figure VI-36. The frequency and amplitude of all other vibration data measured on AC-18 are shown in table VI-XI.

Longitudinal vibrations were excited at lift-off due to launch release transients. The amplitude and frequency of these vibrations were similar to those observed on prior vehicles. Atlas intermediate bulkhead pressure oscillations were the most significant effects produced by the launcher-induced longitudinal vibrations. These oscillations presented no problem because the measured minimum differential pressure was 11.2 N/cm^2 (16.2 psi, fig. VI-23), while the minimum design allowable differential pressure across the bulkhead was 1.4 N/cm^2 (2.0 psi).

Between T + 91 and T + 149 seconds, intermittent longitudinal vibrations of 0.06 g, 12 hertz were observed on the Atlas fuel tank skin. These vibrations are caused by dynamic coupling between structure, engines, and propellant lines (commonly referred to as "POGO"). For a detailed discussion of this "POGO" effect see reference 1.

During Atlas booster engine thrust decay, short-duration longitudinal vibrations of 0.7 g, 14 hertz were observed. Post-flight load analysis indicate that these transients did not produce any significant structural loading.

During the Atlas booster phase of flight the vehicle vibrates in the pitch and yaw planes as an integral body at its natural frequencies. Previous analyses and tests have defined these natural frequencies and the modes which the vehicle assumes when it is dynamically excited. The rate gyros on the Centaur provide data for determining modal deflections. The maximum first-mode deflection occurred in the pitch plane at T + 141 seconds (fig. VI-37). This pitch deflection was less than 6 percent of the allowable. The maximum second-mode deflection occurred in the yaw plane at T + 31 seconds (fig. VI-38). The yaw deflection was less than 25 percent of the allowable.

Structural loading due to upper-air winds is minimized during the booster phase of Atlas flight by the preflight selection of pitch and yaw programs from within a family of available preset programs. The pitch and yaw programs are chosen just prior to launch on the basis of calculated vehicle response to measured upper-air wind profiles. The wind profiles are obtained from weather balloons released at established intervals during the hours prior to launch. The programs selected are those that are calculated to give the least critical predicted peak booster engine gimbal angle and predicted peak vehicle structural load.

Vehicle structural loads are expressed as structural capability ratios, the ratios of predicted load to allowable load at each of the locations being considered. Structural capability ratio is the algebraic sum of the ratio of predicted to allowable axial load plus the ratio of predicted to allowable bending moment. Predicted bending moment includes the root-sum-square of bending moments due to random dispersions, in addition to the bending moments calculated to result from angles of attack predicted from measured wind profiles.

The flight time envelope of maximum predicted structural capability ratios for this flight is shown in figure VI-39. The peak structural capability ratio predicted for this flight was 0.74 at station 906 at T + 86 seconds. These capability ratios are based on pitch program 31, yaw program 0, and the calculated response to the winds measured by the T-minus-48-minute weather balloon.

Angles of attack experienced during actual flight are computed from differential pressure measurements in the fairing nose cap. Figures VI-40 and VI-41 compare these pitch and yaw angle-of-attack histories to those calculated from the winds measured by the T - 48 minute weather balloon. Analysis of dynamic pressure and angle-of-attack data showed the structural capability ratio was maximum at T + 87.5 seconds and occurred 1.5 seconds later than the predicted time of T + 86.0 seconds. The combined pitch and yaw angle of attack at T + 87.5 seconds slightly exceeded the maximum value predicted to occur at T + 86.0 seconds. This would indicate that the actual structural capability ratio slightly exceeded the predicted value of 0.74 at the critical Atlas station 906. However, the predicted structural capability ratio equation includes a sizeable allowance for dispersions. From an evaluation of the flight dispersions, it was judged that the actual dispersions were appreciably less than the equation allowance. It was therefore concluded that the maximum structural capability ratio was no greater than the predicted value of 0.74.

Local shock and vibration were measured by two piezoelectric high-frequency accelerometers installed on the spacecraft adapter inner surface at Centaur station 113. These accelerometers together with their amplifiers had a flat frequency response to 2100 hertz. However, the telemetry channel Inter-Range Instrumentation Group (IRIG) filter frequency was less than 2100 hertz. Therefore, the frequency range (for unattenuated data) was limited by the standard IRIG filter frequency for that channel. An analysis of the flight data indicated that the two telemetry channels which transmitted the high-frequency accelerometer data were cross connected. However, no data were lost due to this anomaly.

In addition to these accelerometers, there were six low-frequency accelerometers located on the payload transition adapter at Centaur station 148. Three accelerometers were sensitive in the tangential and three in the longitudinal directions.

A summary of the most significant shock and vibration levels measured by these eight accelerometers on AC-18 is shown in table VI-XI. The vibration levels were highest near lift-off, as expected. The maximum shock loads (over 20 g's) occurred at insulation panel jettison, Atlas/Centaur separation, and spacecraft separation. These shock loads were of short duration (about 0.025 sec) and did not provide significant loads.

TABLE VI-XI. - MAXIMUM SHOCK AND VIBRATION LEVELS OBSERVED AT MARK EVENTS, AC-18

Time of dynamic disturbance, sec after lift-off	Mark event	Acceleration in g's; and frequency in Hz	Accelerometer measurement number							
			CY113O	CY114O	CA647A	CA648A	CA649A	CA650A	CA651A	CA652A
			Accelerometer station location (referenced to Centaur stations)							
			113	112	148					
			Axis or direction of sensitivity							
			Radial	Longitudinal				Tangential		
			Accelerometer system gain of 0 db limited to approximately-							
			2100 Hz		100 Hz			70 Hz		
			Standard telemetry channel cutoff filter frequency, Hz							
			790	790	110	160	220	330	450	600
			Accelerometer range, g's							
			±20		-2.9 to 8.9			-1.14 to 1.16		
1.0 to 5.0	Launch	g's (rms) g's (zero to peak) Hz	3.7 13.5 400	2.5 8.5 540	0.33 ---- 0.9 [a]0.8 200 [a]150	0.58 ---- 1.6 [a]1.5 270 [a]290	0.87 2.7 250	0.29 0.95 120	0.24 0.75 110	0.41 1.0 120
58 to 62	Transonic region	g's (rms) g's (zero to peak) Hz	1.1 4.1 380	0.76 2.8 540	0.09 0.26 200	0.18 0.6 250	0.26 0.9 [a]0.9 250 [a]290	0.10 0.27 150	0.10 0.25 140	0.11 0.24 130
151.76	Booster engine cutoff	g's (zero to peak) Hz	0.7 500	0.6 540	0.6 13	0.5 13	0.6 13	0.20 75	0.16 75	0.16 [a]0.12 75 [a]6
154.85	Booster jettison	g's (zero to peak) Hz	(b) (b)	(b) (b)	(b) (b)	(b) (b)	(b) (b)	0.05 5.1	0.05 5.2	0.08 5.2
196.49	Insulation panel jettison	g's (zero to peak) Hz	(c) 550	(c) 550	0.8 29	1.0 29	1.0 29	0.4 100	0.3 50	0.4 100
233.26	Nose fairing jettison	g's (zero to peak) Hz	3.7 400	1.3 [a]2.6 30 [a]540	1.0 33	1.0 33	1.1 33	0.37 25	0.34 33	0.28 25
251.59	Sustainer engine cutoff	g's (zero to peak) Hz	(d) (d)	(d) (d)	0.3 85	0.2 85	0.2 85	0.4 85	0.35 85	0.35 85
253.57	Atlas/Centaur separation	g's (zero to peak) Hz	(c) 520	(c) 520	0.1 30	0.1 30	0.1 30	0.34 100	0.30 100	0.32 100
263.06	Main engine first start	g's (zero to peak) Hz	0.5 200	0.4 30	0.30 30	0.36 30	0.24 30	0.07 17	0.05 17	0.04 17
639.00	Main engine first cutoff	g's (zero to peak) Hz	(d) (d)	2.1 39	1.4 33	1.5 33	1.5 33	0.16 20	0.11 20	0.14 20
2143.14	Main engine second start	g's (zero to peak) Hz	(d) (d)	1.1 29	0.74 30	0.64 30	0.70 30	0.32 [a]0.16 33 [a]20	0.39 [a]0.16 33 [a]20	0.16 [a]0.08 33 [a]20
2213.94	Main engine second cutoff	g's (zero to peak) Hz	1.1 380 to 400	2.4 32	1.4 33	1.6 33	1.5 33	0.2 30	0.2 50	0.2 30
2348.99	Spacecraft separation	g's (zero to peak) Hz	(c) 430	(c) 520	2.3 100	1.6 70	2.4 100	0.4 100	0.4 100	0.5 70

[a]Double entries indicate that the recorded vibration consisted of two or more predominant frequencies.

[b]Telemetry signal dropout.

[c]The maximum amplitude observed for this flight event exceeded the intelligence band for its telemetry channel.

[d]No detectable response.

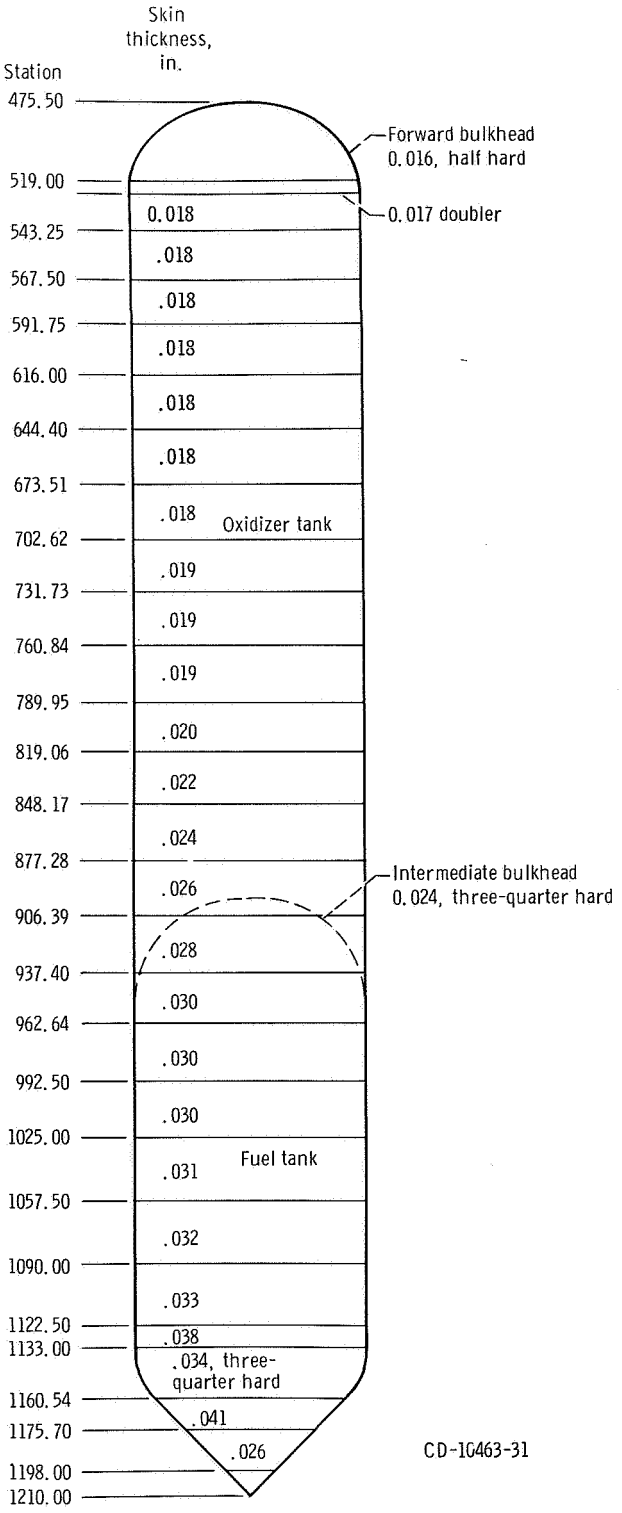

Figure VI-22. - Atlas propellant tanks, AC-18.

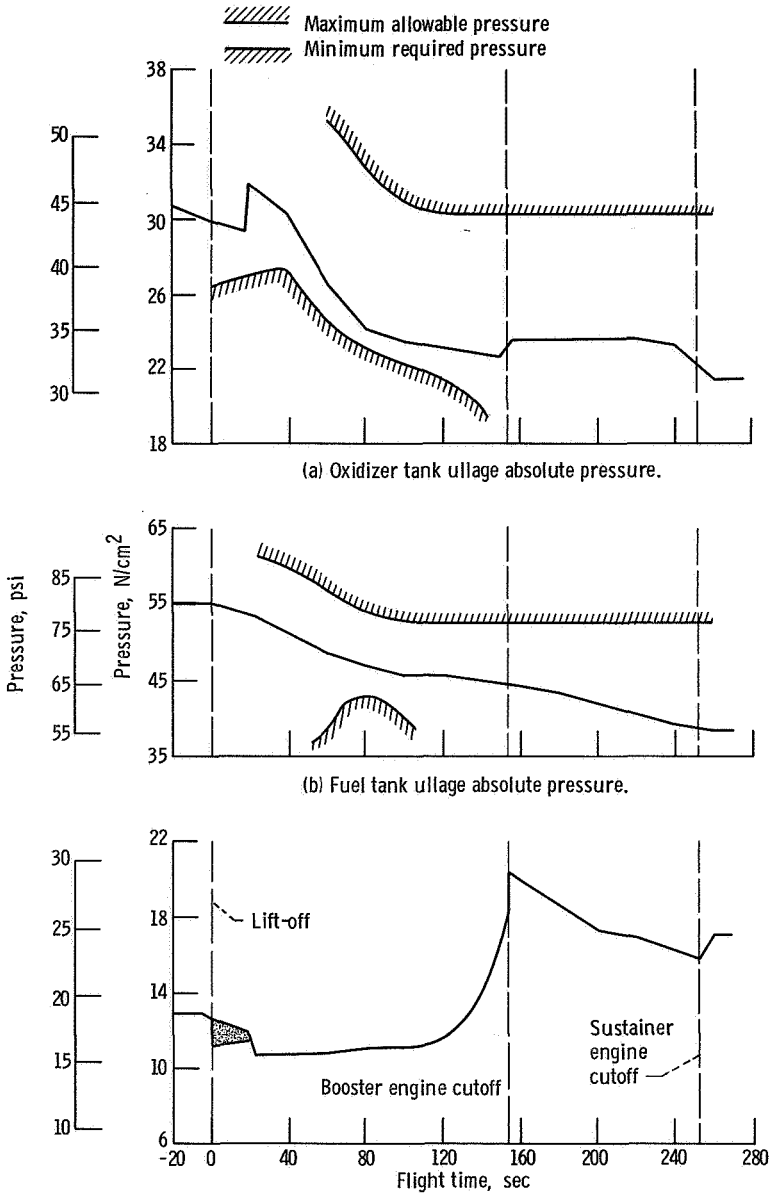

Figure VI-23. - Atlas fuel and oxidizer tank pressures, AC-18.

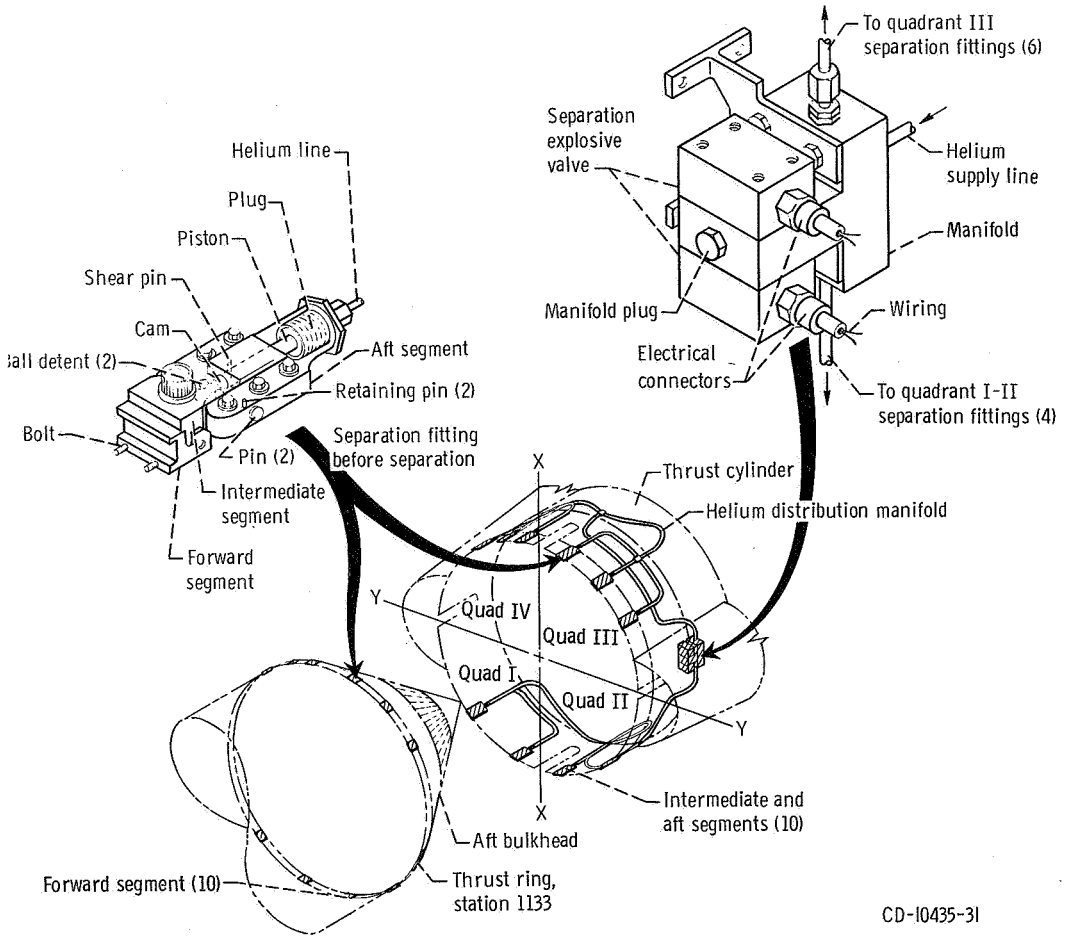

(a) Details.

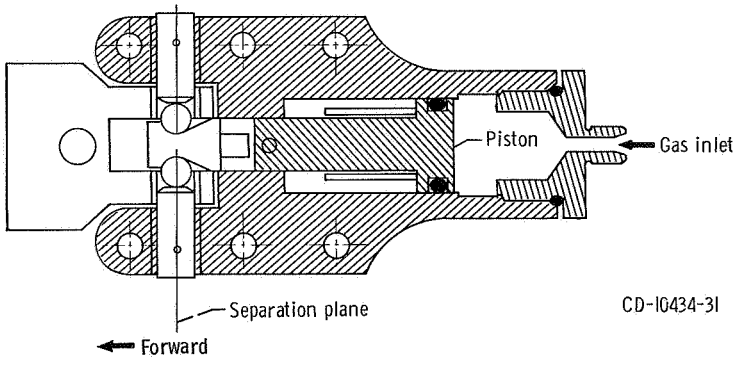

(b) Separation fitting.

Figure VI-24. - Atlas booster engine section separation system, AC-18.

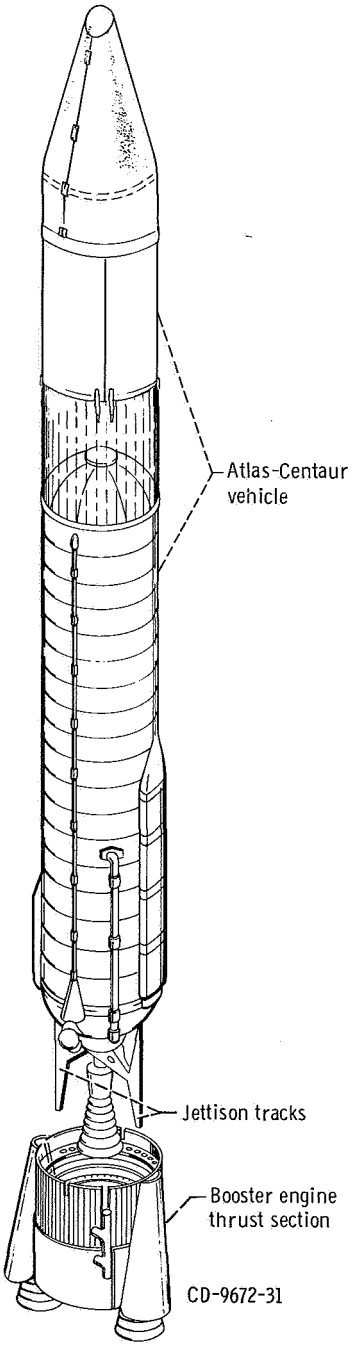

Figure VI-25. - Atlas booster engine section staging system, AC-18.

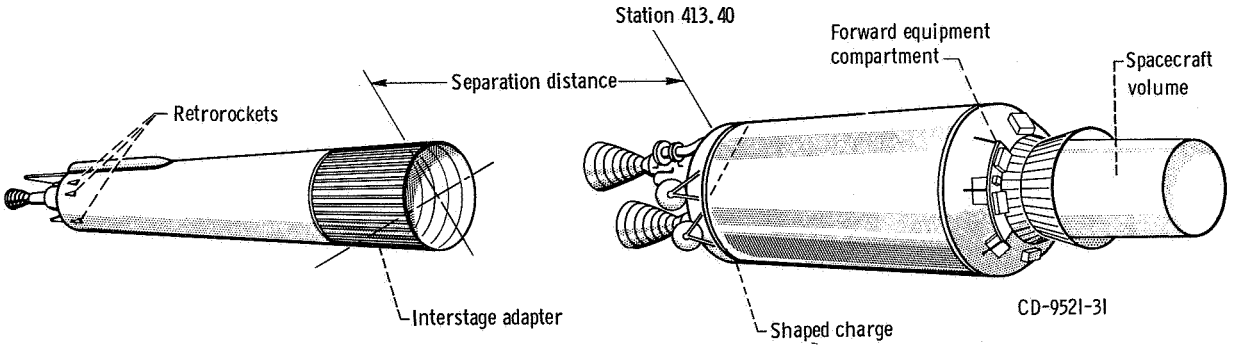

Figure VI-26. - Atlas/Centaur separation system, AC-18.

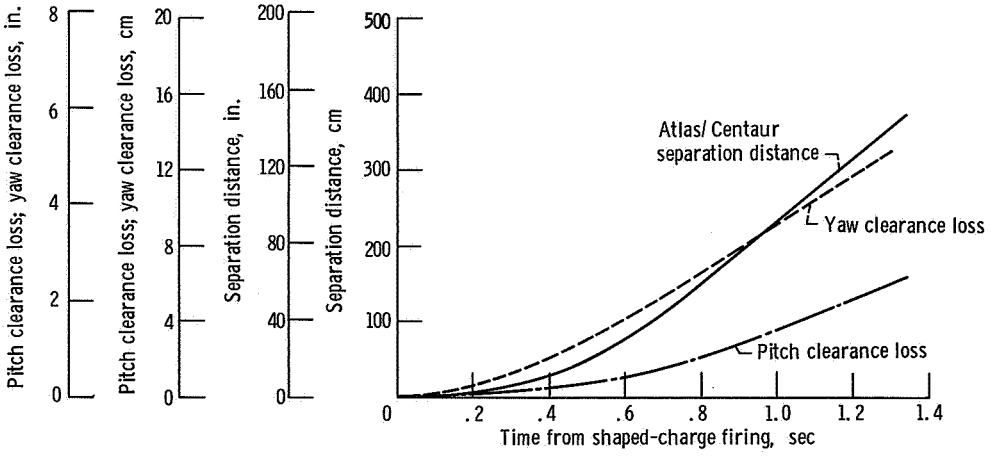

Figure VI-27. - Atlas/Centaur separation distances and clearances, AC-18. All clearance losses referenced to forward end of interstage adapter.

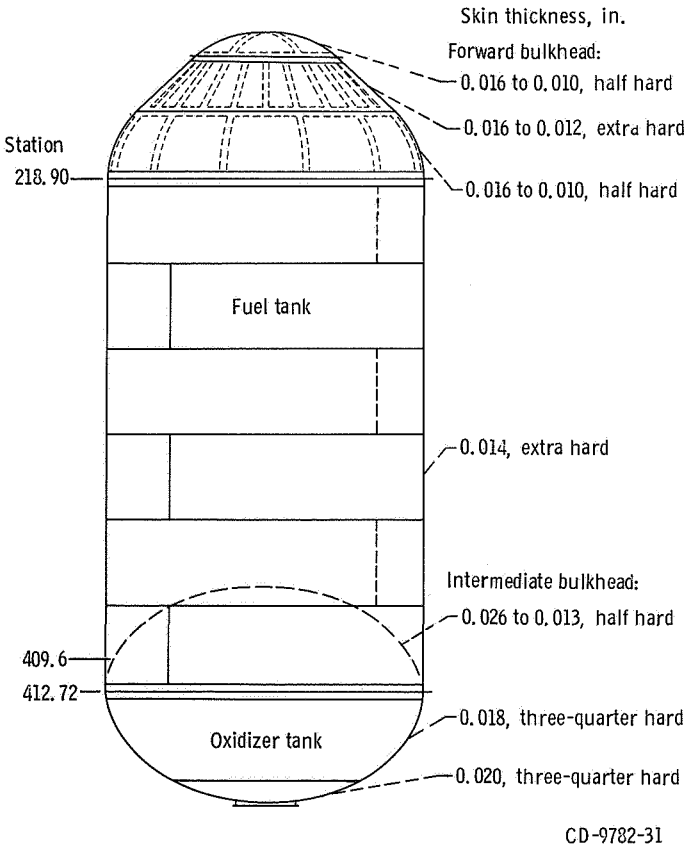

Figure VI-28. - Centaur propellant tanks, AC-18. (All material 301 stainless steel, of hardness indicated.)

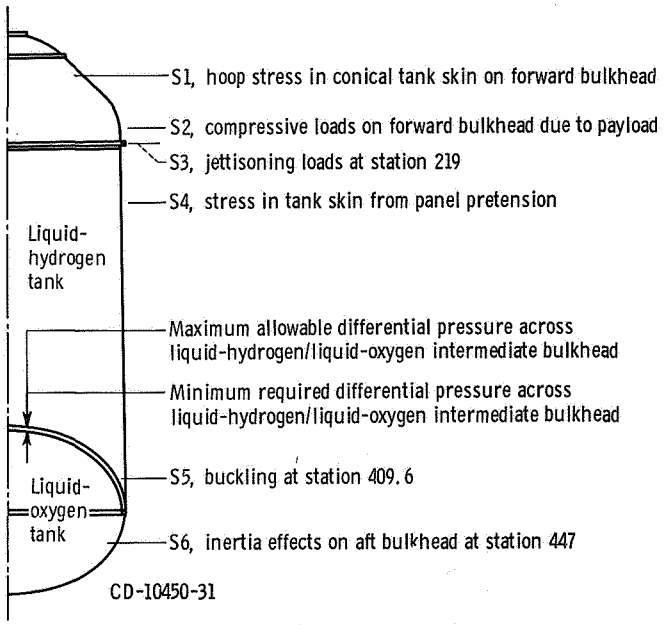

Figure VI-29. - Tank locations and criteria which determine allowable pressures, AC-18.

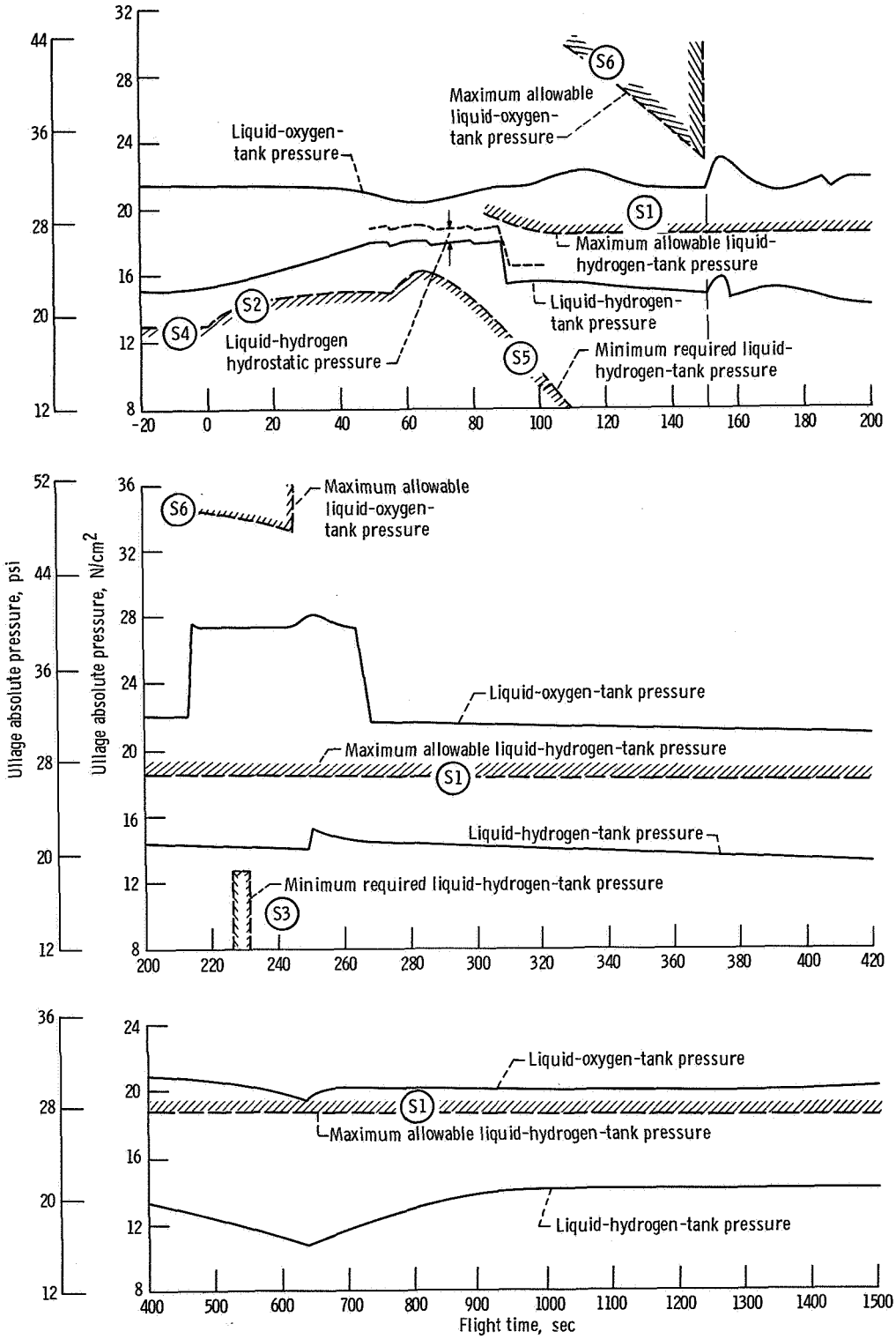

Figure VI-30. - Centaur fuel and oxidizer tank pressures, AC-18. S1, S2, etc., indicate tank structure areas which determine the allowable tank pressure (see fig. VI-29).

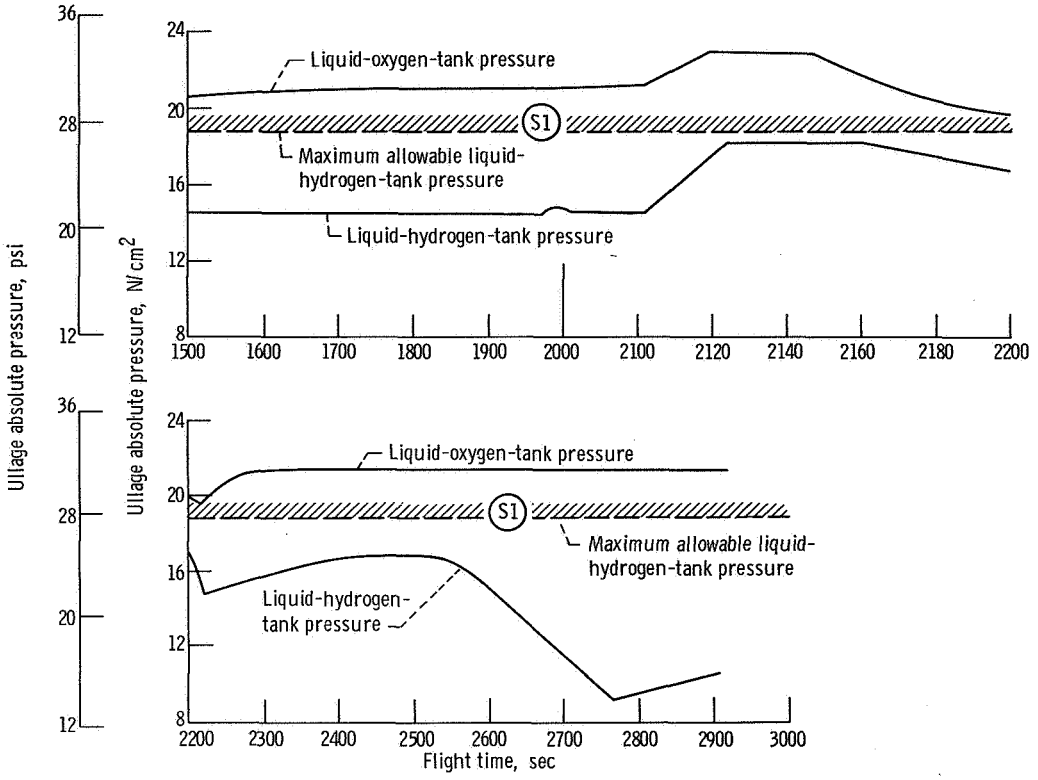

Figure VI-30. - Concluded.

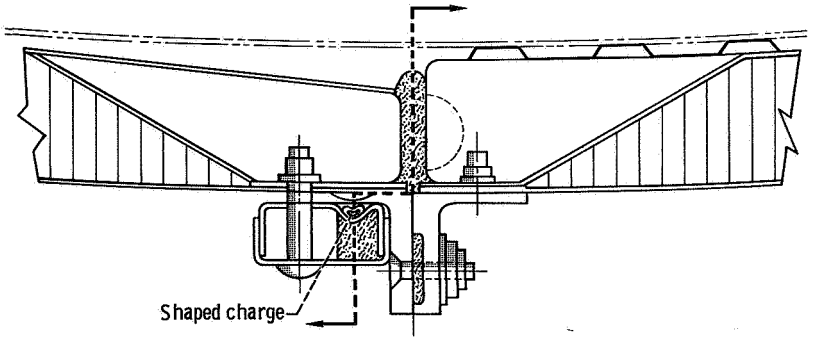

Section B-B: Longitudinal joint

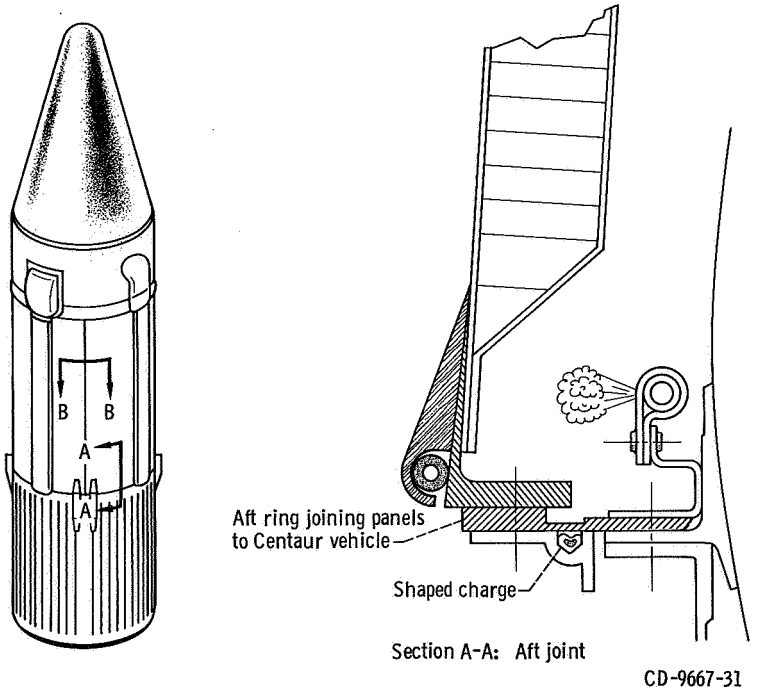

Figure VI-31. - Hydrogen tank insulation panels and separation system, AC-18.

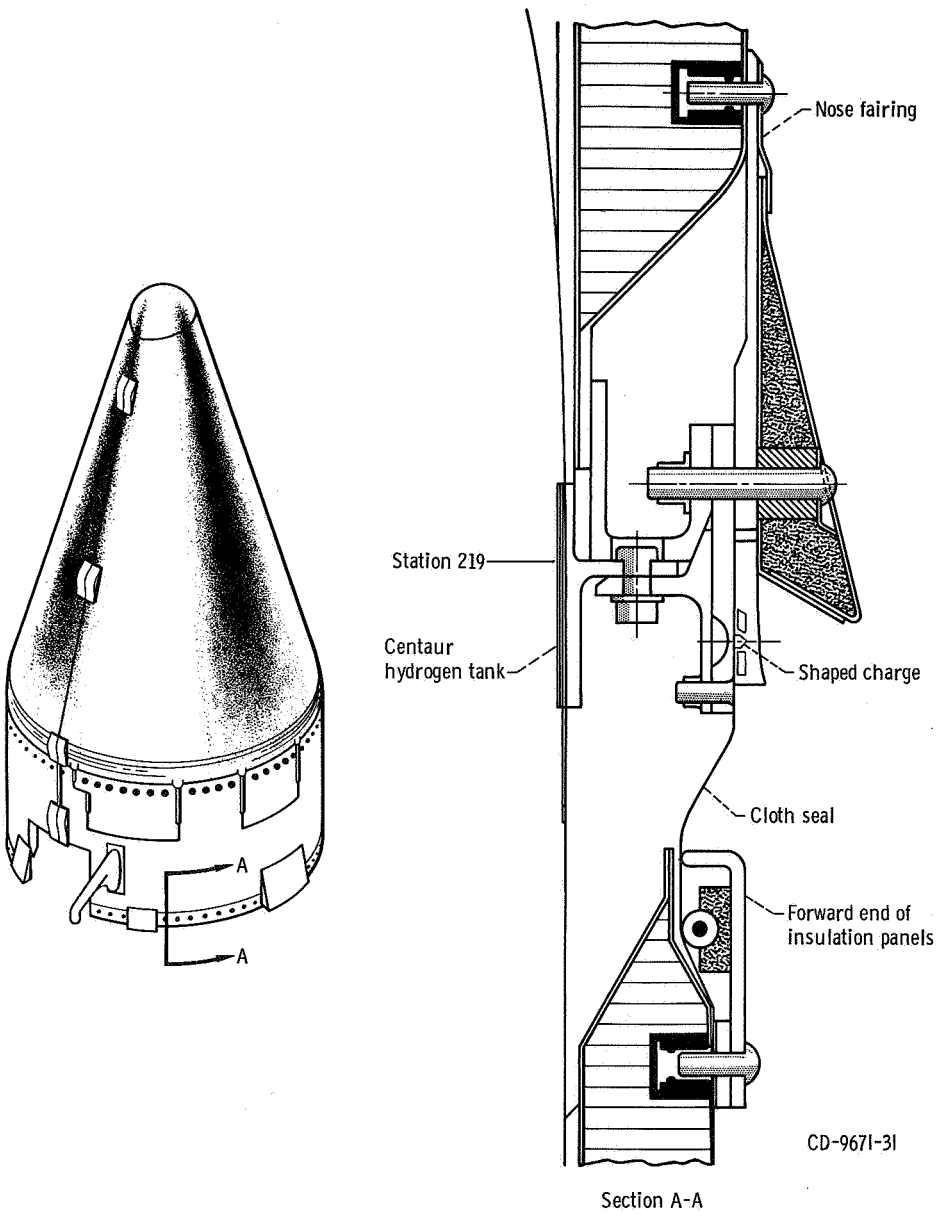

Figure VI-32. - Nose fairing aft separation system, AC-18.

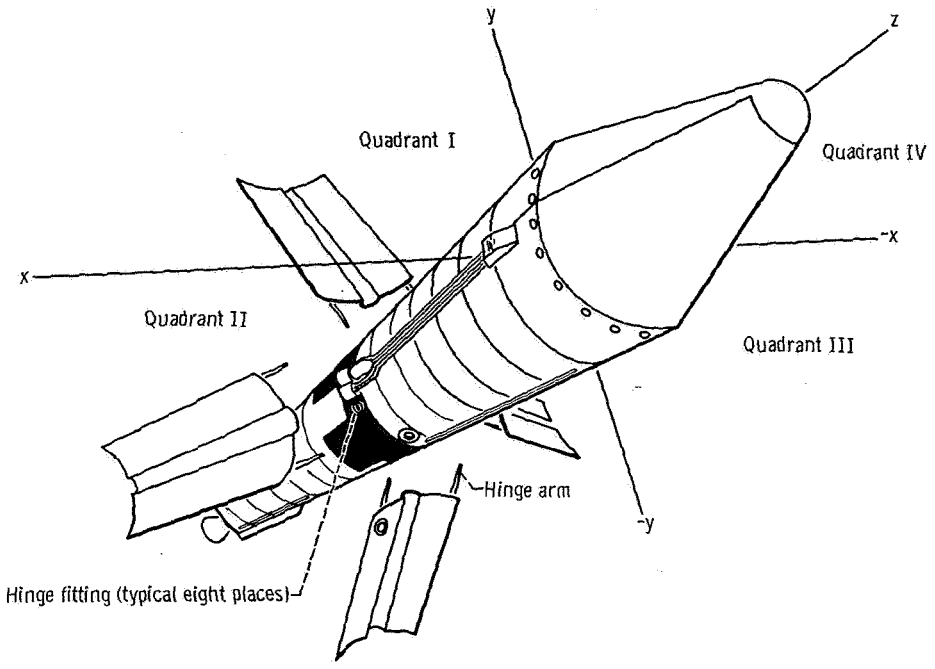

Figure VI-33. - Hydrogen tank insulation panel jettison, AC-18.

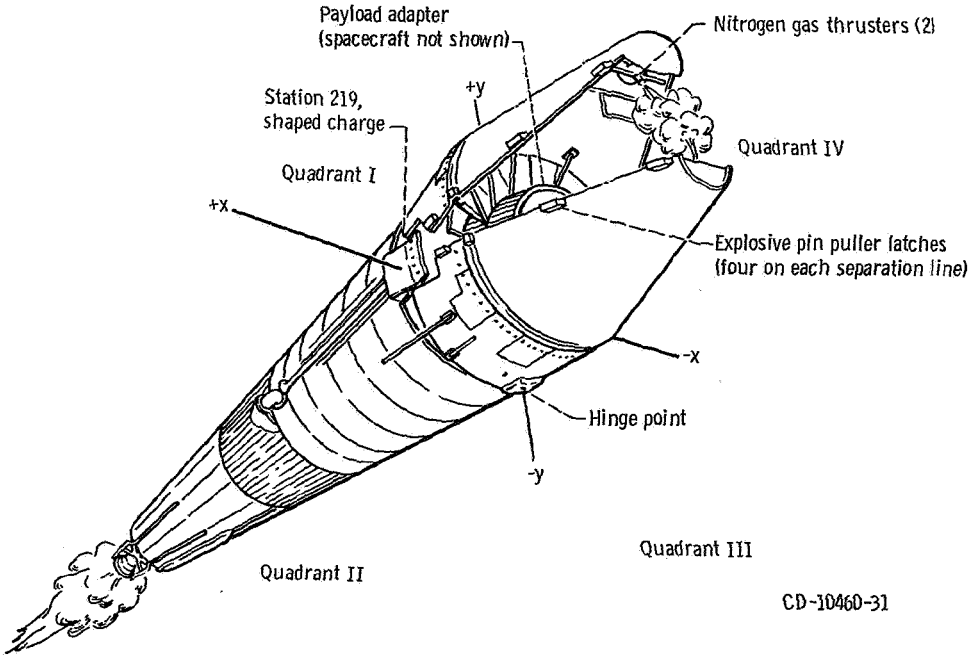

Figure VI-34. - Nose fairing jettison system, AC-18.

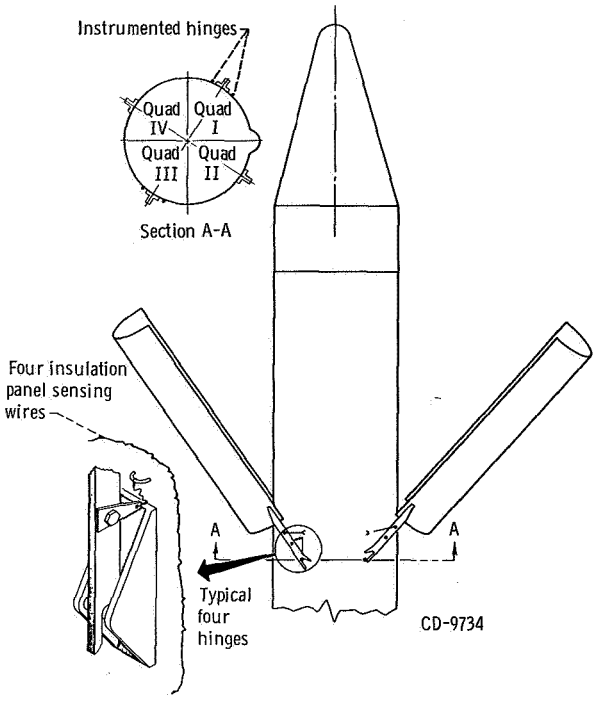

Figure VI-35. - Insulation panel breakwire locations, AC-18.

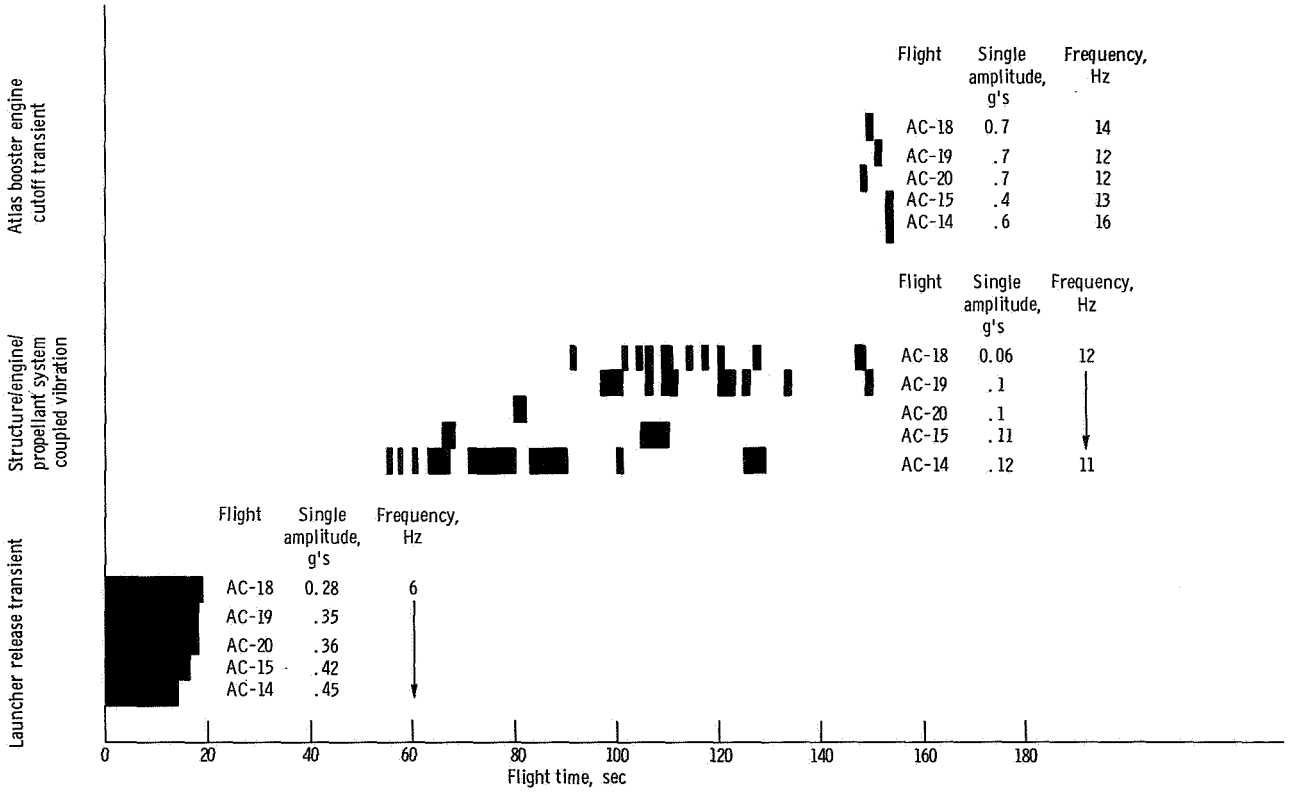

Figure VI-36. - Longitudinal vibrations from Atlas/Centaur flights.

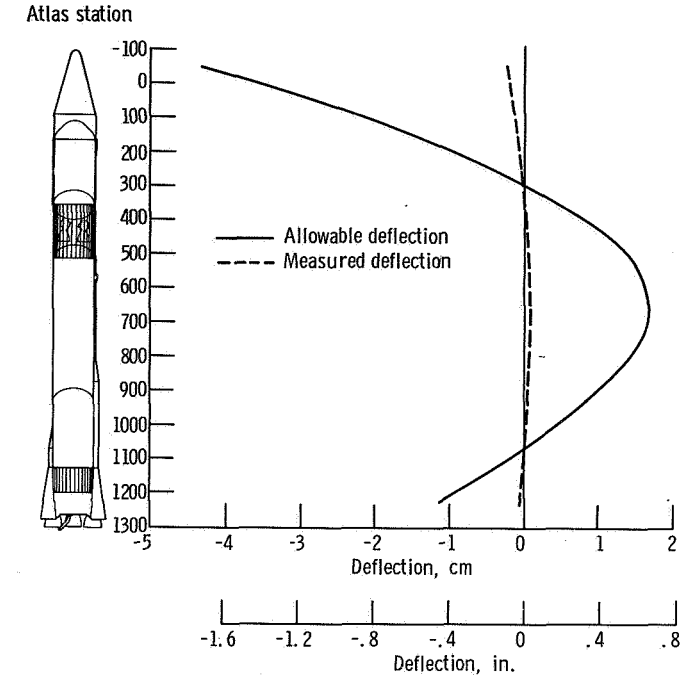

Figure VI-37. - Maximum pitch plane first-bending-mode amplitudes at T + 141 seconds, AC-18.

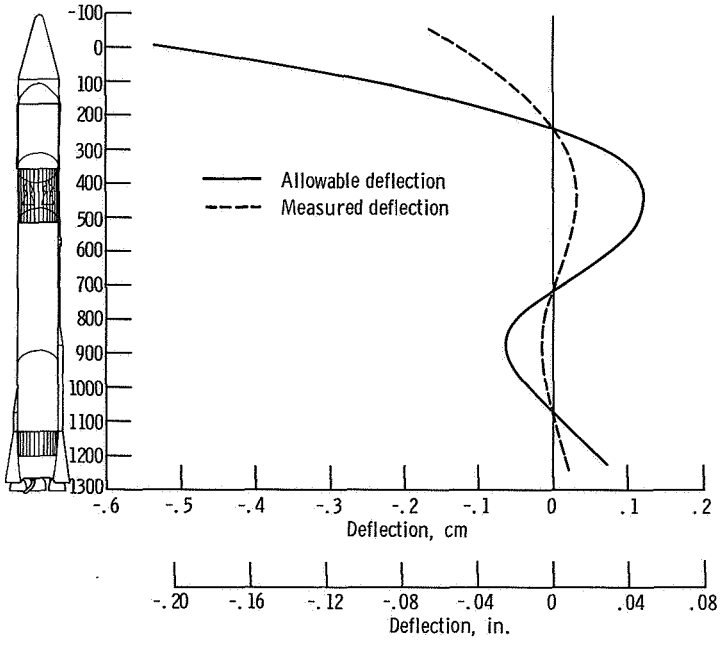

Figure VI-38. - Maximum yaw plane second-bending-mode amplitudes at T + 31 seconds, AC-18.

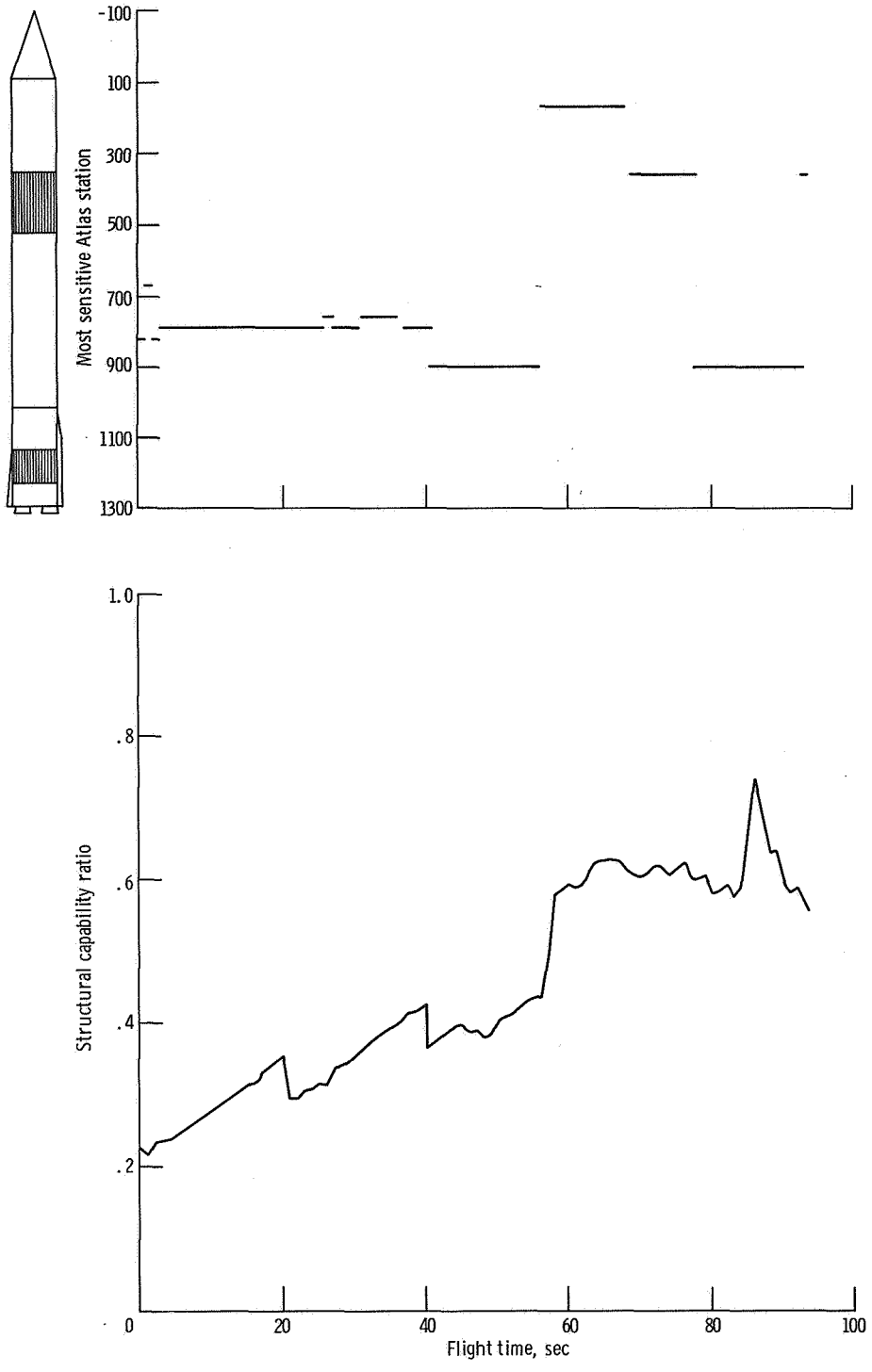

Figure VI-39. - Maximum predicted structural capability ratio (see text) and sensitive station (based on T - 48-min weather balloon), AC-18.

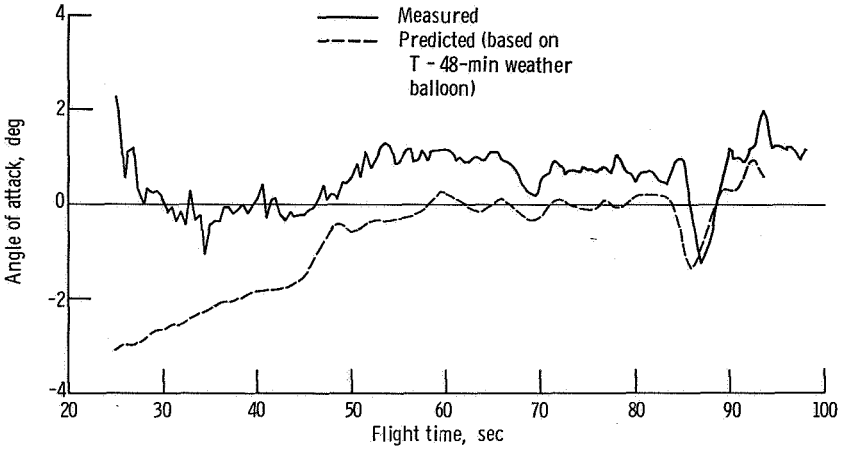

Figure VI-40. - Predicted and actual pitch angles of attack, AC-18.

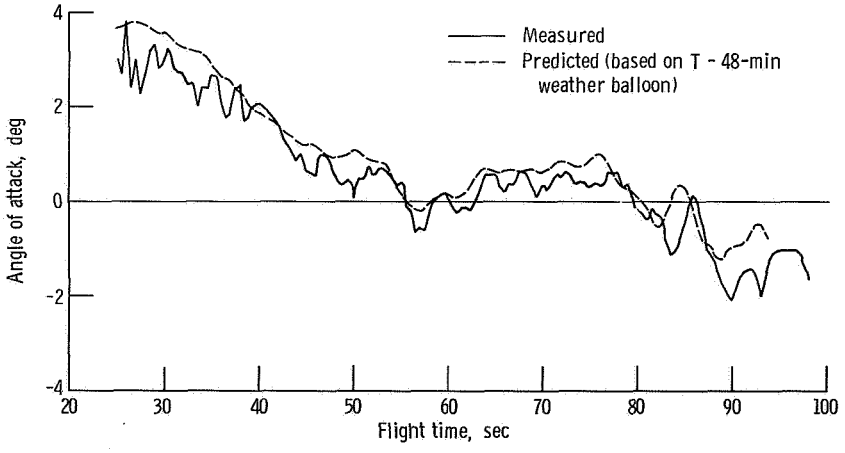

Figure VI-41. - Predicted and actual yaw angles of attack, AC-18.

ELECTRICAL SYSTEMS

by John M. Bulloch and John B. Nechvatal

Power Sources and Distribution

System description - Atlas. - The power supply consists of a power changeover switch; one main battery; one telemetry battery; two independent range safety command (vehicle destruct) system batteries; and a three phase, 400-hertz rotary inverter. (See fig. VI-42 for the system block diagram.)

System performance - Atlas. - Transfer of the Atlas electrical load from external to internal power was accomplished by the main power changeover switch at T - 2 minutes. Performance of the Atlas electrical system was normal throughout the flight. Voltages and current levels furnished to the dependent systems were within specification limits.

The Atlas main battery supplied the requirements of the user systems at normal levels (25 to 30 V). The battery voltage was 27.4 volts at lift-off and 27.8 volts at sustainer engine cutoff. This is a normal rise of voltage, due to battery temperature increase.

The telemetry battery and the two range safety command batteries provided normal voltage levels throughout Atlas flight. The voltages at lift-off were 28.1 volts for the telemetry system and 29.2 and 29.0 volts for the two range safety command systems.

The Atlas rotary inverter supplied 400-hertz power within specified voltages and frequency limits. The voltage at lift-off was 115.0 volts and increased to 115.3 volts at sustainer engine cutoff (T + 251.6 sec). The inverter frequency at lift-off was 401.9 hertz and rose to 402.5 hertz by the end of Atlas flight. The gradual rise in frequency is typical of the Atlas inverter. The required frequency difference of 1.3 to 3.7 hertz between the Atlas and Centaur inverter frequencies was properly maintained. This difference prevents undesirable beat frequencies in the Atlas flight control system. (Beat frequencies resonant with the slosh and natural structural resonant frequencies of the vehicle may cause the flight control system to issue false commands which may degrade vehicle stability.)

System description - Centaur. - The electrical power system consists of a power changeover switch, a 100-ampere-hour main battery, two independent range safety command (vehicle destruct) batteries, two pyrotechnic system batteries, and a solid-state inverter supplying 400-hertz current to the guidance, flight control, and propellant utilization systems. The system block diagram is shown in figure VI-43.

System performance - Centaur. - Performance of the Centaur electrical system was satisfactory throughout the flight. Transfer of the Centaur electric load from external power to the internal battery was accomplished at T - 4 minutes by the power changeover

switch in 250 milliseconds (specification value, 2.00 sec). The maximum voltage excursion at power transfer was 0.2 volt, which is considered negligible.

The main battery voltage was 28.0 volts at lift-off. A low of 27.7 volts was recorded during the main engine first start sequence, and a high of 28.8 volts was reached during the coast phase. The voltage decreased to 28.4 volts at main engine second start, and recovered to 28.8 volts by spacecraft separation.

Main battery current was 46.5 amperes at lift-off. It peaked at 63 amperes at main engine first start and 62.5 amperes at main engine second start. The flight current profile was consistent with values recorded during preflight tests. The main battery current profile with respect to flight programmed events is shown in figure VI-44.

Short-duration current pulses caused by the spacecraft separation squib bridgewires shorting to ground following squib firing were observed. Thermal relays in these circuits removed the short-circuit loads in approximately 150 to 200 milliseconds. This type of current pulse has been observed on the last four Centaur flights.

The pyrotechnic battery voltages were 35.1 and 35.0 volts at lift-off. Minimum specification limit is 34.7 volts. Proper operation of the pyrotechnic system batteries and associated relays was verified by instrumentation and by the successful jettison of the insulation panels and nose fairing.

Performance of the two range safety command system batteries was satisfactory. At lift-off the battery voltages were 32.4 and 32.2. The minimum specification limit is 30 volts.

The Centaur inverter operated satisfactorily throughout the flight. Telemetered voltage levels compared closely to values recorded during preflight testing. The inverter phase voltages at lift-off were as follows: phase A, 115.3 volts; phase B, 115.2 volts; and phase C, 115.1 volts. Voltage changes during flight were small and well within expected values, with a maximum phase voltage variation of 0.9 volt from lift-off values. Inverter frequency remained constant at 400 hertz throughout flight. Inverter skin temperature was 303 K (86^{o} F) at lift-off and reached 337 K (147^{o} F) at power turnoff (T + 2819 sec). Following power turnoff, the C-band beacon and telemetry systems were the only systems operating.

C-Band Tracking System

System description. - An airborne C-band radar system (fig. VI-45) with associated ground stations provides position and velocity data for range safety tracking. These data are also used for post-flight guidance and flight trajectory data anslysis. The airborne equipment includes a lightweight transponder, a circulator (to channelize receiving and sending signals), a power divider, and two antennas located on opposite sides of the Centaur tank. The locations of the Centaur antennas are shown in figure VI-46. The

ground stations use standard radar equipment and are located as shown in figure VI-47 for AC-18.

System performance. - C-band radar coverage was obtained until T + 5030 seconds (fig. VI-48). Cape Kennedy, Merritt Island, Patrick Air Force Base, Grand Bahama Island, Grand Turk, Bermuda, and Antigua provided coverage during Atlas-Centaur powered flight. Antigua also provided data for near-real-time calculations of the Centaur parking orbit. Ascension and Pretoria provided data for the Centaur/ATS-5 transfer orbit calculations. Carnarvon provided data for determining the Centaur orbit after the post-separation maneuver. Tananarive had data losses during four periods because of weak and lobing signals. Carnarvon had one data loss of 18 seconds (3452 to 3470 sec) because of insufficient signal strength.

Range Safety Command System

System description. - The Atlas and Centaur stages each contain independent vehicle destruct systems. These systems are designed to function simultaneously upon command from the ground stations. Each system includes redundant receivers, power control units, destructor, and batteries and antennas which operate independently of the main vehicle power system. The location of the Centaur range safety antannas is shown in figure VI-46. Block diagrams of the Atlas and Centaur systems are shown in figures VI-49 and VI-50, respectively.

The Atlas and Centaur vehicle destruct systems have the capability of shutting down the engines only or shutting down the engines and destroying the vehicle. Each destruct system consists of an explosive charge which ruptures the propellant tanks of the Atlas and Centaur stages and the liquid propellants are dispersed. In addition, a shaped charge was located on the payload adapter to destroy the spacecraft apogee motor.

System performance. - The Atlas and Centaur range safety command systems were prepared to execute destruct commands throughout the flight. The command from the Antigua ground station to disable the Centaur range safety command system shortly after Centaur main engine cutoff was properly received and executed. The ground transmitter coverage to support the vehicle destruct systems for AC-18 is shown in figure VI-51.

Signal strength at the Atlas and Centaur range safety command receivers was satisfactory throughout the flight, as indicated by telemetry measurements.

Instrumentation and Telemetry

System description - Atlas. - The Atlas telemetry system (fig. VI-52) consists of a radiofrequency telemeter package, two antennas, a telemetry battery, and transducers.

It is a pulse amplitude modulation/frequency modulation/frequency modulation (PAM/FM /FM) telemetry system and operates at a carrier frequency of 229.0 megahertz. The PAM technique is used on all Atlas-Centaur commutated (sampled) channels and makes possible a large number of measurements on one subcarrier channel. This increases the data handling capability of the telemetry system. The FM/FM technique uses analog values from transducers to frequency modulate the subcarrier oscillators which, in turn, frequency modulate the main carrier (radiofrequency link).

System performance - Atlas. - The telemetry coverage for the Atlas portion of the flight (fig. VI-53) extended well beyond Atlas/Centaur separation and met all telemetry coverage requirements. The location of telemetry stations for this flight is shown in figure VI-47.

Of the 106 measurements (table VI-XII) made on Atlas, the following four measurements showed unexpected outputs:

(1) The vernier engine number 1 and number 2 thrust chamber pressure measurements (AP28P and AP29P, respectively) exhibited characteristics of carbon deposit buildup at the inlet port shortly after booster engine section jettison. Subsequently only qualitative data were obtained from these measurements. This type of measurement anomaly has been observed on previous flights.

(2) The sustainer fuel pump discharge pressure measurement (AP330P) exhibited negative "spiking" which is characteristic of wiper arm lift-off within the transducer. No data were lost because of this "spiking."

(3) The sustainer yaw position measurement (AS256D) exhibited a step bias level shift of 8-percent information bandwidth (IBW) during the engine ignition sequence. The bias level remained 8 percent low throughout the flight. No data were lost because of this shift. This bias shift has occurred on several previous flights and is believed to be caused by slippage between the transducer and the gimbal block shafts.

System description - Centaur. - The Centaur telemetry system (fig. VI-54) consists of two radiofrequency telemetry packages (RF1 and RF2), one antenna, and transducers. It is a PAM/FM/FM system which operates at frequencies of 225.7 and 259.7 megahertz for RF1 and RF2 telemetry packages, respectively. The RF1 telemetry package was used for Centaur operational measurements and the RF2 package was installed for special measurements in order to obtain (1) transition adapter and spacecraft data, (2) spacecraft compartment environmental data, and (3) spacecraft separation indication. The major difference between the AC-18 and the AC-17 instrumentation was additional measurements to provide analysis of the AC-18 hydrogen peroxide system configuration changes.

System performance - Centaur. - The telemetry coverage for AC-18 was excellent (fig. VI-55). The station locations for AC-18 are shown in figure VI-47. Of the total

241 measurements (table VI-XIII) that were made on the Centaur, the following six measurements showed unexpected results:

(1) The C-2 engine thrust controller vibration measurement (CP769O) failed to provide any vibration output during the flight. The cause of the failure is unknown.

(2) The C-1 engine thrust chamber outboard temperature measurement at station 518 (CP741T) went off-scale high at 2152 seconds. This is indicative of an open circuit in the measurement circuitry. No valid data were obtained beyond this time.

(3) The C-1 engine fuel pump temperature measurement (CP122T) exhibited a slow response to temperature changes. The cause of this problem is unknown; however, it has occurred before on Centaur flights.

(4) The longitudinal acceleration fine range (±0.001 g) measurement (CM294A) and the longitudinal acceleration (±0.01 g) measurement (CM295A) exhibited a positive acceleration transient at spacecraft separation. The indication should have been in the negative direction.

(5) The liquid-hydrogen boost pump H_2O_2 supply line temperature measurement (CP361T) near the overspeed valve indicated unexpected data throughout the flight. (Refer to section PROPULSION SYSTEMS.)

TABLE VI-XII. - ATLAS MEASUREMENT SUMMARY, AC-18

System	Measurement type									
	Acceleration	Rotation rate	Displacement	Pressure	Frequency	Rate	Temperature	Voltage	Discretes	Totals
Airframe				3			2		4	9
Range safety								3	1	4
Electrical					1			4		5
Pneumatics				7			1			8
Hydraulics				6						6
Dynamics	1								2	3
Propulsion		3	3	18			6		6	36
Flight control			11			3		4	13	31
Propellant	1			2				1		4
Totals	2	3	14	36	1	3	9	12	26	106

TABLE VI-XIII. - CENTAUR MEASUREMENT SUMMARY, AC-18

System	Measurement type												
	Acceler-tion	Rota-tion rate	Cur-rent	Dis-place-ment	Vibra-tion	Pres-sure	Fre-quency	Rate	Tem-per-ature	Digi-tal	Volt-age	Dis-cretes	Totals
Airframe	8			5					19			3	35
Range safety											2	3	5
Electrical			1				1		2		4		8
Pneumatics						7			6			2	15
Hydraulics						2			2				4
Guidance									3	1	16		20
Propulsion		4			1	21			54			20	100
Flight control								6			4	35	45
Propellant				2							2		4
Spacecraft					2	1	1		1				5
Totals	8	4	1	7	3	31	2	6	87	1	28	63	241

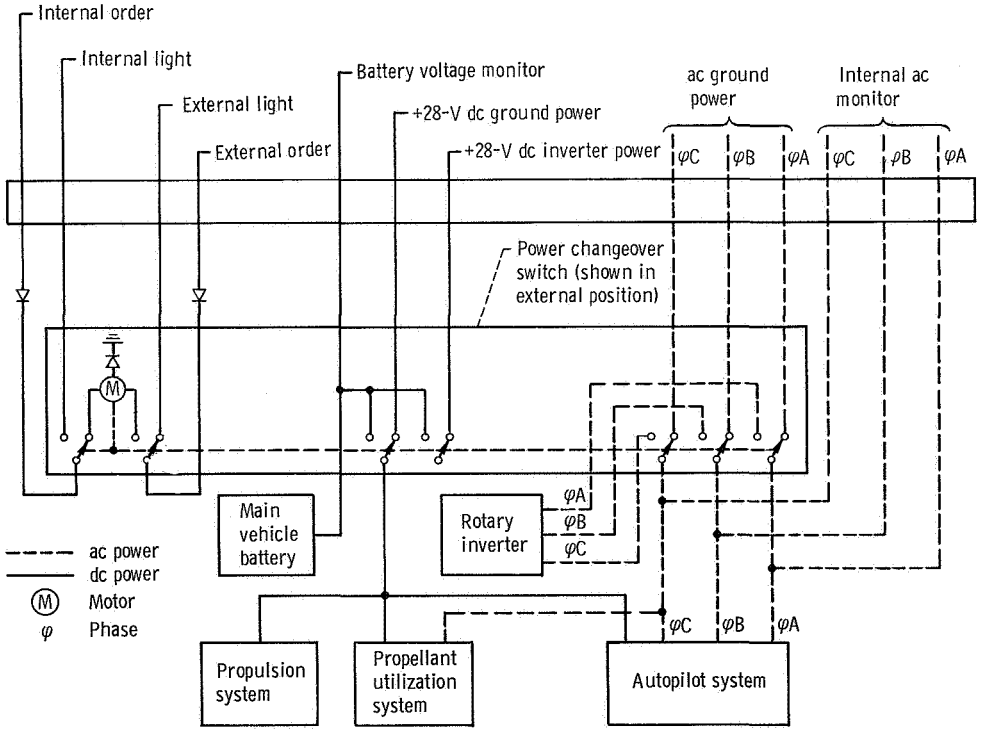

Figure VI-42. - Block diagram of Atlas electrical system, AC-18.

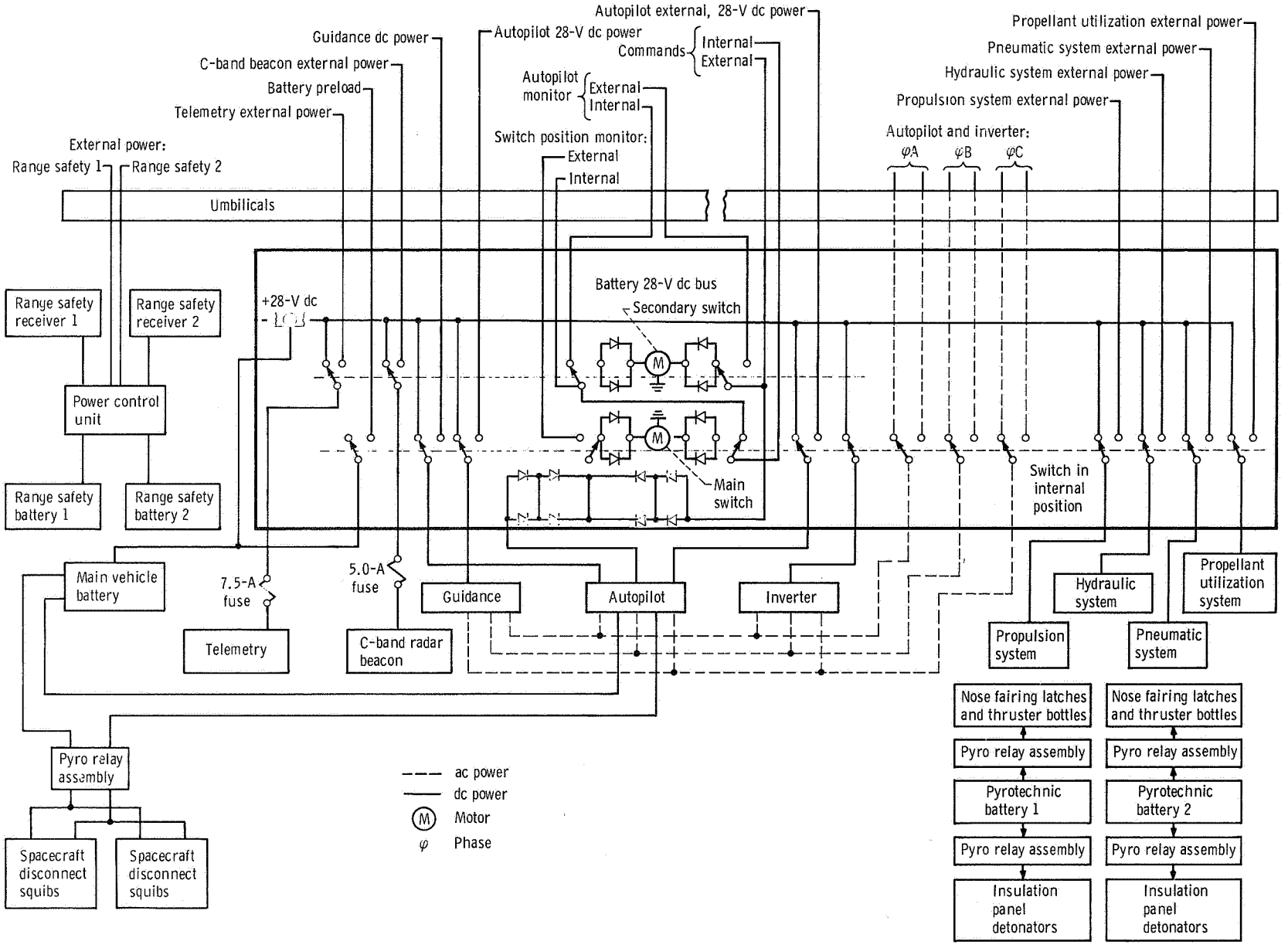

Figure VI-43. - Block diagram of Centaur electrical system, AC-18.

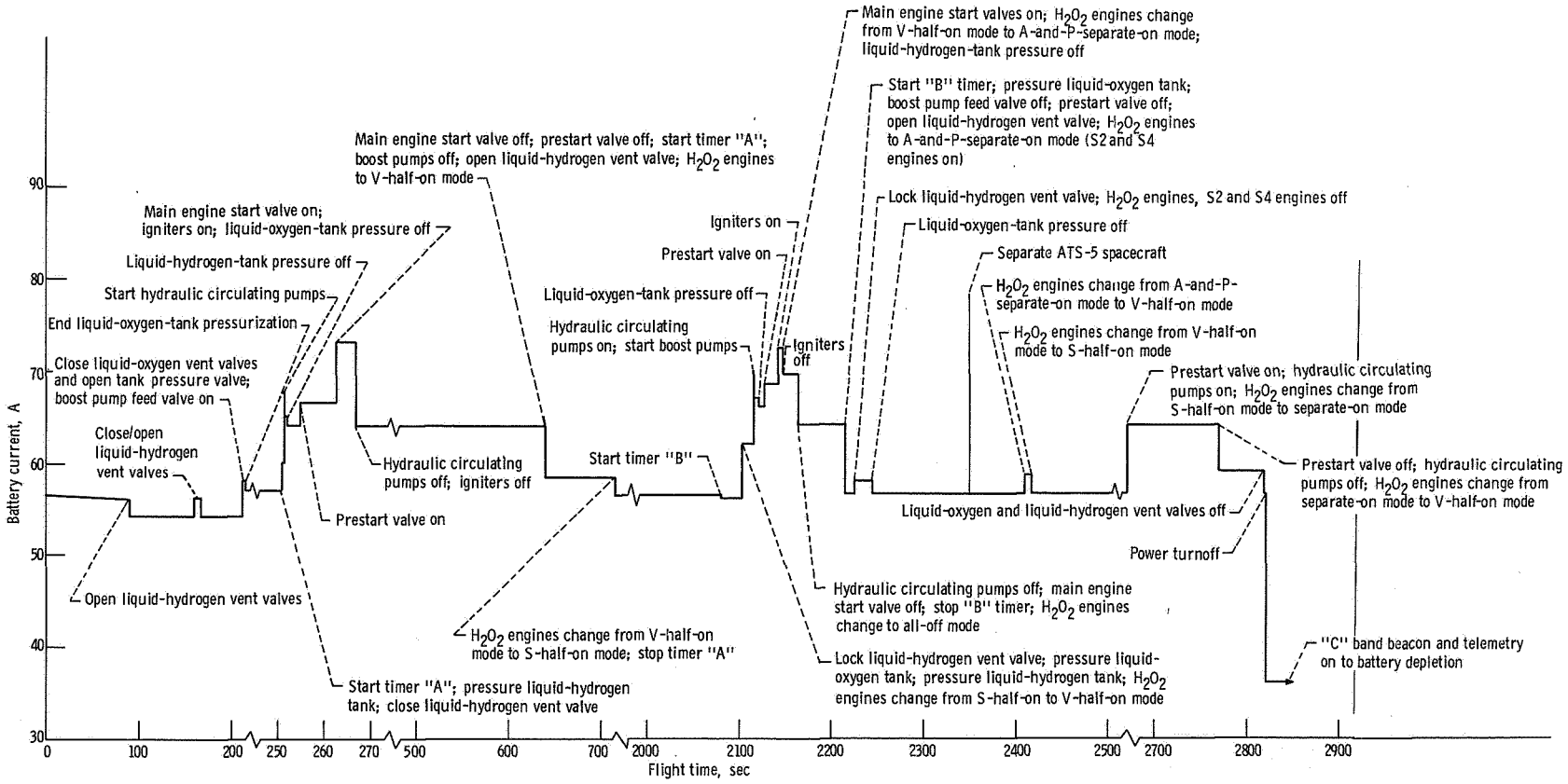

Figure VI-44. - Centaur main battery current profile, AC-18. (Note breaks and scale changes in time scale. See table VI-XVI, GUIDANCE AND FLIGHT CONTROL SYSTEMS section, for description of hydrogen peroxide engine flight modes.)

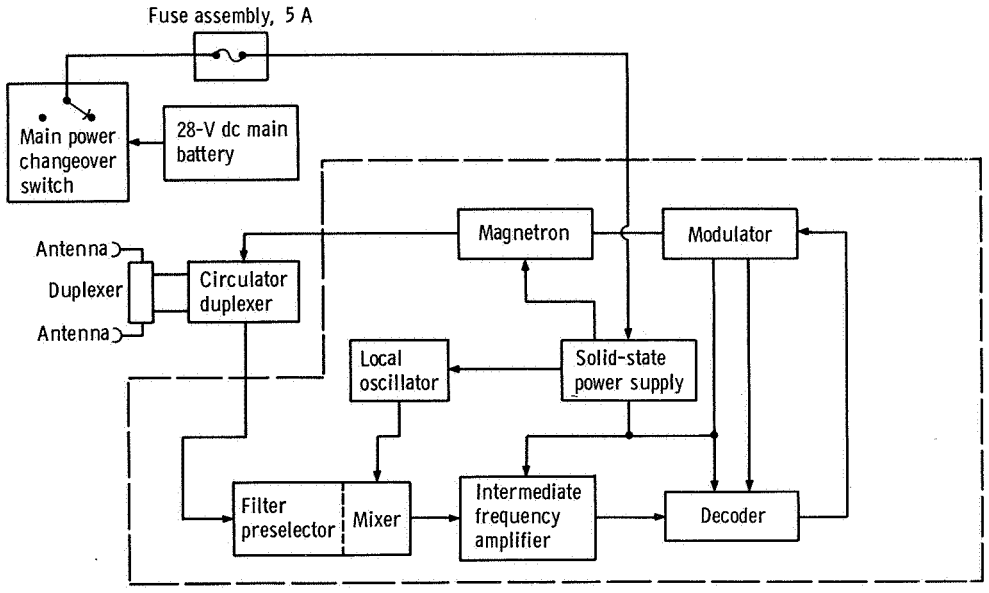

Figure VI-45. - Centaur airborne C-band radar system, AC-18.

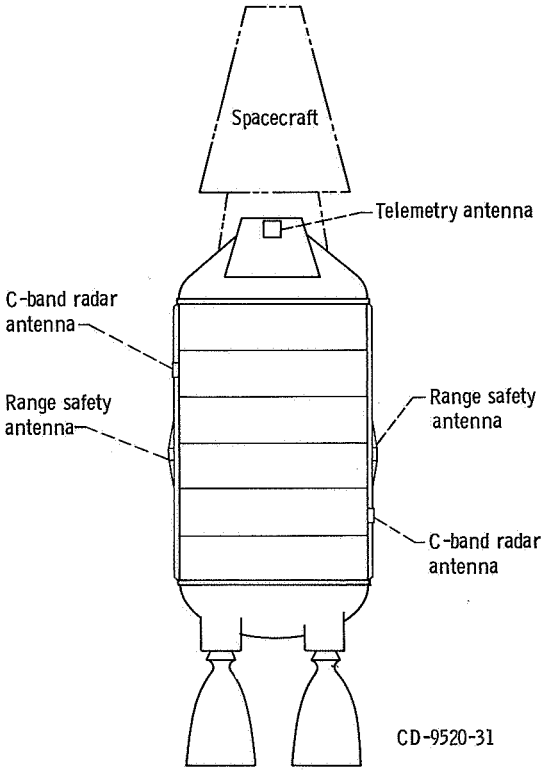

Figure VI-46. - Location of Centaur antennas, AC-18.

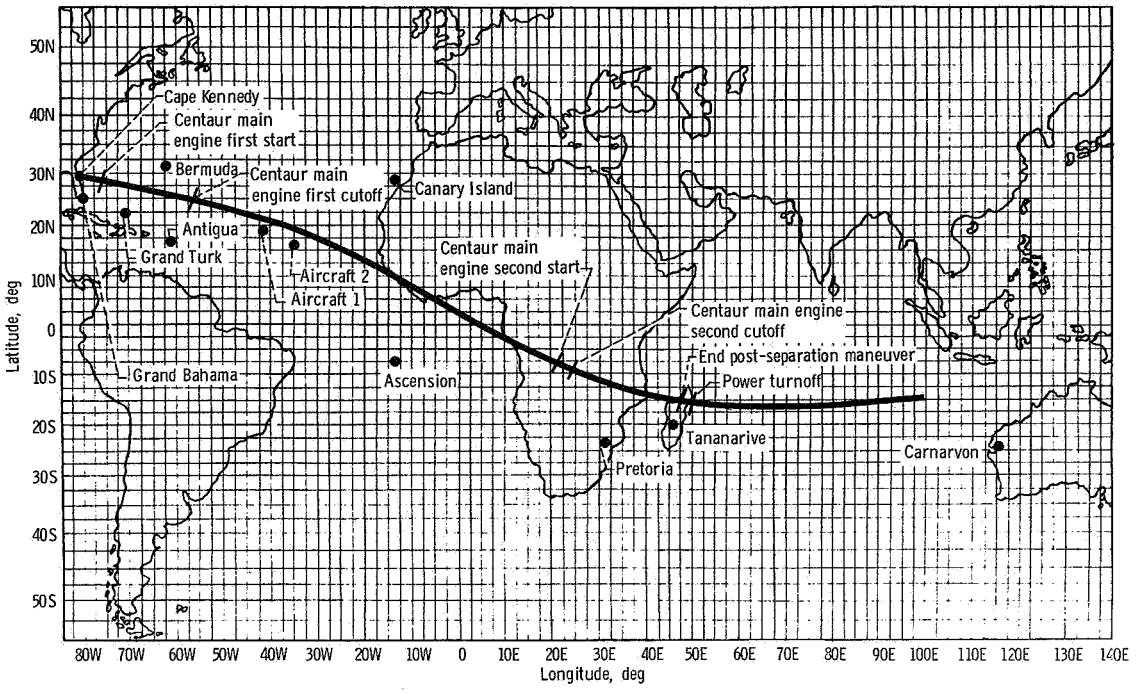

Figure VI-47. - Tracking station location and vehicle trajectory, earth track, AC-13.

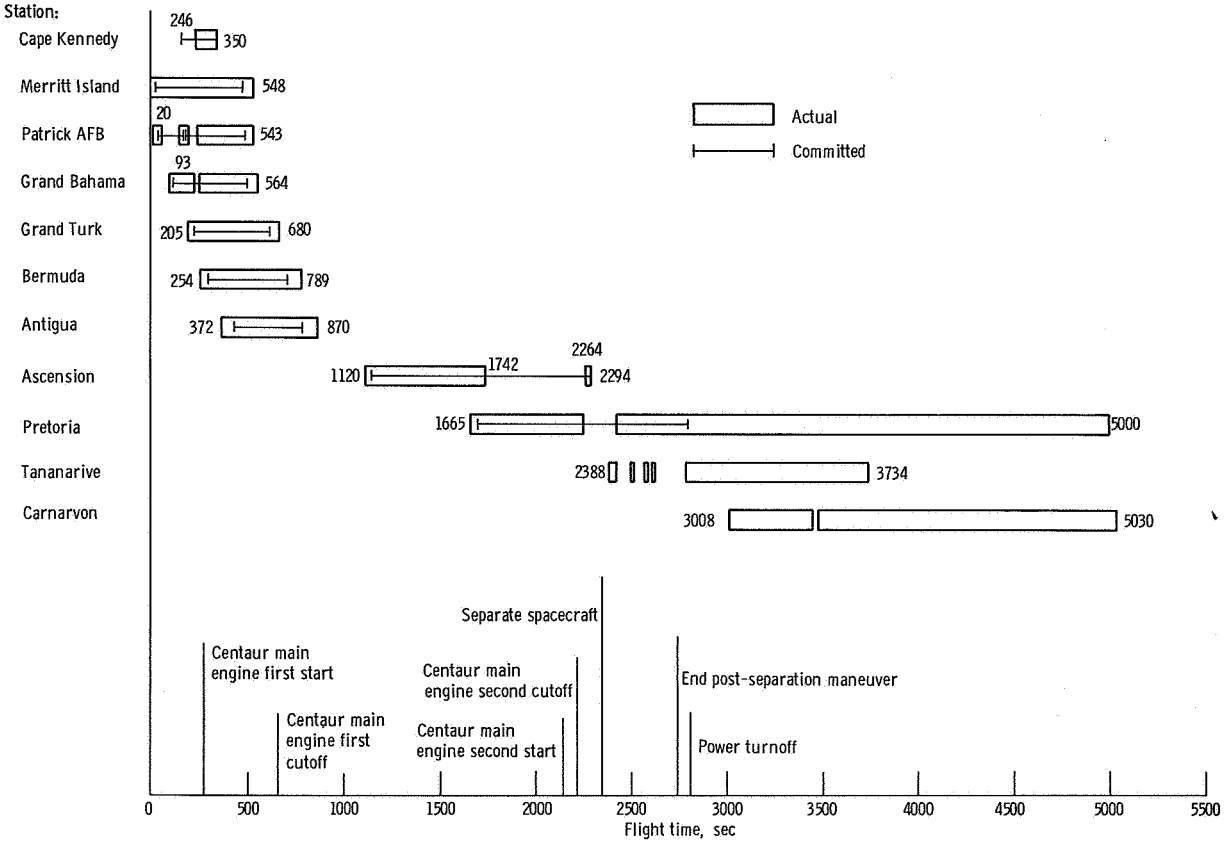

Figure VI-48. - C-band radar coverage, AC-18. Coverage shown is for autobeacon track only.

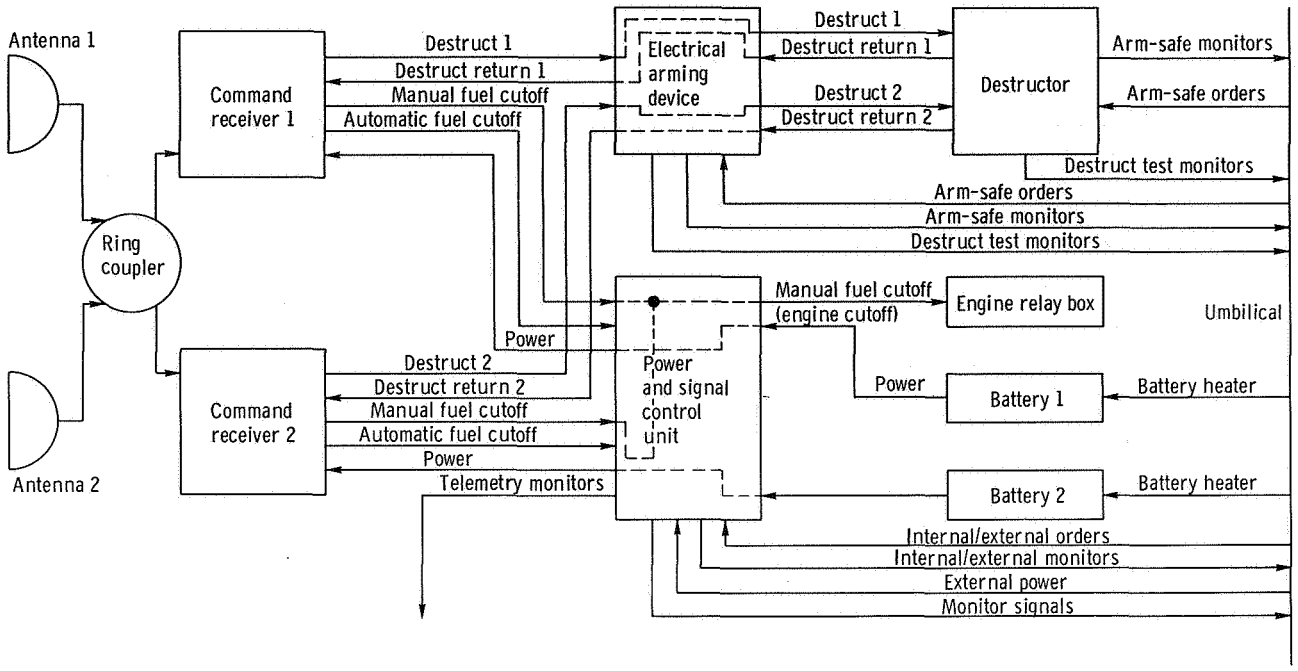

Figure VI-49. - Block diagram of Atlas vehicle destruct subsystem, AC-18.

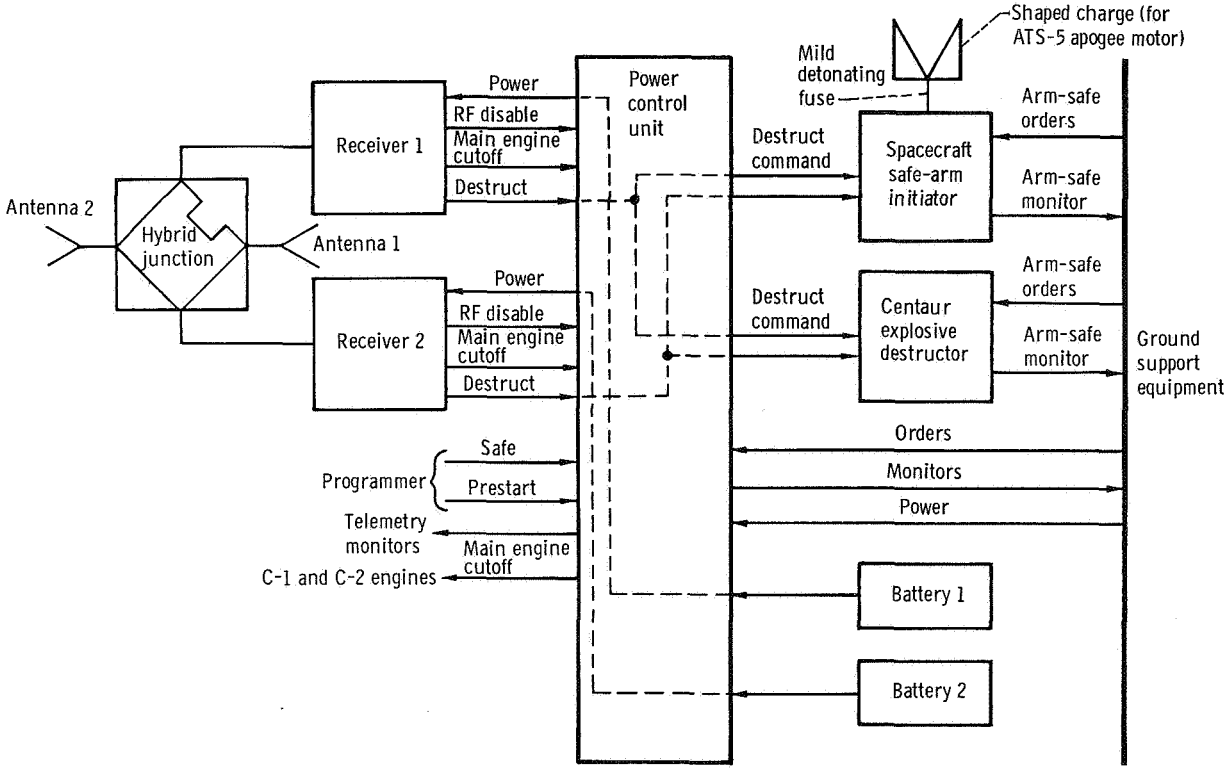

Figure VI-50. - Block diagram of Centaur vehicle destruct subsystem, AC-18.

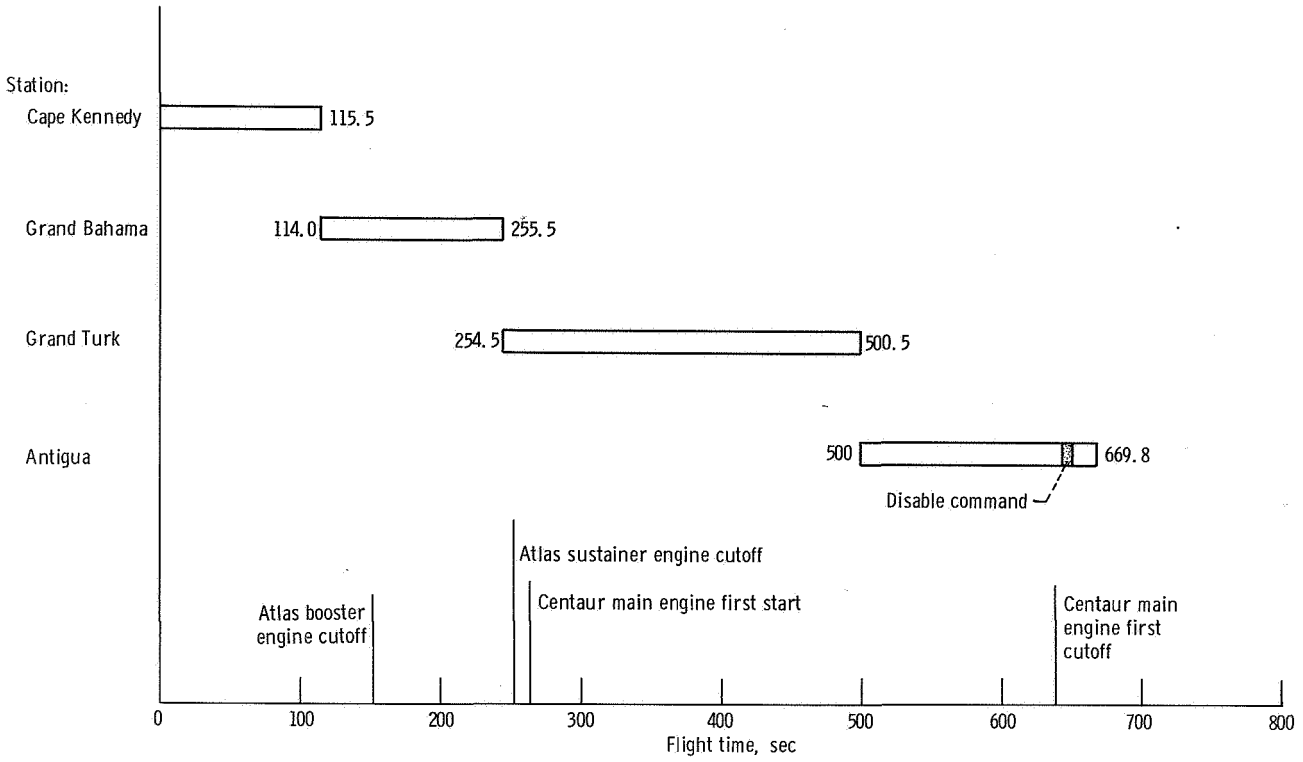

Figure VI-51. - Range safety command system transmitter utilization, AC-18.

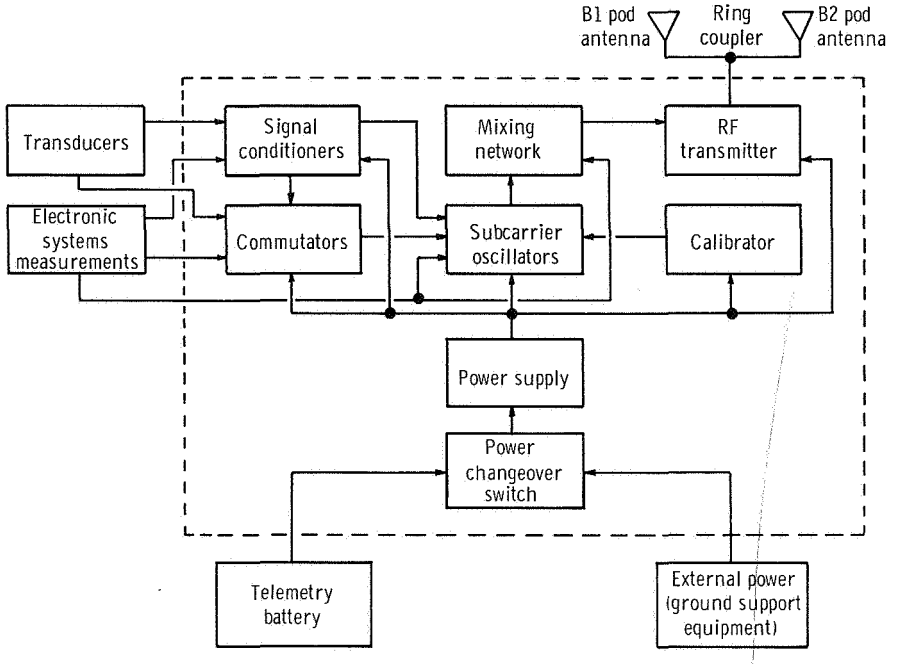

Figure VI-52. - Block diagram of Atlas telemetry system, AC-18.

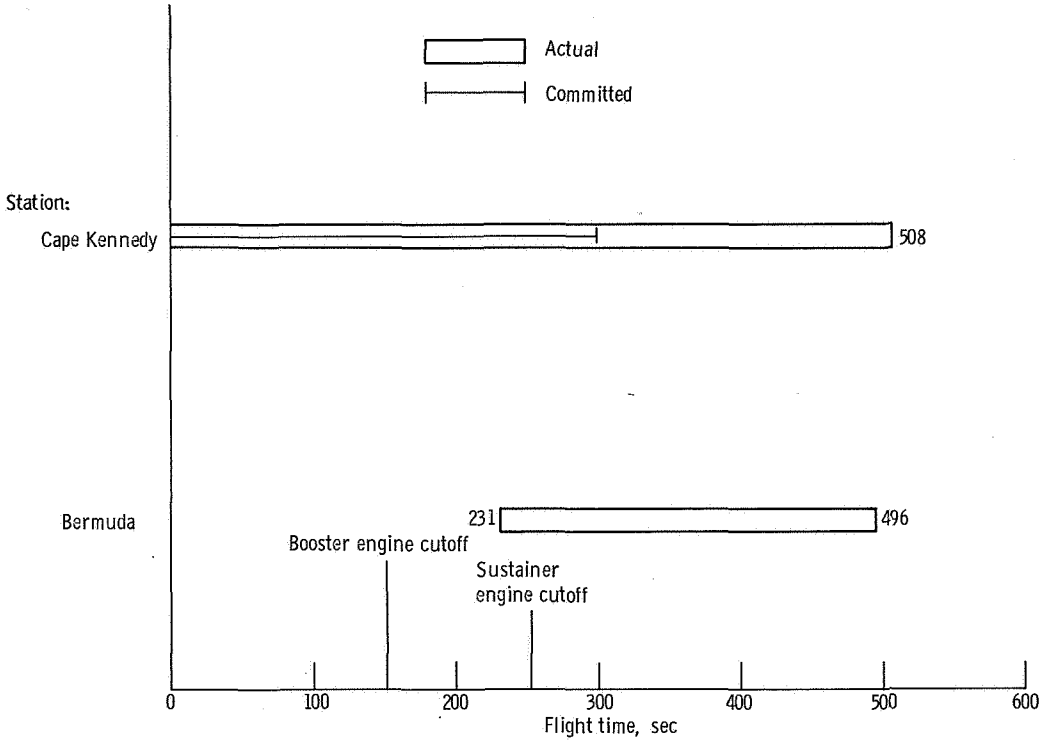

Figure VI-53. - Atlas telemetry coverage, AC-18.

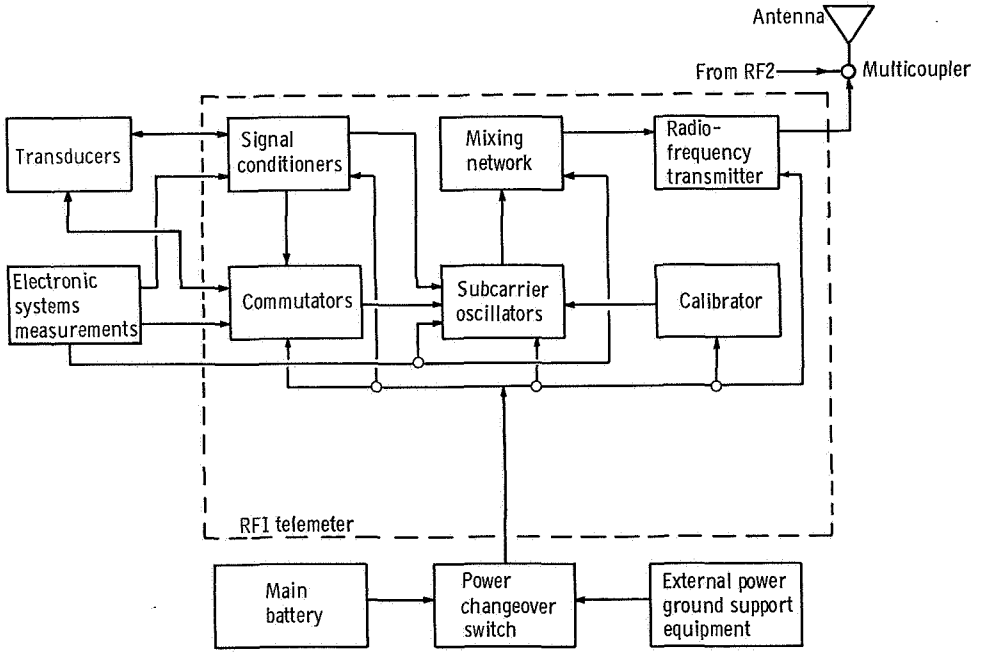

Figure VI-54. - Centaur telemetry system, typical each telemeter, AC-18.

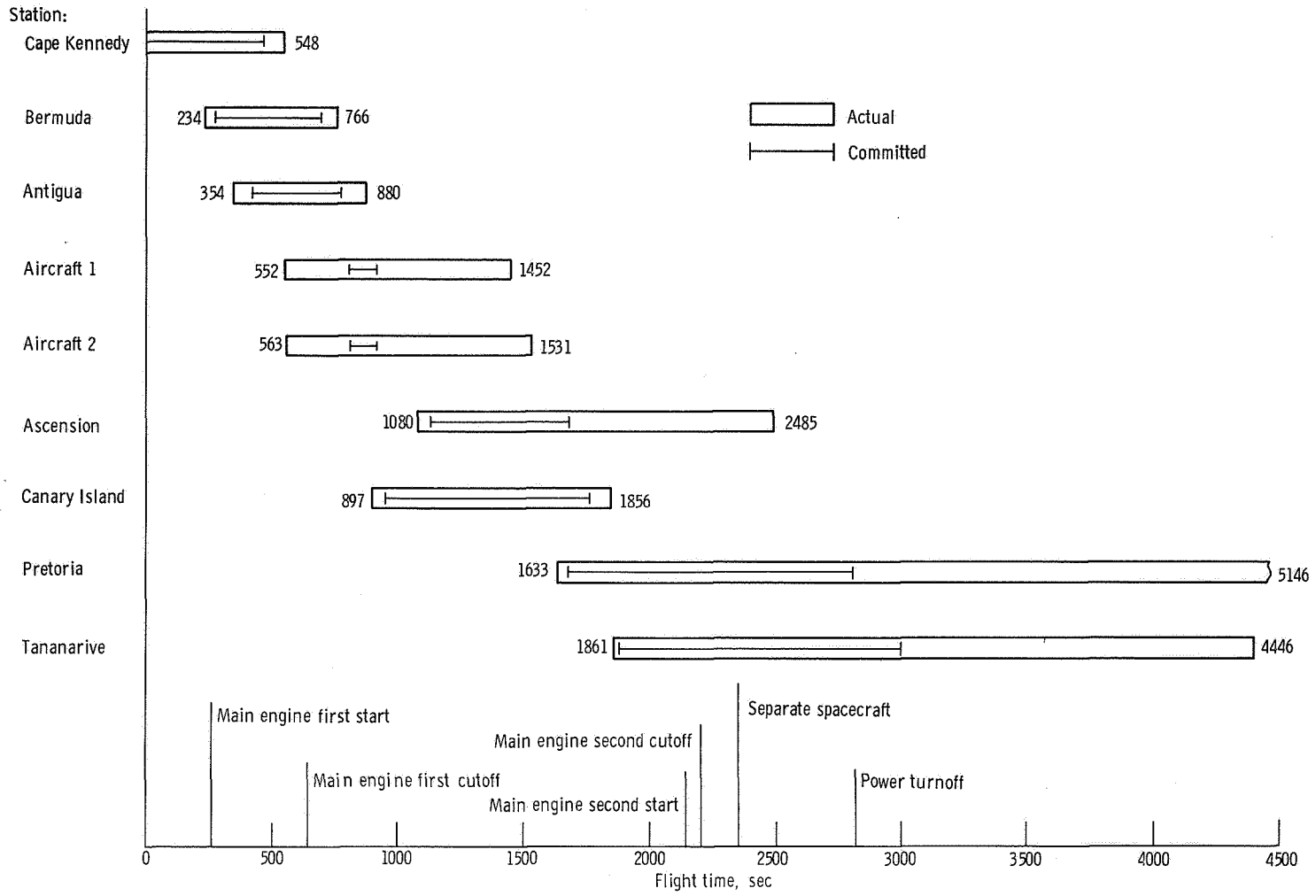

Figure VI-55. - Centaur telemetry coverage, AC-18.

GUIDANCE AND FLIGHT CONTROL SYSTEMS

by Dean H. Bitler, Donald F. Garman, Edmund R. Ziemba, and Corrine Rawlin

The objectives of the guidance and flight control systems are to stabilize and control the launch vehicle; to steer the vehicle along the required flightpath; to determine when the vehicle has reached the velocity required to place the spacecraft in the desired orbit; and to provide command signals to other vehicle systems to start flight events such as jettison insulation panels, separate stages, start main engines, etc. An inertial guidance system is installed on the Centaur stage. Separate flight control systems are installed on the Atlas and Centaur stages.

The Atlas flight control system controls the Atlas-Centaur vehicle by gimbaling the Atlas booster, sustainer, and vernier engines to provide thrust vector control. The Centaur flight control system controls the Centaur by gimbaling the main engines to provide thrust vector control while the main engines are operating or by commanding various combinations of the hydrogen peroxide attitude control engines on or off during coast periods, when the main engines are not operating.

Three modes of operation are used for stabilization, control, and guidance of the launch vehicle. These modes are "rate stabilization only," "rate stabilization and attitude control," and "rate stabilization and guidance control." Block diagrams of the three modes are shown in figure VI-56. The flight times during which a particular mode or a combination of modes is used are shown in figure VI-57. Figure VI-57 also shows the modes of operation of the Centaur hydrogen peroxide attitude control system which are discussed in the following section Flight Control Systems.

The rate-stabilization-only mode stabilizes the roll axis of the Centaur stage continuously after Atlas/Centaur separation. This mode is also used to stabilize the pitch and yaw axes of the Centaur stage for 4.0 seconds following both Centaur main engine starts. In this mode, output signals from rate gyros are used to control the vehicle. The output signal of each rate gyro is proportional to the angular rate of rotation of the vehicle about the input axis of each gyro. The output signal is then used to control gimbaling of the engines in a direction to minimize the output signal; hence, the vehicle angular rate is also minimized. Rate stabilization is also combined with position (attitude) information in the other two modes of operation.

The rate-stabilization-and-attitude-control mode is used for pitch, yaw, and roll control during the Atlas booster phase of flight and for roll control only during the Atlas sustainer phase. This mode is termed "attitude control" since the displacement gyros (one each for the pitch, yaw, and roll axes) provide a reference attitude to which the vehicle is to be alined. However, if the actual flightpath differs from the desired flightpath, there is no way of determining the difference and correcting the flightpath. The

reference attitude is programmed to change during booster phase. These changes in reference attitude cause the vehicle to roll to the programmed flight azimuth angle and to pitch downward and yaw if required. Vehicle stabilization is accomplished in the same manner as in the rate-stabilization-only mode. The rate-stabilization signals are algebraically summed with the attitude reference signals. These resultant signals (one signal for each axis) are then used to control and stabilize the vehicle by gimbaling the engines to minimize (null) the signal.

The rate-stabilization-and-guidance-control mode is used for the pitch and yaw axes during Atlas sustainer phase, during Centaur main engine firing, and during the coast period following main engine cutoff. In this mode, the guidance system provides the attitude and direction reference. If the resultant flightpath, as measured by the guidance system, is not the required flightpath, the guidance system issues steering signals to direct the vehicle to the required flightpath. Vehicle stabilization is accomplished in the same manner as in the rate-stabilization-only mode. The pitch and yaw rate stabilization signals are algebraically summed with the appropriate pitch and yaw steering signals from the guidance system. These resultant signals (one for pitch and one for yaw) are used to control and stabilize the vehicle.

Figure VI-58 is a simplified diagram of the interface between the guidance system and the flight control systems.

Guidance System

The Centaur guidance system is an inertial system which becomes completely independent of ground control at approximately T - 12 seconds.

System description. - The guidance system performs the following functions:

(1) Measures vehicle acceleration in fixed inertial coordinates

(2) Computes the values of actual vehicle velocity and position, and computes the vehicle flightpath to attain the trajectory injection point

(3) Compares the actual position to the desired flightpath and issues steering signals

(4) Issues discrete commands

The guidance system consists of five separate units. Three of the units form a group called the "inertial measurement units." The other two units are the navigation computer unit and the signal conditioner unit. A simplified block diagram of the guidance system is shown in figure VI-59.

Inertial measurement units: The inertial measurement units measure vehicle acceleration and consist of

(1) The inertial platform unit, which contains the platform assembly, the gyros, and the accelerometers

(2) The pulse rebalance, gyro torquer, and power supply unit, which contains the electronics associated with the accelerometers

(3) The platform electronics unit, which contains the electronics associated with the gyros

The platform assembly uses four gimbals which provide a three-axes coordinate system. The use of four gimbals, instead of three, allows complete rotation of all three vehicle axes about the platform without gimbal lock. Gimbal lock is a condition in which two axes coincide, causing loss of 1 degree of freedom. A gimbal diagram is shown in figure VI-60. The azimuth gimbal is isolated from movements of the vehicle structure by the other three gimbals. The inertial components (three gyros and three accelerometers) are mounted on the azimuth or inner gimbal. A gyro and an accelerometer are mounted as a pair with their sensing axes parallel. The gyro and accelerometer pairs are also alined on three mutually perpendicular (orthogonal) axes corresponding to the three axes of the platform.

The three gyros are identical and are of the signal-degree-of-freedom, floated-gimbal, rate-integrating type. Each gyro monitors one of the three axes of the platform. These gyros are elements of control loops, the sole purpose of which is to maintain each axis fixed in inertial space. The output signal of each gyro is connected to a servoamplifier whose output controls a direct-drive torque motor which moves a gimbal of the platform assembly. By controlling each gimbal, the inner gimbal is fixed in inertial space and provides a stable known reference for the accelerometers. Since the inner gimbal is fixed in inertial space and the outer roll gimbal is attached to the vehicle, the angles between the gimbals provide a means for transforming steering signals from inertial coordinates to vehicle (body) coordinates. The transformation is accomplished by electromechanical resolvers mounted between gimbals. The resolvers produce electrical signals proportional to the sine and cosine functions of the gimbal angles. These electrical signals are used to provide an analog solution of the mathematical equations for coordinate transformation by interconnecting the resolvers in the proper manner.

The three accelerometers are identical and are of the single-axis, viscous-damped, hinged-pendulum type. The accelerometer associated with each axis measures the change in vehicle velocity along that axis by responding to acceleration. Acceleration of the vehicle causes the pendulum to move off center. The associated electronics then produce precise current pulses to re-center (rebalance) the pendulum. These rebalance pulses are either positive or negative depending on an increase or decrease in vehicle velocity. These rebalance pulses, representing changes in velocity (incremental velocity), are also routed to the navigation computer unit for computation of vehicle velocity.

Proper flight operation requires alinement and calibration of the inertial measuring unit during launch countdown. The characteristic constant torque drift rate and mass unbalance along the input axis of each gyro are measured. The scale factor and zero bias offset of each accelerometer are also measured. These prelaunch-determined

values are stored in the navigation computer for use during flight. The inner gimbal of the platform is alined to the reference azimuth direction by ground-based optical equipment. This gimbal is also alined perpendicular to the local vertical by using the two accelerometers in the horizontal plane.

Navigation computer unit: The navigation computer computes velocity and other navigation and guidance parameters. It is a digital computer with a magnetic drum memory. The memory drum has a capacity of 2816 words (25 bits per word) of permanent storage, 256 words of temporary storage, and six special-purpose tracks. Permanent storage is prerecorded and cannot be altered by the computer. The temporary storage is the working storage of the computer. The six special tracks are for addressing, instruction register, multiplication, and integration.

The operation of the navigation computer is controlled by the prerecorded program. This program directs the computer to use the prelaunch equations, navigation equations, and guidance equations. The prelaunch equations establish the initial conditions for the navigation and guidance equations. Initial conditions include (1) a reference trajectory, (2) launch site values of geographical position, and (3) initial values of navigation and guidance functions. Based on these initial conditions the guidance system starts flight operation approximately 12 seconds before lift-off.

The navigation equations are used to computer vehicle velocity and actual position. Velocity is determined by algebraically summing the incremental velocity pulses from the accelerometers. An integration is then performed on the computed velocity to determine actual position. Corrections for the prelaunch-determined gyro and accelerometer constants are also made during the velocity and position computation to improve the navigation accuracy. For example, the velocity data derived from the accelerometer measurements are adjusted to compensate for the accelerometer scale factors and zero offset biases measured during the launch countdown. The direction of the velocity vector is also adjusted to compensate for the gyro constant torque drift rates measured during the launch countdown.

The guidance equations continually compare actual position and velocity with the position and velocity required for orbital injection. Based on this position comparison, steering signals are generated to steer the vehicle along an optimized flightpath to obtain the desired injection conditions. The guidance equations are used to generate six discrete commands: (1) booster engine cutoff, (2) sustainer engine cutoff backup, (3) Centaur main engine first cutoff and Centaur main engine second cutoff, (4) propellant utilization system "null", and (5) B timer start. The booster engine cutoff command and the sustainer engine cutoff backup command are issued when the measured vehicle acceleration equals predetermined values. The Centaur main engine cutoff commands are isused when the computed angular momentum equals that required for injection into the apprpriate orbit. The command to "null" the propellant utilization system is issued

15 seconds before the computed-predicted second Centaur main engine cutoff command. The command to start the B timer is issued when a predetermined range angle from the launch pad to vehicle position, measured at the center of the earth, is attained. This command begins the sequence for the main engine second start.

During the booster phase of flight, the navigation computer supplies pitch and yaw signals for steering the Atlas stage. From a series of predetermined programs, one pitch program and one yaw program are selected based on prelaunch upper-air wind soundings. The selected programs are entered and stored in the computer during launch countdown. The programs consist of discrete pitch and yaw turning rates for specified time intervals from T + 15 seconds until booster engine cutoff. These programs permit changes to be made in the flight reference trajectory during countdown to reduce anticipated aerodynamic heating and structural loading conditions on the vehicle.

Before AC-18, on a Centaur-two-powered-phase mission, the navigation computer issued the command which started the sequence for main engine second start. When the engines started, the acceleration rise was sensed and the guidance equations were automatically branched to the second-firing flight mode. Seventy seconds later an enable was actuated so that at engine shutdown, for any reason, the acceleration drop could be sensed and a discrete issued to separate the spacecraft. With this mechanization, spacecraft separation could not occur if ignition failed since there would be no acceleration rise. Beginning with AC-18, if second-firing ignition is not sensed within 17.5 seconds of the "start main engines" command, the guidance equations assume engine failure and would issue a command which would result in spacecraft separation after 135 seconds.

Signal conditioner unit: The signal conditioner unit is the link between the guidance system and the vehicle telemetry system. This unit modifies and scales guidance system parameters to match the input range of the telemetry system.

System performance. - The accuracy of the guidance system was satisfactory as proven by the orbit in which the spacecraft was placed. See Section V. - TRAJECTORY AND PERFORMANCE.

Discrete Commands

All discrete commands were issued properly. Table VI-XIV lists the discretes, with the criteria for the issuance of the discretes. Actual and predicted times from liftoff are shown only for reference since measured performance is the real basis for issuance rather than time.

Guidance steering loops. - The pitch and yaw steering signals are proportional to the components of the steering vector (desired vehicle pointing vector) along the vehicle

pitch and yaw axis. In this section of the report, the steering signals have been converted into the approximate angular attitude errors between the steering vector and the vehicle roll axis (vehicle pointing vector) in the pitch and yaw planes.

Guidance steering was activated 8.0 seconds after the booster engine cutoff command. During the sustainer phase of flight and during Centaur main engine firing, the attitude errors were maintained near null in pitch and yaw except for short durations following the times when guidance steering was enabled. Attitude errors at these times are as follows:

Event	Time, sec	Attitude displacements, deg	
		Pitch	Yaw
Sustainer phase	T + 160	4.8 (nose up)	0
Centair first powered phase	T + 268	2.0 (nose down)	16.3 (nose left)
Centaur second powered phase	T + 2148	3.2 (nose down)	4.1 (nose right)

The large yaw maneuver during the Centaur first powered phase was used to obtain the planned parking orbit inclination for this flight. During Centaur second powered phase, another left-turn maneuver was accomplished to lower the orbital inclination as previously planned. At T + 2215 seconds, another yaw maneuver started to ensure the vehicle would turn to the spacecraft separation attitude in less than 180^{o}. This total maneuver was completed by T + 2296 seconds.

Accelerometer loops and gyro control loops: The gimbal control loops operated satisfactorily throughout the flight and maintained the platform's inertial reference. The fourth gimbal uncaged at T + 53 seconds when the vehicle had pitched over approximately 18^{o}. The maximum displacement errors were less than 20 arc-seconds. Normal low-frequency oscillations (<2 Hz) were observed in the gyro control loops, and are attributed to vehicle dynamics. The accelerometer loops operated satisfactorily throughout the flight. Accelerometer pendulum null offsets were less than 2 arc-seconds in any loop.

Temperature measurements: The accelerometer, gyro, and coupler oven temperature control amplifiers operated within their control ranges throughout the flight. The unit skin temperatures were within specifications throughout the flight. The temperatures are recorded in table VI-XV.

System description - Atlas. - The Atlas flight control system provides the primary functions required for vehicle stabilization, control, sequencing, and the execution of guidance steering signals and consists of the following major units:

(1) The displacement gyro unit, which contains three single-degree-of-freedom, floated-gimbal, rate-integrating gyros and associated electronic circuitry for gain selection and signal amplification: These gyros are mounted to the vehicle structure in an orthogonal triad configuration alining the input axis of a gyro to its respective vehicle vehicle axis of pitch, yaw, or roll. Each gyro provides an electrical output signal proportional to the integral of the angular rate of rotation of the vehicle about the input (reference) axis.

(2) The rate gyro unit, which contains three single-degree-of-freedom, floated-gimbal, rate gyros and associated electronic circuitry: These gyros are mounted in the same manner as the displacement gyro unit. Each gyro provides an electrical output signal proportional to the angular rate of rotation of the vehicle about the gyro input (reference) axis.

(3) The servoamplifier unit, which contains electronic circuitry to amplify, filter, integrate, and algebraically sum combined position and rate signals with engine position feedback signals: The electrical outputs of this unit direct the hydraulic actuators which gimbal the engines to provide thrust vector control.

(4) The programmer unit, which contains an electronic timer; arm-safe switch; high-, low-, and medium-power electronic switches; and circuitry to set the roll program from launch ground equipment: The programmer issues discrete commands to other units of the Atlas flight control system, the Atlas propulsion system, the Atlas pneumatic system, the vehicle separation systems, and the Centaur flight control system.

System description - Centaur. - The Centaur flight control system provides the primary means for vehicle stabilization and control, execution of guidance steering signals, and timed switching sequences for programmed flight events. The Centaur flight control system (fig. VI-61) consists of the following major units:

(1) The rate gyro unit, which contains three single-degree-of-freedom, floated-gimbal, rate gyros with associated electronics for signal amplification gain selection and conditioning of guidance steering signals: These gyros are mounted to the vehicle in an orthogonal triad configuration alining the input axis of each gyro to its respective vehicle axis of pitch, yaw, or roll. Each gyro provides an electrical output signal proportional to the angular rate of rotation of the vehicle about the gyro input (reference) axis.

(2) The servoamplifier unit, which contains electronics to amplify, filter, integrate, and algebraically sum combined position and rate signals with engine position feedback signals: The electrical outputs of this unit issue signals to the hydraulic actuators which

control the gimbaling of the engines. In addition, this unit contains the logic and threshold circuitry to control the engines of the hydrogen peroxide attitude control system.

(3) The electromechanical sequence timer unit, which contains a 400-hertz synchronous motor to provide the time reference and actuate switches at program times: Two timer units, designated "A" and "B," are needed because of the large number of discrete commands required for this two-powered-phase mission.

(4) The auxiliary electronics unit, which contains logic, relay switches, transistor switches, power supplies, control circuitry for the electromechanical timer, circuitry for conditioning computer-generated discretes, and an arm-safe switch: The arm-safe switch electrically isolates valves and pyrotechnic devices from the control switches. The combination of the electromechanical timer units and the auxiliary electronics unit issues discretes to other units of the Centaur flight control system and to the propulsion, pneumatic, hydraulic, separation, propellant utilization, telemetry, spacecraft, and electrical systems.

Vehicle steering during Centaur powered flight is by thrust vector control through gimbaling of the two main engines. There are two actuators for each engine to provide pitch, yaw, and roll control. Pitch control is accomplished by moving both engines together in the pitch plane. Yaw control is accomplished by moving both engines together in the yaw plane, and roll control is accomplished by moving the engines differentially in the yaw plane. Thus, the yaw actuator responds to an algebraically summed yaw/roll command. By controlling the direction of thrust of the main engines, the flight control system maintains the flight of the vehicle on a trajectory directed by the guidance system. After main engine cutoff, control of the vehicle is maintained by the flight control system through selective firing of hydrogen peroxide engines. A more complete description of the engines and the propellant supply for the attitude control system is presented in the section PROPULSION SYSTEMS.

The logic circuitry, which commands the 14 hydrogen peroxide engines either on or off, is contained in the servoamplifier unit of the flight control system. Figure VI-62 shows the alphanumeric designations of the engines and their locations on the aft end of the vehicle. Algebraically summed position and rate signals are the inputs to the logic circuitry. The logic circuitry provides five modes of operation designated "all off," "separate on," "A and P separate on," "V half on," and "S half on." These modes of operation are used during different periods of the flight and are controlled by the electromechanical sequence timer unit. A summary of the modes of operation is presented in table VI-XVI. In this table "threshold" designates the vehicle rate in degrees per second that has to be exceeded before the engines are commanded "on."

System performance - Atlas. - The flight control system performance was satisfactory throughout the Atlas phase of the AC-18 flight and compared well with previous flights. The corrections required to control the vehicle because of disturbances were

well within the system capabilities. The vehicle dynamic responses resulting from each flight event were evaluated in terms of amplitude, frequency, and duration as observed on rate gyro data (table VI-XVII). In this table, the control capability is the ratio of engine gimbal angle used to the available total engine gimbal angle, in percent. The percent control capability used at the times of the flight events includes that necessary for correction of the vehicle transient disturbances and for steady-state requirements. The programmer was started at 1.1-meter (42-in.) rise, which occurred at approximately T + 1 second. At this time the flight control system began to gimbal the engines for vehicle control. The significant vehicle transients were quickly damped and required a maximum of 12 percent of the control capability. The roll program was initiated at approximately T + 2 seconds and rolled the vehicle approximately 8^{o} to the desired flight azimuth. The roll rate, which depended on the launch pad and flight azimuth orientations, continued for approximately 13 seconds. The pitch program (code PP31) and yaw program (code YP0), which were selected in accordance with launch-day upper-wind data, were initiated at T + 15 seconds and continued until booster engine cutoff.

Centaur rate gyro data indicated that the period of maximum aerodynamic loading was approximately from T + 77 to T + 95 seconds. During this period a maximum of 28 percent of the control capability was required to compensate for steady-state and transient loading.

Atlas booster engine cutoff occurred at T + 151.8 seconds. The rates imparted to the vehicle by this transient required only 2 percent of the sustainer engine gimbal capability. The Atlas booster engine section was jettisoned at about 3 seconds after booster engine cutoff. The rates imparted by this disturbance were nearly damped out by the time Centaur inertial guidance was admitted.

During the Atlas booster phase of the flight, the Atlas flight control system provided the vehicle attitude reference. At approximately 5 seconds after booster engine section jettison, the Centaur guidance system provided the attitude reference for pitch and yaw. At this time, guidance issued a steering vector which required a maximum of 30 percent of the Atlas engine gimbal angle capability. The maximum vehicle rate transient during this change was a pitch rate of 2.86 degrees per second peak-to-peak (table VI-XVII).

Insulation panels and nose fairing were jettisoned at T + 196.5 and T + 233.3 seconds, respectively. The observed vehicle rate transients due to these disturbances were damped within 2.1 seconds and required a maximum control capability of 14 percent. Only small transients were observed at sustainer engine cutoff. Transients rates resulting from Atlas/Centaur separation were damped within 2.1 seconds.

System performance - Centaur. - The Centaur flight control system performance was satisfactory. Vehicle stabilization and control were maintained throughout the flight. All events sequenced by the timers were executed at the required times. The following evaluation is presented in paragraphs related to time sequenced portions of the flight.

For typical time periods of guidance/flight control modes of operation and attitude control system modes of operation, refer to figure VI-57. Vehicle dynamic responses for selected flight events are tabulated in table VI-XVII.

Sustainer engine cutoff (SECO) to Centaur main engine first cutoff (MECO-1) (T + 251.6 sec to T + 639.0 sec): Appropriate commands were issued to separate the Centaur stage from the Atlas stage and to initiate the Centaur main engine first firing sequences. There were no significant vehicle transients during separation. Vehicle control was maintained during the period between Atlas/Centaur separation and main engine start by gimbaling the main engines as they were discharging boost pump turbine exhaust and chilldown flow.

Guidance steering was enabled 4 seconds after main engine start. At this time the steering command was 2^{o} down and 16^{o} to the left. Vehicle rates resulting from the guidance steering commands and main engine start disturbances were damped within 12 seconds. Vehicle steady-state angular rates during the remainder of the first powered phase were less than 1 degree per second. The angular rates imparted to the vehicle at main engine first cutoff were damped within 1.4 seconds.

Main engine first cutoff (MECO-1) to main engine second prestart (from T + 639 sec to approximately T + 2125 sec): At main engine first cutoff the hydrogen peroxide attitude control system was activated. At T + 695.9 seconds, during the V-half-on mode, the rate gyro and low-frequency accelerometer data indicated an unexpected low-level disturbance. The maximum peak-to-peak rate was 0.53 degree per second in pitch at 20 hertz with a 1-second duration. No other unusual disturbances were observed throughout this period.

Main engine second prestart to main engine second cutoff (approximately T + 2125 sec to T + 2213.9 sec): During main engine second prestart, the attitude control system is in the V-half-on mode to control the prestart disturbances. Main engine second start occurred at T + 2143.1 seconds. Coincident with main engine second start was a 20-second period of A-and-P-separate-on mode to provide control for the emergency separation sequence (refer to flight control system description). The maximum angular rate caused by main engine start transients was 2.14 degrees per second in pitch. Vehicle rates for the remainder of the second powered phase did not exceed 1 degree per second.

Main engine second cutoff (MECO-2) to retrothrust (from T + 2213.9 sec to T + 2519 sec): The hydrogen peroxide attitude control system was activated in the A-and-P-separate-on mode at the time of Centaur main engine cutoff. The S2 and S4 engines commenced firing at MECO-2 for a period of 10 seconds to settle propellants. For the AC-18 flight the autopilot was in a nonlinear gain configuration from MECO-2 until MECO-2 + 197 seconds. This configuration enabled rapid alinement maneuvers and pointing vector accuracy at spacecraft separation. The Centaur began turning to the

separation vector at approximately T + 2213.9 seconds and completed the turn at approximately T + 2303.0 seconds. The ATS-5 was separated from the Centaur at T + 2349 seconds. At spacecraft separation, the residual rates were extremely low. However, a positive transient was seen on the longitudinal accelerometers instead of the expected negative transient. It is believed that these measurements did not respond correctly because guidance data and integration of the transition adapter low-frequency accelerometer data verify the expected negative impulse (see section ELECTRICAL SYSTEM, Instrumentation and Telemetry).

At approximately T + 2355.1 seconds the Centaur began its post-separation maneuver by turning approximately 101^{o}. This turn was essentially complete by the time the V-half-on mode, for propellant settling, was commanded on at T + 2411 seconds. This was followed by a 100-second S-half-on period to increase relative separation distance. At T + 2519 seconds the engine prestart valves were opened to allow the residual propellants to discharge through the main engines. Simultaneously the separate-on mode and gimbaling of the main engines provided vehicle control. The post-separation maneuver was completed satisfactorily. A V-half-on mode followed later as an experiment to determine the amount of remaining hydrogen peroxide.

TABLE VI-XIV. - DISCRETE COMMANDS ISSUED BY GUIDANCE, AC-18

Command	Criterion for issuance	Time,[a] T + sec	
		Actual	Predicted
Booster engine cutoff	When square of vehicle thrust acceleration is greater than 2640 $(m/sec^2)^2$ (28 500 $(ft/sec^2)^2$)	152	153±2.6
Sustainer engine cutoff backup	When square of vehicle thrust acceleration is greater than 51.1 $(m/sec^2)^2$ (550 $(ft/sec^2)^2$)	258	Not predicted
Main engine first cutoff	When vehicle has achieved required angular momentum for parking orbit	639	641±8.6
Start timer for main second engine start	When vehicle has achieved required range angle (Range angle is angle at center of earth from launch pad to vehicle position.)	2083	2081±8.6
Null propellant utilization system	Fifteen seconds prior to computed predicted time of main engine second cutoff	2198	2196±2.3
Main engine second cutoff	When vehicle has achieved required angular momentum for transfer orbit	2215	2211±10.4

[a]Times shown are for reference only.

TABLE VI-XV. - UNIT SKIN TEMPERATURES, AC-18

Parameter	Units	Flight values at-	
		T - 0 sec	T + 2400 sec
Inertial platform skin temperature	K	296	304
	^{o}F	73.6	88
Pulse rebalance, gyrotorquer, and power supply skin temperature	K	288	294
	^{o}F	58	70
Navigation computer skin temperature	K	291	315
	^{o}F	64	107.2

TABLE VI-XVI. - DESCRIPTION OF ATTITUDE CONTROL SYSTEM MODES OF OPERATION, AC-18

[Thrust; A engines, 15.6 N (3.5 lbf); P engines, 26.7 N (6.0 lbf); S engines, 13.3 N (3.0 lbf); V engines, 222.4 N (50.0 lbf).]

Mode	Flight period	Description
All off	Powered phases	This mode prevents operation of all attitude control engines regardless of error signals.
Separate on	Main engine second cutoff (MECO-2) + 305 seconds to MECO-2 + 555 seconds, during post-separation maneuver	When in separate-on mode, a maximum of two A and two V engines and one P engine fire. A engines: When 0.2-deg/sec threshold is exceeded, suitable A engines fire to control in yaw and roll. A1/A4 and A2/A3 combinations are inhibited. P engines: When 0.2-deg/sec threshold is exceeded, suitable P engine fires to control in pitch. P1/P2 combination is inhibited. S engines: Off. V engines: When 0.3-deg/sec threshold is exceeded, suitable engines fire (as back-up for higher rates). V1/V3 and V2/V4 combinations are inhibited.
A and P separate on	1. Main engine second start (MES-2) to MES-2 + 20 seconds 2. MECO-2 to MECO-2 + 197 seconds	This mode is the same as separate-on, except engines are inhibited. This mode, in flight period 1, provides control for a possible spacecraft separation in the event of no second firing. In flight period 2, alinement and retromaneuver are accomplished. (For this mission the S2/S4 engines were commanded on by the timer from MECO-2 until MECO-2 + 10 seconds to settle propellants.)
V half on	1. MECO-1 to MECO-1 + 76 seconds 2. MES-2 - 40 seconds to MES-2 3. MECO-2 + 197 to MECO-2 + 205 seconds during post-separation maneuver 4. Last 50 seconds prior to Centaur power turnoff	A engines: When 0.2-deg/sec threshold is exceeded, suitable A engines fire to control in roll only. P engines: Off. S engines: Off. V engines: When 0.2-deg/sec threshold is exceeded, a minimum of two and a maximum of three V engines fire to control in pitch and yaw. When there are no error signals, V2/V4 combination fires continuously. This continuous firing serves various purposes: to settle propellants, in flight periods 1 and 2; to provide lateral and added longitudinal separation between Centaur and spacecraft, in flight period 3; and to deplete hydrogen peroxide supply to determine the amount of usable propellant remaining at end of mission, in flight period 4.
S half on	1. MECO-1 + 76 seconds to MES-2 - 40 seconds 2. MECO-2 + 205 seconds to MECO-2 + 305 seconds	A engines: When 0.2-deg/sec threshold is exceeded, suitable A engines fire to control in roll only. P engines: S engines: When 0.2-deg/sec threshold is exceeded, a minimum of two and a maximum of three S engines fire to control in pitch and yaw. When there are no error signals, S2/S4 combination fires continuously for propellant retention purposes. V engines: When 0.3-deg/sec threshold is exceeded, a minimum of one and a maximum of three V engines fire to control in pitch and yaw. When a V engine fires, the corresponding S engine is commanded off. This mode is used to retain settled propellants, in flight period 1; and to provide lateral and added longitudinal separation between Centaur and spacecraft at a low peroxide consumption rate, in flight period 2.

TABLE VI-XVII. - VEHICLE DYNAMIC RESPONSE TO FLIGHT DISTURBANCES, AC-18

Event	Time,[a] sec	Measurement	Rate gyro peak-to-peak amplitude, deg/sec	Transient frequency, Hz	Transient duration, sec	Required control capability, percent
Lift-off	T + 0	Pitch	0.54	33	0.4	(b)
		Yaw	1.20	5.0	.1	(b)
		Roll	.51	.83	.2	(b)
1.1-Meter (42-in.) rise	T + 1	Pitch	2.59	7.1	0.2	12
		Yaw	1.37	25	.1	4
		Roll	2.05	7.1	.2	4
Region of maximum aerodynamic pressure (T + 77 to T + 95 sec)	T + 85 T + 84 T + 87.5	Pitch Yaw Roll	2.41 1.45 1.71	0.21 .27 .37	10 10 5.5	28 20 20
Booster engine cutoff	T + 151.9	Pitch	1.25	6.7	3.0	2
		Yaw	1.54	5.0	3.0	2
		Roll	2.05	1.1	1.7	2
Booster engine jettison	High frequency, T + 154.9	Pitch	4.82	35	0.8	(c)
		Yaw	6.15	35	.8	(c)
		Roll	7.68	40	.8	(c)
	Low frequency, T + 155.7	Pitch	1.07	0.77	Transient damped by time of admit-guidance	(c)
		Yaw	2.35	.12		(c)
		Roll	1.97	.71		(c)
Admit guidance	T + 159.9	Pitch	2.86	0.17	8	30
		Yaw	1.37	1.2	4	8
		Roll	1.37	.77	6	8
Insulation panel jettison	T + 196.5	Pitch	2.86	30	0.4	6
		Yaw	1.37	30	.2	4
		Roll	1.88	6.7	.7	4
Nose fairing jettison	T + 234.1	Pitch	5.54	30	0.9	14
		Yaw	2.12	30	2.1	6
		Roll	1.54	30	.7	4
Sustainer engine cutoff	T + 251.1	Pitch	1.43	30	0.7	---
		Yaw	.68	30	.7	---
		Roll	.34	30	.4	---
Atlas/Centaur separation	T + 253.5	Pitch	2.14	30	0.7	---
		Yaw	.34	30	2.1	---
		Roll	.85	33	.1	---
Main engine first start	T + 264.3	Pitch	2.14	30	1.1	24
		Yaw	.68	30	.5	8
		Roll	.34 2.39	30 .71	.2 .6	8 8
Admit guidance	T + 268.3	Pitch	1.52	0.24	12	28
		Yaw	2.90	.1	9	34
		Roll	.33	1.0	1.3	34
Main engine first cutoff	T + 639.1	Pitch	6.08	30	1.4	20
		Yaw	3.93	30	1.4	16
		Roll	1.71	30	.8	16
Main engine second start	High frequency, T + 2144.4	Pitch	2.14	30	1.8	8
		Yaw	1.11	30	1.8	24
		Roll	----	-----	----	24
	Low frequency, T + 2144.4	Pitch	1.78	0.5	2	8
		Yaw	2.05	.5	2	24
		Roll	2.05	.38	2.6	24
Admit guidance	T + 2148.3	Pitch	2.32	0.5	15	12
		Yaw	3.25	.42	15	32
		Roll	.34	.71	5	32
Main engine second cutoff	T + 2214	Pitch	5.00	35	1.0	20
		Yaw	3.59	35	.4	16
		Roll	1.45	35	.2	16

[a]Time of transient as indicated on rate gyro data.
[b]Autopilot not yet active.
[c]Sustainer engine control inactive during booster engine jettison.

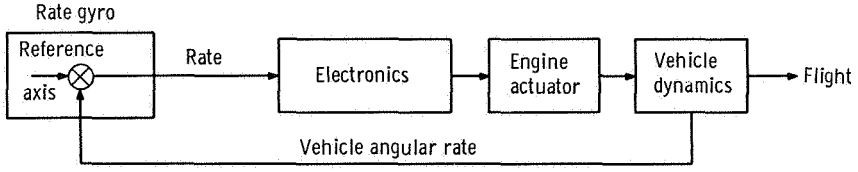

(a) Rate-stabilization-only mode.

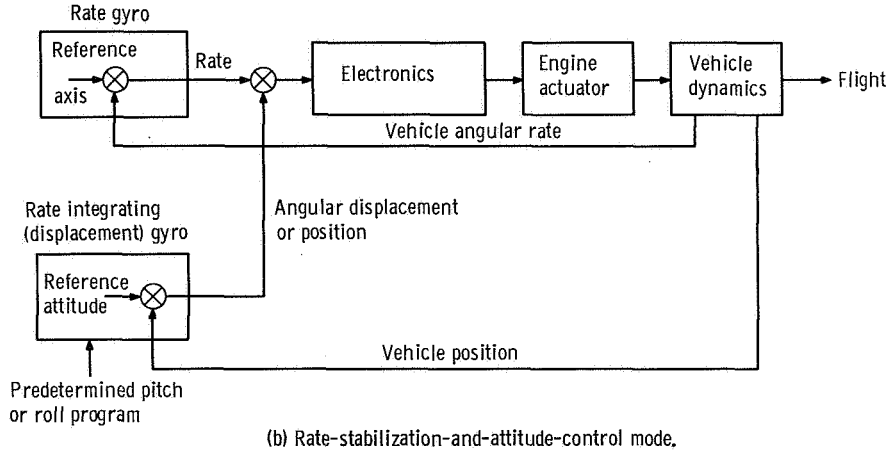

(b) Rate-stabilization-and-attitude-control mode.

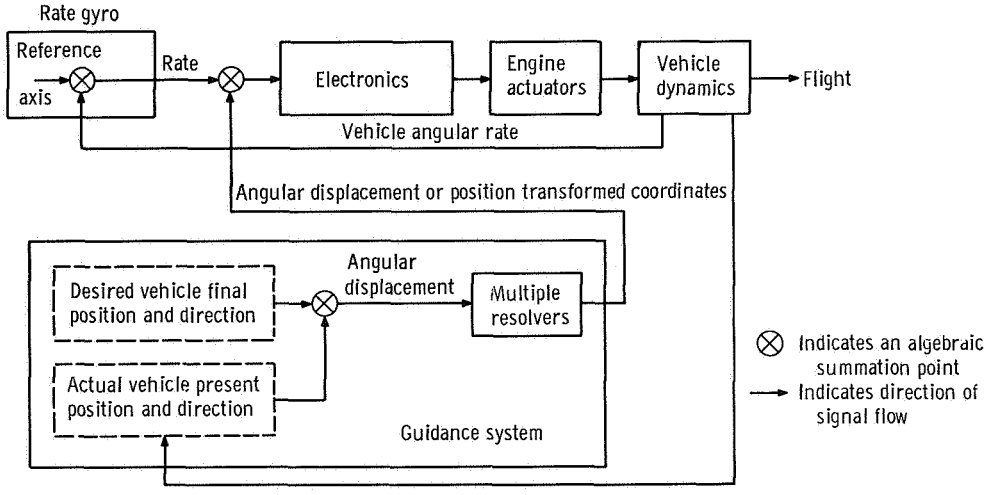

(c) Rate-stabilization-and-guidance-control mode.

Figure VI-56. - Guidance and flight control modes of operation, AC-18.

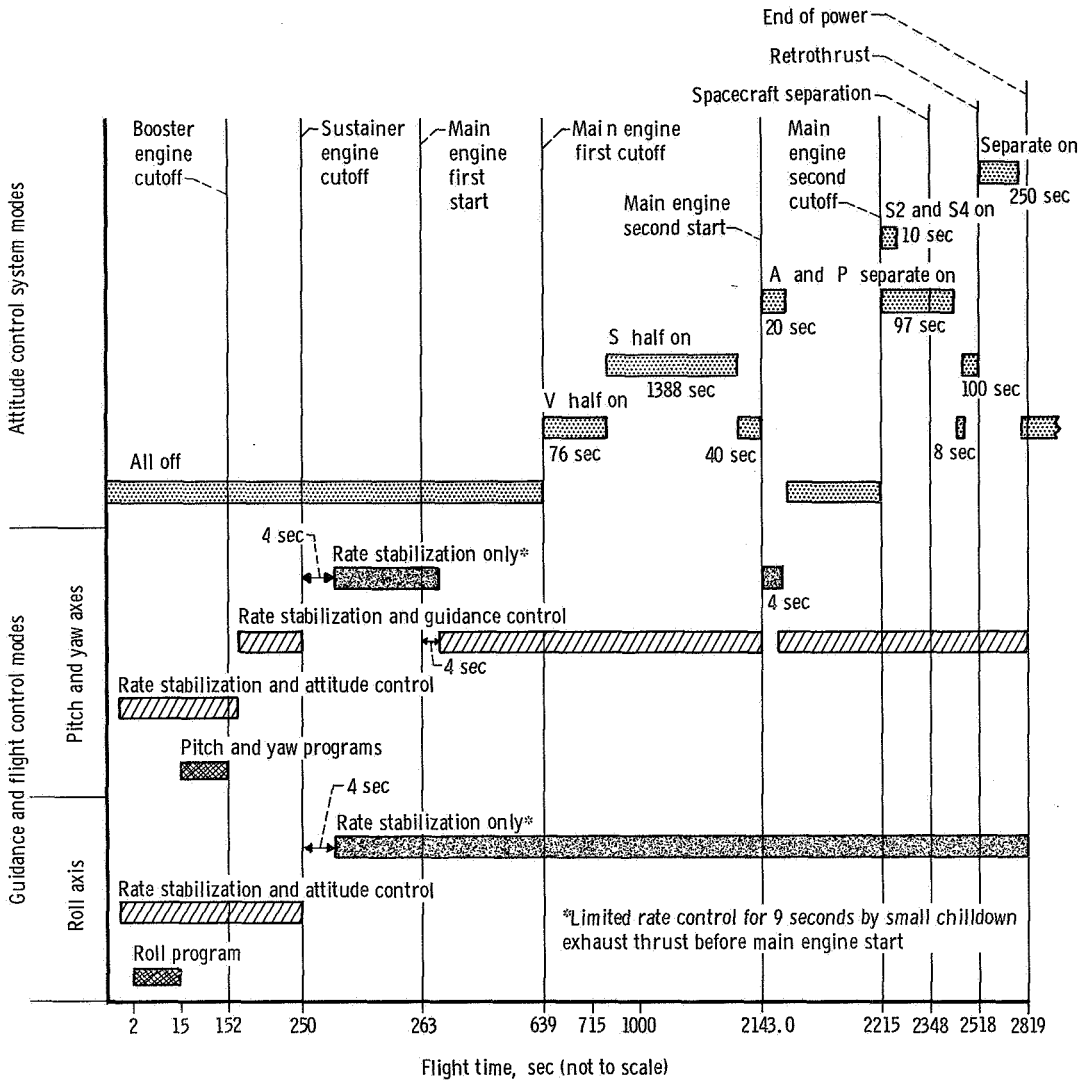

Figure VI-57. - Time periods of guidance and flight control mode and attitude control system mode of operation, AC-18. Times shown are for reference only.

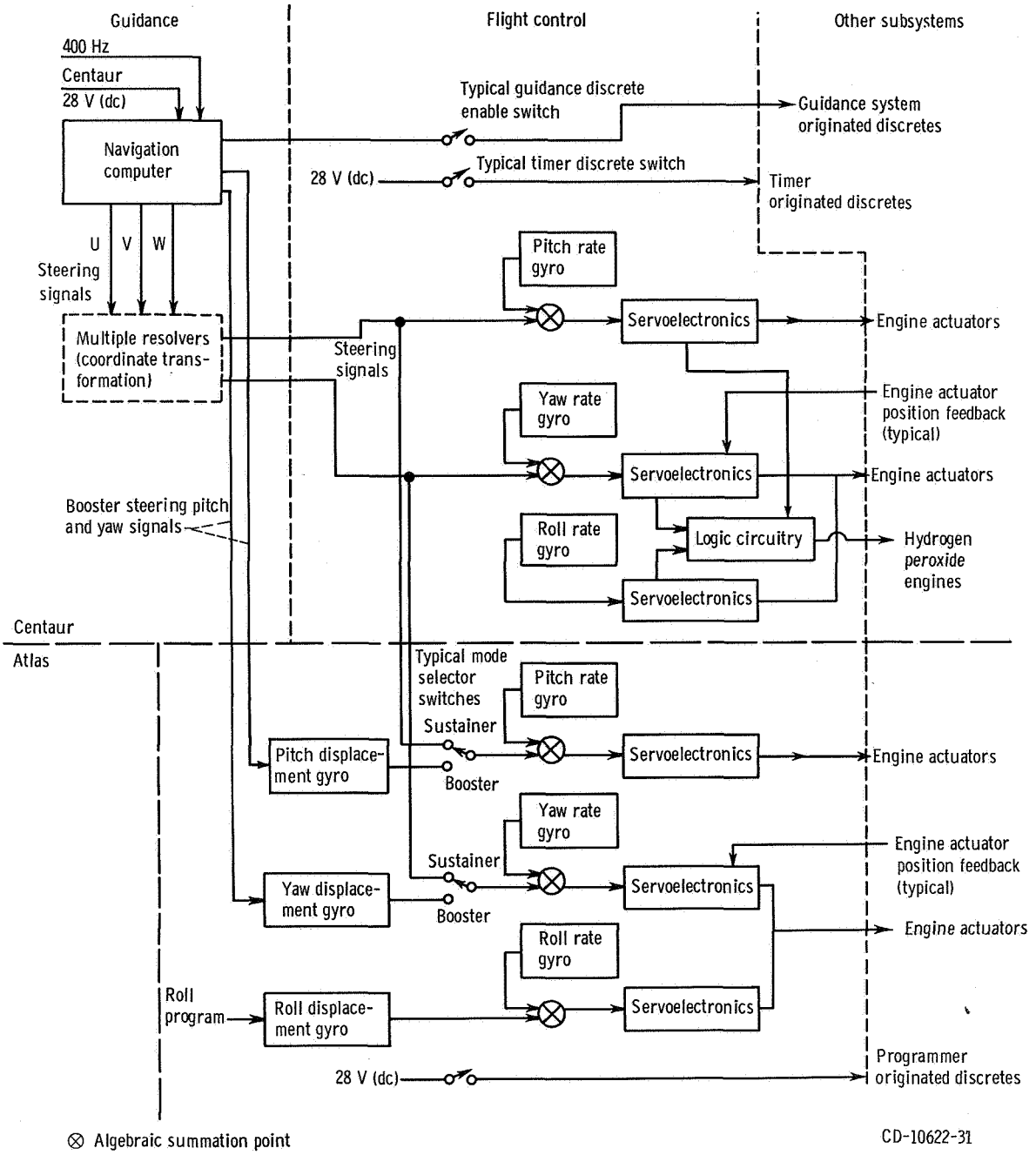

Figure VI-58. - Simplified guidance and flight control systems interface, AC-18.

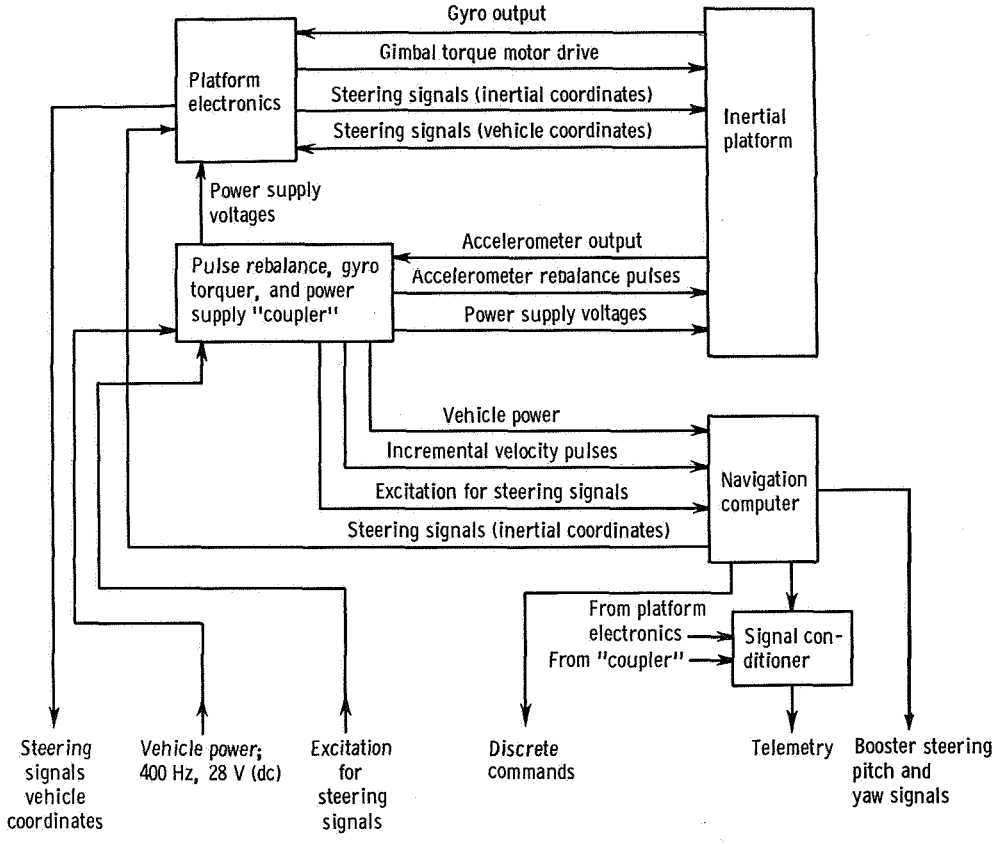

Figure VI-59. - Simplified block diagram of Centaur guidance system, AC-18.

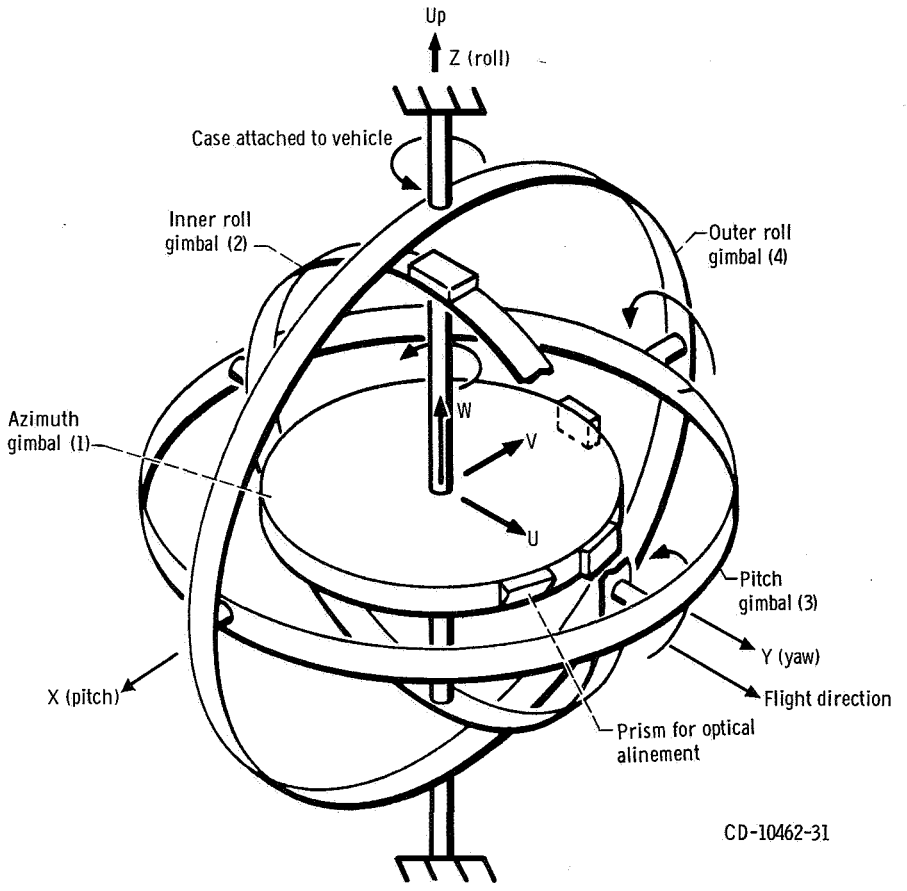

Figure V1-60. - Gimbal diagram, AC-18. Launch orientation: inertial platform coordinates, U, V, and W; vehicle coordinates, X, Y, and Z.

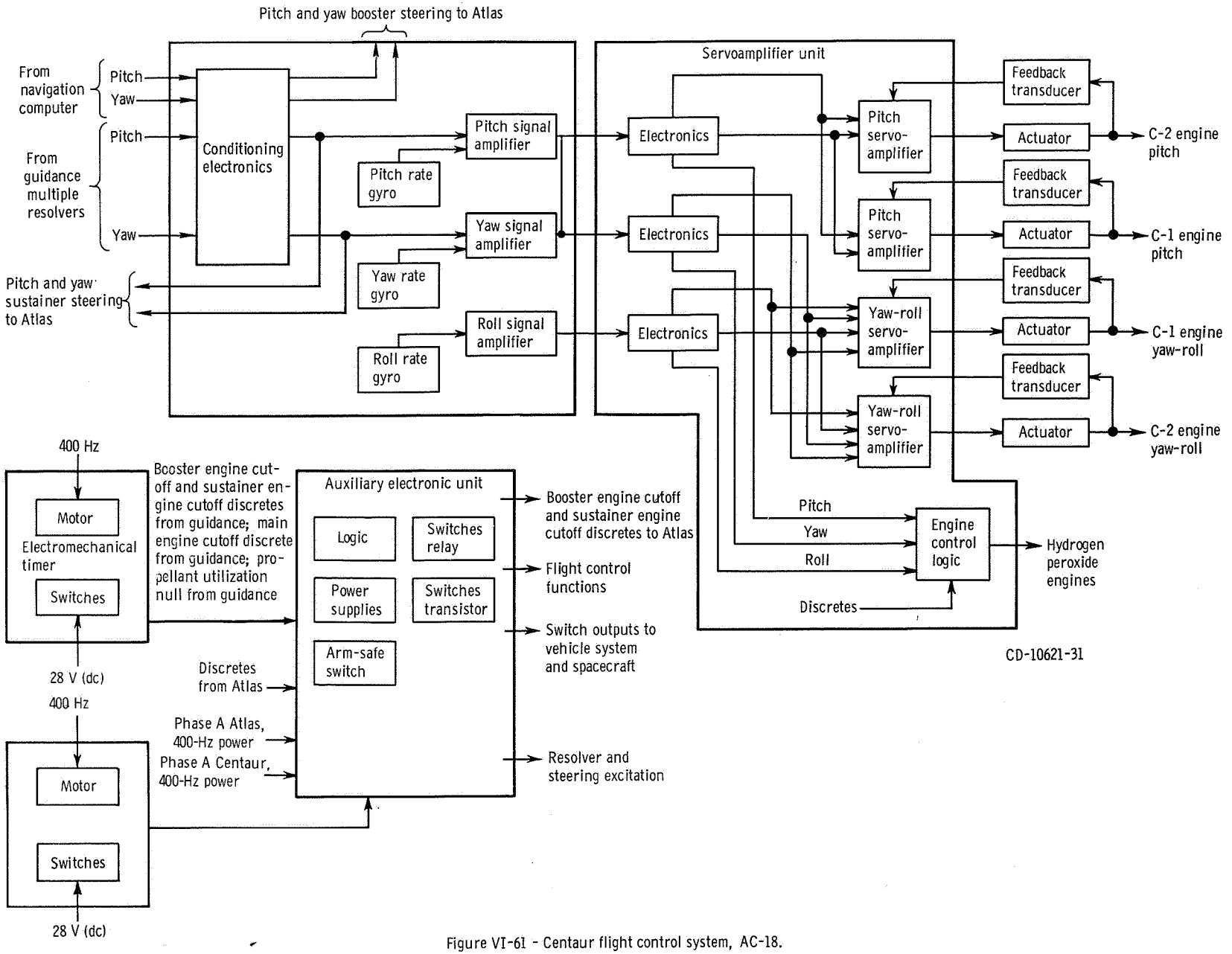

Figure VI-61 - Centaur flight control system, AC-18.

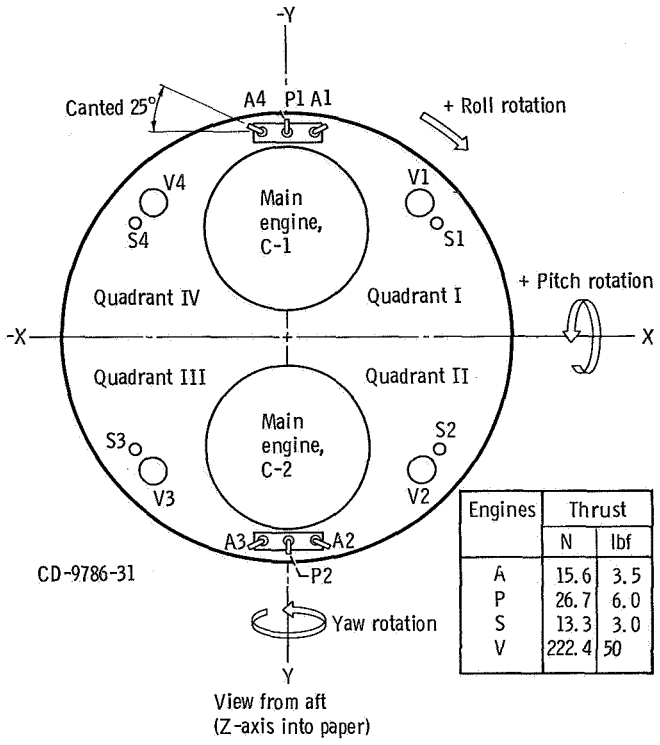

Engines	Thrust	
	N	lbf
A	15.6	3.5
P	26.7	6.0
S	13.3	3.0
V	222.4	50

Figure VI-62. - Attitude engines alphanumeric designations and locations, AC-18. Signs of axes are convention for flight control system.

VII. CONCLUDING REMARKS

The Atlas-Centaur (AC-18) performed satisfactorily and met all launch vehicle flight objectives. Centaur main engine restart occurred as planned, indicating the modifications made because of the Centaur failure on ATS-4 were satisfactory. The ATS-5 with firing of its apogee motor attained the desired near-synchronous orbit; however, gravity gradient stabilization was not achieved because of stability control problems. This was the fifth launch in support of the ATS program and concluded a planned series of five ATS missions.

Lewis Research Center,
National Aeronautics and Space Administration,
Cleveland, Ohio, June 16, 1971,
491-02.

REFERENCE

1. Gerus, Theodore F.; Housely, John A.; and Kusic, George: Atlas-Centaur-Surveyor Longitudinal Dynamics Test. NASA TM X-1459, 1967.

NASA-Langley, 1971 —— 31 E-6284

"The aeronautical and space activities of the United States shall be conducted so as to contribute . . . to the expansion of human knowledge of phenomena in the atmosphere and space. The Administration shall provide for the widest practicable and appropriate dissemination of information concerning its activities and the results thereof."

—NATIONAL AERONAUTICS AND SPACE ACT OF 1958

NASA SCIENTIFIC AND TECHNICAL PUBLICATIONS

TECHNICAL REPORTS: Scientific and technical information considered important, complete, and a lasting contribution to existing knowledge.

TECHNICAL NOTES: Information less broad in scope but nevertheless of importance as a contribution to existing knowledge.

TECHNICAL MEMORANDUMS: Information receiving limited distribution because of preliminary data, security classification, or other reasons.

CONTRACTOR REPORTS: Scientific and technical information generated under a NASA contract or grant and considered an important contribution to existing knowledge.

TECHNICAL TRANSLATIONS: Information published in a foreign language considered to merit NASA distribution in English.

SPECIAL PUBLICATIONS: Information derived from or of value to NASA activities. Publications include conference proceedings, monographs, data compilations, handbooks, sourcebooks, and special bibliographies.

TECHNOLOGY UTILIZATION PUBLICATIONS: Information on technology used by NASA that may be of particular interest in commercial and other non-aerospace applications. Publications include Tech Briefs, Technology Utilization Reports and Technology Surveys.

Details on the availability of these publications may be obtained from:

SCIENTIFIC AND TECHNICAL INFORMATION OFFICE

NATIONAL AERONAUTICS AND SPACE ADMINISTRATION

Washington, D.C. 20546